Republic of Iraq

Ministry of Higher Education and Scientific Research

Kerbala University/College of Engineering

Civil Engineering Department

Structural Behaviour of Self-Compacted Concrete Box Girders with In-Place Openings

A Thesis

Submitted to the Civil Engineering Department /College of Engineering/

Kerbala University in Partial Fulfilment of the Requirements for the Master Degree of Science in Civil Engineering/Infrastructure Engineering

Prepared by

Saif Ali Hassan

(B. Sc. in Civil Engineering-2016)

Supervised by

Assist Prof. Dr. Sadjad Amir Hemzah

Dr. Wajde Shober Saheb Alyhya

2020, A.D. **1441, A.H.**

بِسم الله الرَّحمَن الرَّحِيم

وَقُل رَّبِّ زِدْنِي عِلْمًا

صدق الله العلي العظيم

سورة طه الآية ﴿114﴾

SUPERVISOR CERTIFICATE

We certify that this thesis entitled "**Structural Behaviour of Self-Compacted Concrete Box Girders with In-Place Openings**" is prepared by "**Saif Ali Hassan** " under our supervision at Kerbala University in partial fulfilment of the requirements for the master degree of science in Civil Engineering /Infrastructure Engineering.

Signature:

Assist. Prof. Dr. Sadjad Amir Hemzah

(Supervisor)

Date: / / 2020

Signature:

Dr. Wajde Shober Saheb Alyhya

(Supervisor)

Date: / / 2020

Dedication

This thesis is dedicated to my parents, my family, brothers, sisters and friends for their love and continuous support

Acknowledgements

In the name of **ALLAH**, the most compassionate and the most merciful. Praise be to **ALLAH** as well as pray and peace be on his prophet Mohammed and his family.

First, I would like to express my gratitude and thanks to our supervisors, **Assist. Prof. Dr. Sadjad Amir Hemzah** and **Dr. Wajde Shober Saheb** for their excellent assistance, guidance and valuable suggestions during the research period.

I would like to thank the head and the staff of the Civil Engineering department as well as the construction materials laboratory. I also would like to thank my friends: **Mohammed**, **Karrar**, and **Basel** for their help and support to complete this work.

A special thank and gratitude are due to my family, especially **my parents and my wife** for their care, patience and encouragement during the research period.

Finally, I would like to express my extreme love and appreciation to everyone who has supported this work.

Abstract

This research aims to investigate the structural behaviour of a reinforced self-compacted concrete hollow beam with in-place openings that are non-strengthened or externally strengthened by CFRP strips. The aim is achieved by implementing experimental and numerical work by ABAQUS 2019.

The experimental program comprised casting fourteen reinforced self-compacting concrete hollow beams, which are tested under two concentrated and symmetrical loading.The beams have identical properties (i.e. dimensions, flexural reinforcement, concrete compressive strength, and opening size). The specimens are categorised into three groups, in addition, to two additional beams without openings as control beams. The first group includes six beams with an opening in the front or the front and rear of the web, while the second group contains three beams with openings in the bottom flange of the beam. Besides, the third group comprises three beams with an opening in the front and rear of the web and strengthened with CFRP laminates. The studied parameters were the number and locations of openings.

The experimental results for the first group of specimens revealed that creating openings in the flexure or shear zone or both can cause reductions in the ultimate failure loads by about (5% to 16 %). Furthermore, increase in the deflections of the specimens were observed by about (20% to 70%) owing to the reductions in their stiffness from (16% to 41%) when compared with the hollow control beam. The second group specimens, on the other hand, suffered from reductions' ratios in the ultimate failure loads within the ranged (5% to 9 %). Furthermore, all beams in the second group suffered from higher deflections ranged from (28% to 63 %) owing to the reductions in the stiffness of these beams from (22% to 39%) if compared to control beam. In contrast, the reductions' ratios in the ultimate failure loads for the third group of beams were nearly (2% to 8 %), while the increases in the deflections ratios were (22% to 43 %) due to the reductions in the beams' stiffness from (18% to 23%) if compared with the control beam.

Moreover, the strengthening by CFRP laminates enhanced the post-cracking behaviour of specimens and delayed the appearing of the cracks compared with the unstrengthened beams in the first group. Regarding the first group of beams, the values of the ductility indices ranged from (1.5 to 2.8) if compared with the control beam, while the values for the second group were ranged from (2.2 to 2.5) if compared with the control beam. On the other hand, higher

values for the ductility indices were recorded for the third group of beams (2.4 to 3.2) compared with the unstrengthened beams in the first group.

Non-linear finite element analysis was performed using ABAQUS (2019) to conduct a numerical investigation for the reinforced self-compacting concrete hollow beams with or without openings and strengthened or unstrengthened by CFRP laminates. New parametric study of various variables was also numerically examined. Full bond was assumed between the concrete and steel reinforcement and between the concrete surface and CFRP. There was a good convergence between the experimental and numerical results in terms of the ultimate load, maximum deflection, load-deflection curves, and mode of failure. The average difference in the ultimate load and the maximum deflection found to be equalled to 1.8 and 9.2 %, respectively that ensure the veracity of numerical results.

Furthermore, numerical results obtained from the analyzed beams revealed that the ultimate failure loads for hollow beams with openings decreased with the increase in the opening's diameter from nearly 4 to 18.2 % for opening located at the middle web and from about 2 to 27 % for openings located near the supports in comparison with the control beam. The increase in the number of opening with the same diameter caused a decrease in the ultimate failure loads by 10 to 36 % if compared with the control beam. Furthermore, the ultimate hollow beam load with an opening (s) of identical diameter near the supports increased with the increase in the compressive strength of concrete. The bottom flange-strengthening scheme by CFRP was the best in terms of the ultimate strength viewpoint for hollow beams with a near supports' openings or mid-span's openings, in which the increases were 29 and 37 % for both beams respectively if compared with the unstrengthened beams.

List of Contents

List of Figures

List of Plates

List of Tables

Notation

Symbol	Description
A	Cross-sectional area of a section (mm^2)
Av	Area of vertical shear reinforcing bar (mm^2)
d	Effective Depth (mm)
E_c	Concrete modulus of elasticity (GPa)
E_s	Steel modulus of elasticity (GPa)
f_{cu}	Compressive strength of concrete (MPa)
f_y	Yield stress of steel reinforcement (GPa)
f_s	Strength of steel reinforcement (MPa)
f_u	Ultimate strength of steel reinforcement (MPa)
f_{sp}	Splitting tensile strength of concrete (MPa)
f_t	Tensile strength of concrete (MPa)
f_r	Concrete modulus of rupture (MPa)
D/h	Diameter of opening/ effective depth
ε	Strain
ε_{cu}	Ultimate strain of concrete
$\varepsilon_{\circ}$	Strain corresponding to the maximum compressive stress of concrete
υ	Poisson's ratio
υ_s	Poisson's ratio of steel
h	Total depth of beam (mm)
L	Total length of the beam (mm)
M_u	Ultimate moment capacity (kN.m)
M_n	Nominal moment capacity (kN.m)
P	Maximum applied load (kN)
P_{cr}	Cracking load (kN)
P_u	Ultimate load (kN)
V_c	Shear strength of concrete (kN)
V_s	Shear strength of steel bar (kN)
V_u	Ultimate shear strength (kN)

Vn	Nominal shear strength (kN)
ϕ	Size of steel bar (mm)
ρ	The ratio of longitudinal tensile reinforcement
ρ_{min}	Minimum ratio of longitudinal tensile reinforcement

Abbreviations

Symbol	Description
SCC	Self-compacting concrete
CFRP	Carbon fibre reinforcement polymer
ACI	American Concrete Institute
ASTM	American Society for Testing and Materials
BS	British Standard
FRP	Fibre reinforcement polymer
FEA	Finite Element Analysis
IQS	Iraqi specification
MPa	Mega Pascal
pp	Page number
RC	Reinforced concrete
No.	Number
mm	Millimetre
ANSYS	Analysis System program
AFRP	Aramid fibre reinforcement polymer
GFRP	Glass fibre reinforcement polymer
EFNARC	European Federation of National Associations Representing for Concrete

CHAPTER ONE
INTRODUCTION

1.1 General

Hollow or box beams are commonly utilized in girders, especially for bridges with long spans to reduce the construction charge and minimize the dead load **Aziz *et al.*, (2018**). Furthermore, hollow beams have been increasingly used in towers, buildings construction, offshore structures and bridges to pass different utilities such as mechanical and electrical pipes as shown in **Plate 1.1 Hassan *et al.*, (2018**).

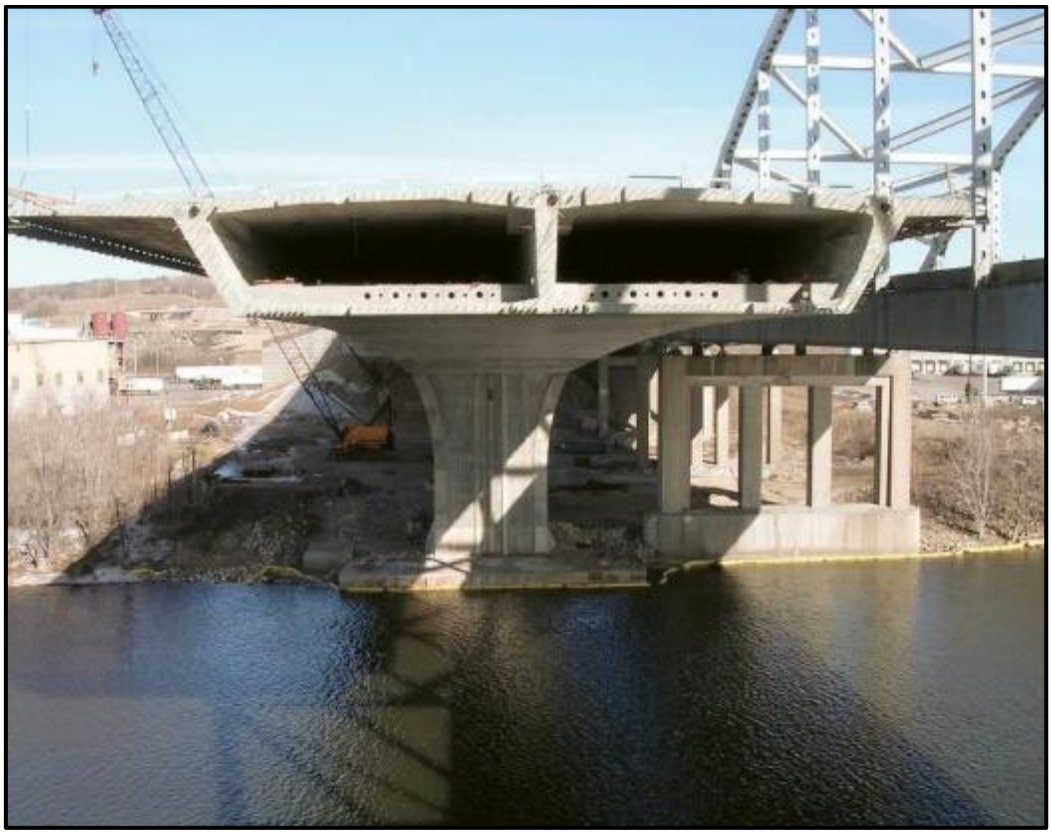

Plate 1. 1: Application of hollow beam in Wakota Bridge American Segmental Bridge, (2005)

In the construction of modern buildings, a network of pipes and ducts is necessary to accommodate essential services like water supply, sewage, air-conditioning, electricity, telephone, and computer network. Usually, these services are placed underneath the beam soffit and, they are, for aesthetic reasons, covered by a suspended ceiling creating a dead space. Passing these pipes and ducts through a transverse opening in the floor beams can reduce the dead space and result in a more compacting design, as shown in **Plate. (1.2).** In small buildings, decreasing the dead spaces may not be remarkable in contrast to multi-storey buildings owing

to the decreasing in the altitude for each story of the multi-storey that produces a significant reduction in the whole altitude **Mansur *et al.***, (**1992**).

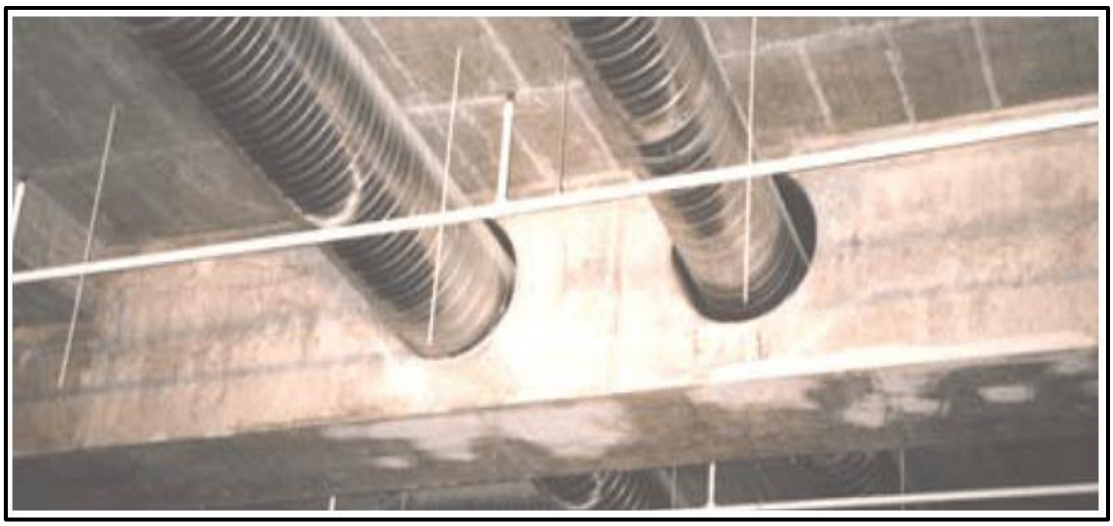

Plate 1.2: An ordinary beam with a circular opening (Amiri et al., 2011)

1.2 Self-Compacting Concrete (SCC)

New types of concrete, such as self-compacting concrete (SCC) have been produced owing to the rapid evolution in concrete technology and construction techniques. As the name indicates, it is a type of concrete that does not require external or internal compaction, as it levels and compacts under its self-weight only. SCC is a recent innovation in concrete technology and one of the most promising developments in the construction industry, owing to its numerous advantages over normal vibrated concrete (NVC) **Naik *et al.***, (**2012**)a. SCC was invented at the University of Tokyo/Japan in 1988 to tackle the problem associated with the shortage in the skilled labour required for the compaction process of NC **Okamura and Ouchi**, (**1998**). Concrete can be classified as an SCC when it has three fundamental fresh properties: filling ability, passing ability, and resistance to segregation. Filling ability is the ability of concrete to flow into and fill all spaces within the formwork under its own weight. Passing ability, on the other hand, is the ability of concrete to flow through tight openings (e.g. congested reinforcement) without any blocking. Resistance to segregation is the ability of concrete to meet the filling ability and passing ability requirements while maintaining homogeneous mix (hence, no separation of aggregate from the paste, or water from the solids) **Douglas**, (**2004**).

The major advantages of SCC application are as follows **Okrajnov-Bajic *et al.***, (**2009**):

1. There is no need for vibration during placement of fresh concrete into formworks.
2. Placement of concrete is more natural.
3. Placement of fresh concrete achieved is faster and more efficient.
4. Lower noise level on the construction site. Thus, the number of working hours on the construction site can be increased
5. Lower consumption of energy.
6. Lower number of workers required in the construction site.
7. Safer and healthier working environment.
8. High quality of the achieved concrete.
9. Better bond between concrete and steel reinforcement even in congested reinforcement.
10. High quality of concrete surface finish is obtained
11. Improved durability of structures.
12. Reduced cost of maintenance.

Some of the disadvantages of SCC are **Naik *et al.***, (**2012**):

1. Compared with normal concrete. Self-Compacted Concrete has many stringent requirements regarding the selection of materials
2. More accurate measurement and monitoring of the constituent materials. Where the uncontrolled variation of 1% in the moisture content of the fine aggregate could have a much bigger impact on the rheology of SCC.
3. Requires more trial batches at the laboratory as well as at ready mixed concrete plants.
4. It is more cost than normal concrete owing to the use of high volumes of Portland cement and chemical admixtures.
5. Experienced and highly skilled workers are required for the production of SCC
6. The higher amount and rate of shrinkage of SCC compared to normal concrete

1.3 Reinforced Concrete Hollow Beams with an Openings

A box girder bridge is a bridge in which the main beams comprise girders in the shape of a hollow box. Typically, it comprises either pre-stressed concrete, structural steel, or a composite of steel and reinforced concrete of rectangular or trapezoidal in cross-section. Box girder bridge is frequently used for highway flyovers and modern elevated structures of light rail transport. Although the box girder bridge is usually a form of a beam bridge, it may also be used on cable-stayed bridges and other forms. Recently, hollow structural sections have been increasingly used in various construction application. These hollow sections are used for passing electrical and mechanical utilities, as well as reducing the height of the story and the cost of construction. Hollow beams could be appropriately used as ground beams in residential buildings. Furthermore, the use of hollow beams allows other beams to cross on another without the need for relocating these pipes. The presence of web openings in a reinforced concrete beam can definitely reduce the capacity of the beam to carry the load and increase its service-load deflections and crack widths. Rectangular and circular openings are the shapes of the most widespread openings in practice. The need for circular openings comes out through providing passages to pass service pipes, such as electrical pipes while the rectangular openings allow the passing of air-conditioning ducts. Concerning the opening size, the expression “small” and “large” have been used without any clarification or definition by many researchers **Mansur and Hasnat,** (**1979**). **Corley** (**1974**) stated that when the diameter of the circular opening is more than a quarter the web depth, the effect can be considered owing to the reduction in the strength of the beam by introducing of such openings. The author, however, considered that the essence of classifying an opening either small or large lie in the structural response of the beam. When the opening is small enough to maintain the beam-type behaviour or, in other words, if the general beam theory applies, then the opening may be termed as a small opening. On the other hand, large openings are those that prevent beam-type behaviour from developing to frame- type behaviour **Mansur and Wei, (1999**). Two varying modes of failure were identified for small openings: beam failure and frame failure. On the contrary, the beam behaviour transforms into a Vierendeel action for large openings when the size of the openings increases due to the dependence of the beam behaviour on the size of the openings, as illustrated in **Fig. 1.2 Mansur**, (**1998**).

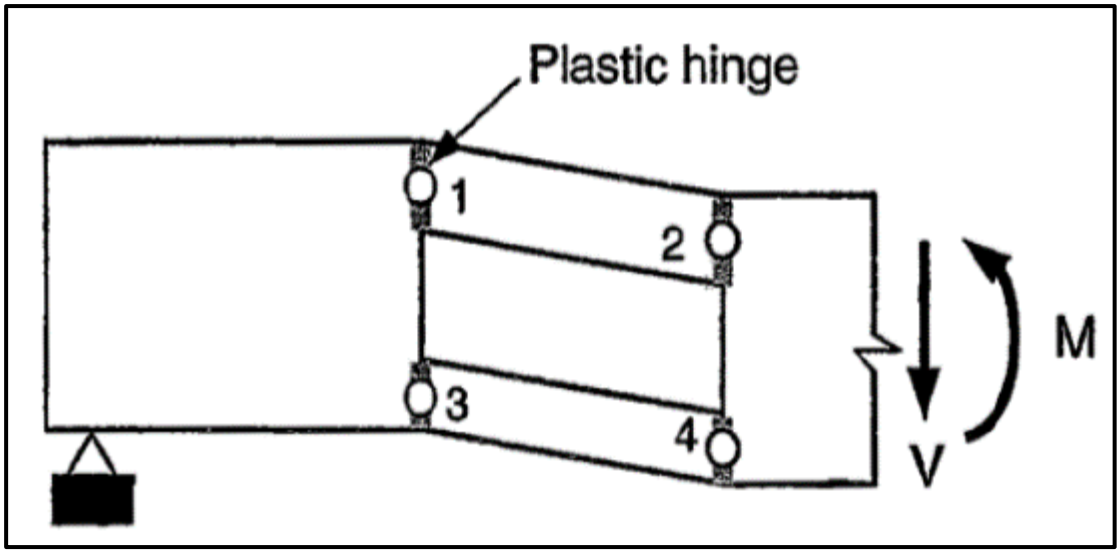

Fig. 1. 1: Large opening (collapses mechanism) (Mansur and Hasnat, (1979)

The following points summarized the effects of introducing an opening on the overall response of a beam:

1. The first load crack decreases as the length and /or the depth of opening increases.
2. The diagonal cracks appear earlier.
3. Unless additional reinforcement is provided to restrict the growth of cracks, the opening corners are liable to exhibit extensive cracking.
4. The increase in the size of opening either by increasing the depth or the length reduces the strength and the stiffness of the beam when using the same amount and scheme of reinforcement. Nevertheless, the opening eccentricity has a slight impact on both stiffness and strength.
5. The chord members below and above the opening conduct in a way identical to the Vierendeel panel chord. The formation of a mechanism with four hinges in the chords caused the final failure, one at each corner of the opening, as shown in **Fig. 1.1.**

1.4 Guidelines for Choosing the Location and Dimensions of the Openings

To simplify the selection of the location and dimensions of the opening, the following points have been suggested, as illustrated in **Fig. 1.2**.

1. Openings are usually located at middle-depth of the section in case of rectangular beams, but they also may be located eccentrically concerning depth. In this case, adequate cover for

concrete should be provided to the chord member reinforcement above and below the opening.

2. The location of the openings should be more than 0.5 of the effective depth of the beam from the supports to avert reinforcement congestion and shear failure in the critical region. Likewise, the location should be not less or equal to half the effective depth (0.5 d) from a concentrated load.
3. The openings depth should not exceed half the effective depth.
4. The length of an opening is limited by two factors: the serviceability requirement of deflection and the chord member's stability, especially the chord of compression.
5. The distance between two adjacent openings should be more than half the effective beam depth when multiple openings are utilized to ensure that each opening behaves alone **Tan and Mansur**, (**1996**).

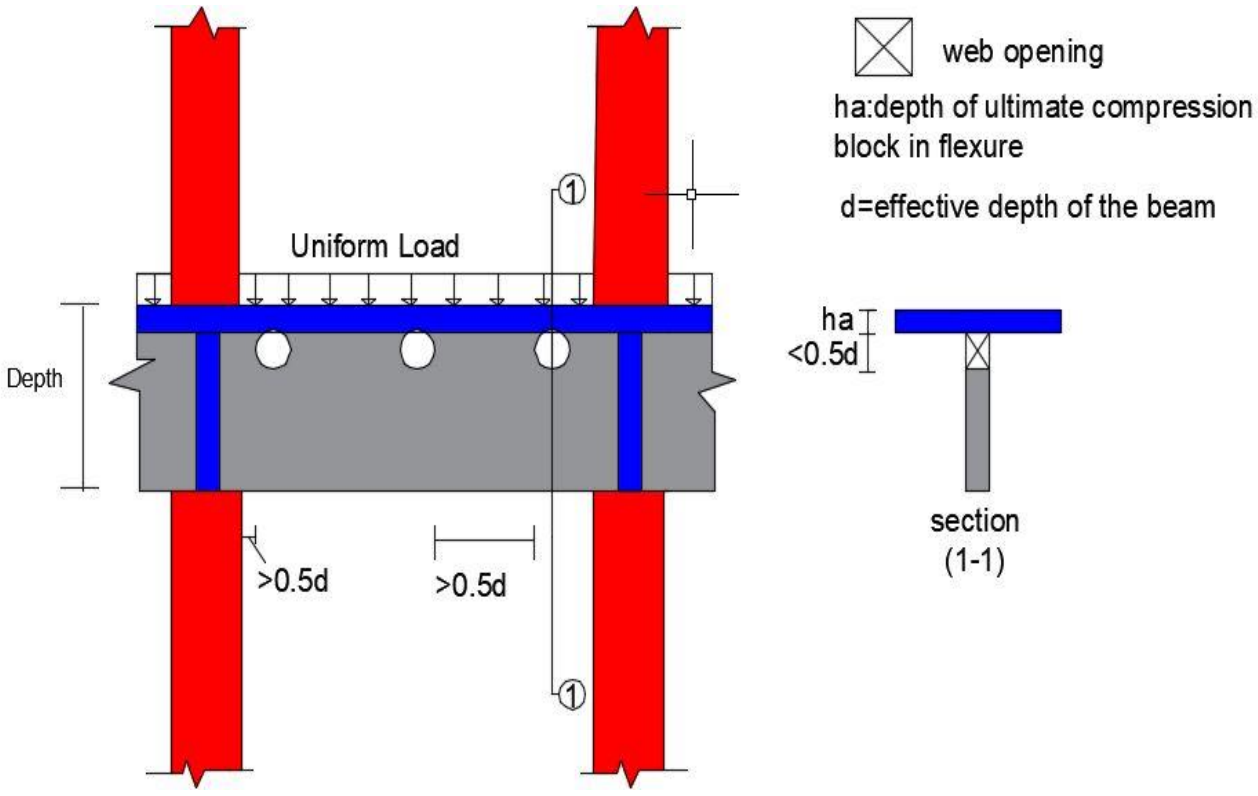

Fig. 1. 2: Web opening location guidelines for straight beam

1.5 Objectives of the Study

The Objectives of this study can be summarized as follows

1. Investigate experimentally the structural behaviour of hollow self-compacting reinforced concrete beams that have an in-place circular opening.
2. Examine the impact of various number and locations of opening (s) on the structural behaviour of hollow self-compacting reinforced concrete beams experimentally.
3. Study experimentally the structural behaviour of hollow self-compacting reinforced concrete beams that have circular in-place openings strengthened by CFRP laminates.
4. Utilize finite element technique to analyze the behaviour of hollow self-compacting concrete beams with an in-place circular opening (s) that are strengthened and unstrengthened by CFRP strips until failure using ABAQUS (2019).

1.6 Layout of Thesis

This thesis involves six chapters that are organized as follows: **Chapter one** provided a general introduction for the common effects and applications of openings in reinforced concrete beams in addition to an introduction about self-compacting concrete as well as its fresh properties and application. The Chapter also covered the guidelines for selecting the size and location of openings. The most previous studies related to the field of the present study were reviewed in **Chapter two**. C**hapter three** devoted to the experimental work, specimens' details, materials properties and test operation**.** The main experimental results and their analyses and discussions **were** presented in **Chapter four. Chapter five** covered the modelling of materials used in the finite element analysis, the nonlinear solution technique, numerical outcomes and the comparing results with the experimental results as well as a parametric study. **Chapter six** drawn the succinct conclusions of the present study and recommendations for future work.

CHAPTER TWO
LITERATURE REVIEW

2.1 Introduction

Beams with an opening are quite often in practice to provide a familiar passage for water supply pipes, ducts, sewage and electrical cables. Generally, the presence of such an opening in the reinforced concrete beam can reduce its load-carrying capacity, increase its service load-deflection, and cracks in the building. Furthermore, the opening's presence can also complicate the normal behaviour of the beams **Hauhnar *et al.***, (**2017**). This chapter will focus on the most useful literature review on the development of self-compacting concrete (SCC), its structural performance, and the behaviour of reinforced SCC beams with and without opening (s) that are strengthened or unstrengthened with CFRP laminates

2.2 Development and Advantages of SCC

For many years, beginning in 1983, the durability problem of concrete structure was of high interest in Japan. The primary reasons for the poor durability of Japanese's structures were the shortage in the numbers of skilled labour resulting in insufficient concrete compaction. One potential solution for achieving durable concrete structures regardless of the quality of construction work was the employment of self-compacting concrete (SCC). Professor Okamura at Kochi University in 1986 proposed the concept of SCC, as an innovative solution to the durability mentioned above problem. SCC can flow into every corner and fill the formwork purely due to its own weight and without the need for vibration compaction **Okamura and Ouchi**, (**2003**). The factors that lead to poor durability can be removed from the process of construction through the development of concrete that consolidate by its own self-weight **Horta**, (**2005**)**.** The low viscosity can be considered as one of the practical advantages of SCC upon NVC that leads to a higher rate of flow.

As a consequence, the required pressure for the pumping machine will be less, the damage in the pumping machine from wearing will be lower, and the cranes needed for delivering concrete at the site job in buckets will be less **Khayat *et al.***, (**1999**). Furthermore, the period of construction can be significantly decreased as well as the men number required to achieve an identical amount of work. Akashi-Kaikyo Bridge building has been considered as the longest suspension span bridge in the world, see **Plate 2.1** regarding SCC use. The bridge was considered as an excellent example, where the two anchorages of the bridge consumed 290,000

m^3 of SCC in casting. As a result, the construction period of the anchorages was reduced by 20% **Okamura and Ouchi**, (**2003**).

Plate 2. 1: The Bridge of Akashi-Kaikyo Okamura and Ouchi, (**2003**)

SCC stands as a strong competitor for designers and contractors in particular problems, such as the casting elements with complicated shapes, congested reinforcement or hard access areas. As SCC does not require any outside or inside vibration, while casting to achieve proper consolidation, it is known as a "healthy" and "silent" concrete. The decrease or full disposal of the vibration process can assist in diminishing the environmental effect because the mechanical vibration is considered as a noisy job for the casting's members participating in the process of construction and the neighbours surrounding **Walraven**, (**2003**). Nevertheless, the production of SCC has a complicated aspect in which it has to be designed based on the performance of the required specification, production practices and obtainable materials **Horta**, (**2005**).

2.2 Structural Performance of SCC

In this section, a summary of the available studies related to the structural behaviour of reinforced SCC is presented. Most previous literature was directed towards the mix

proportioning and characterization of the fresh and hardened properties of SCC, with limited information on its structural performance (**Okamura *et al.*, 199; Okamura *et al.*, 2003; Khayat, 1998; Khayat *et al.*, 2003; Huang, 2005**). Furthermore, the lack of data concerning the structural properties of sections cast with SCC considered as one of the obstructions to the spread acceptance of SCC **Sharifi**, (**2012**).

Luo, (**2005**) examined the behaviour of reinforced beams cast with SCC in flexural and shear**.** The experimental program consisted of four NVC beams and eight corresponding SCC beams. Experimental work investigated the beams' cracking loads, shear and flexural capacities, as well as the failure modes. When testing beams under vertical load, no apparent variations were observed between the behaviour of SCC and NVC beams in terms of flexural or shear failure process. Furthermore, the yielding load of SCC beams was very close to that of NVC beams except for higher ultimate loads of the former beams for similar strength and longitudinal reinforcing amount. The load of the crack in SCC beams was slightly lower than that of NVC beams, and the capacity of shearing was almost identical.

de Corte and Boel, (**2010**) studied the flexural resistance and cracking of reinforced SCC and NVC beams having varying reinforcement ratios, comparable compressive strength and identical maximum nominal size of coarse aggregate. Six reinforced concrete beams with dimensions of 2400 mm in length, 150 mm in width, and 200 mm in depth were tested under static and dynamic tests. The beams, which are tested under a two-point load, were simply supported with a span length of 2000 mm. The maximum failure loads for NVC and SCC beams were almost identical (the differences were within 5%). It is worth to mention that the crack width evolution in the SCC beams was slower in comparison with NVC beams.

Lin and Chen, (**2012**) conducted an experimental investigation to study the shear behaviour of two types of SCC beams. The first type (SCC1) contained a higher amount of coarse aggregate, whereas the second one (SCC2) contained a lower amount of coarse aggregate. Twenty-four beams were tested. Eight beams were prepared using normal vibrated concrete (NVC), while the remaining beams were prepared by using the two types of SCC. The studied parameters included the concrete strength, shear span-depth ratio (a/d), the spacing of shear reinforcement, and strength of shear reinforcement. The results showed that SCC1 beams have higher diagonal cracking and ultimate strengths than NVC beams, whereas SCC2 beams recorded lower strengths when compared with NVC beams. The diagonal cracking and ultimate strengths predicted by ACI 318-08 were conservative for this study. The overall performance of SCC1 beams was better than or as good as NVC beams, whereas SCC2 beams had inferior structural performance than NVC beams in many aspects.

Ra'id *et al.*, (**2016**) investigated the torsional behaviour of reinforced SCC beams with variables including, the spacing of transverse reinforcement, concrete compressive strength, hollow and solid sections experimentally. The experimental work investigated eleven beams that are tested under pure torsion and divided into three groups of various compressive strengths. The results stated that the cracking torque of the hollow SCC beams with longitudinal reinforcement and stirrups were higher than that of the corresponding normal SCC beams. On the other hand, the ultimate torques were slightly higher than those of the corresponding solid normal strength beams or slightly smaller than the ultimate torque of corresponding solid SCC beams.

Keflegen, (**2018**) investigated the structural performance of congested reinforcement beams cast using SCC and NVC. The beams, which had the same stirrup geometry for all specimens, were of different geometric cross-sections, length, and longitudinal reinforcement ratios. Six beams were tested throughout the whole experimental investigation (4 were cast with SCC, and 2 were cast with NVC). The test results showed that SCC beams performed better in reinforcement congested beam element than the NVC beams. It has also been concluded that the difference in mix composition for casting SCC and NVC had no significant effect on the load-deflection response of beams prior yielding. In the process of failure under vertical load, SCC beams sustained for a longer time than NVC beams.

2.3 RC Beams with Openings

Several researchers have implemented numerous experimental and analytical studies on reinforced concrete beams with openings. **Mansur *et al.***, (**1999**) studied the effects of creating an opening in existing beams in which nine T-beams were fabricated with circular openings through the web, and they were tested to failure. The location and the size of openings were the most significant parameters considered in this research. The results showed that creating an opening near the support region decreased the stiffness and the strength of the beam significantly and led to an early diagonal cracking.

The effect of small circular openings on shear, flexural and ultimate strength of beams made by regular and high strength concrete was examined by **Amiri J V**, (**2004**). The main factors in his study were the opening diameter, position, reinforcement location and type around openings as well as the concrete strength. In this investigation, nine and five beams were prepared using NVC and high strength concrete, respectively in which the testing beams been loaded as a simple beam with two concentrated and symmetrical load. For the beams made

from NVC, it was concluded that when the diameter of opening exceeded 0.33 times the beam depth, the reduction in the ultimate strength increased and the beam mode failure were changed. Furthermore, in beams made from high strength concrete, the most critical location of the opening to reach the ultimate strength was near support. Besides, the middle shear span was the optimal location in these beams.

By utilizing a three-dimensional finite element model, the behaviour of RC beams with large transverse openings undergo to flexure was studied by **Al-Shaarbaf *et al.***, (**2007**). In this study, the impact of various parameters and some essential finite elements on the response of the load-deflection various parameters were considered such as the concrete compressive strength, the amount of the longitudinal tensile reinforcement and the opening size. Generally, a good match was obtained between the experimental and theoretical results. Besides that, the increase in the compressive strength and the amount of the bottom steel reinforcement led to an increase in the post-cracking stiffness and ultimate load obtained from the finite element model. Moreover, they decreased with the increase in the opening depth and length.

Alsaeq (2013) reviewed the impacts of location and shape of openings on the structural behaviour of RC deep beam. The ultimate strength obtained by ANSYS 12.1, for RC deep beam with opening, exhibited an excellent match with the experimental results with a divergence by only 20% . It was also obtained that the strength can be doubled if the location of the opening was near the deep beam upper corners. Moreover, up to 40% of deep beam structural strength could be saved when utilizing a small rectangular opening with the long sides in the horizontal direction.

Aykac et al. (2014) investigated the flexural behaviour and strength of reinforced concrete beams with multiple transverse openings**.** Ten rectangular reinforced concrete beams with and without multiple web openings were used in that study. The opening geometry, the use of longitudinal stirrups in the posts between the openings, the use of diagonal reinforcement around openings, and the longitudinal reinforcement ratio on the flexural behaviour of RC beams with openings were investigated (**Plate 2.2)**. The result revealed that the stirrups in the posts were shown to have a significant contribution to the ductility of the RC beams with openings if no diagonal reinforcement was used. For the same reinforcement details, RC beams with circular openings were found to have higher load capacities and ductility than those with rectangular openings. Besides, the experiments indicated that the posts between the openings

need to be prevented from undergoing shear failure to avoid Vierendeel truss action and allow the beam to develop its ductility and bending capacity.

Plate 2. 2: Diagonal reinforcement spiralling around circular openings (Aykac *et al.*, (2014)

Al-sheikh, (**2014**) studied the behaviour of RC beam with various shapes of openings with varying diameters at different locations that were unstrengthened by additional reinforcement. The experimental study consisted of casting 27 beams; one beam was without an opening as a control beam, and the remaining beams were prepared with an opening (s). All beams were tested under two points load. The effect of various parameters was studied in terms of ultimate failure load, maximum deflection and failure mode. From the test results, it was concluded that providing an opening in beam could develop cracks around the opening due to the stress concentration. Moreover, the ultimate load-carrying capacity of the RC beam with an opening at the shear span recorded as the lowest against the highest in the flexure zone. The ultimate failure load in beams with a rectangular opening was lower by 4% than beams with a square opening. Meanwhile, the ultimate failure load in beams with a circular opening was higher by 8% than beams with square opening.

Al-bayati, (**2017**) conducted a study on the structural behaviour of SCC deep beams containing openings. Eleven simple-span reinforced SCC deep beams were tested under symmetrically two points load. The investigated variables involved the shear span to the effective ratio (a/d), the sizes and locations of opening (s), and the amount of inclined reinforcement around the openings. The test results showed that the existence of an opening at the centre of the shear span has significantly affected the behaviour of the tested beams regardless of the investigated a/d ratio and size. Furthermore, it was found a/d ratio has influenced the behaviour of the tested beams as increasing the a/d ratio from 0.8 to 1.2 led to a decrease in the failure load by nearly 23%. The results also showed that increasing the opening

diameter from 75 to 160 mm caused drops in the shear cracking and failure loads by nearly 33 and 29 %, respectively.

Jabbar et al. (2016) examined the behaviour of RC hollow beam with and without an opening by utilizing FEM. The hollow beam with an opening was modelled and analysed under loading of flexural with high-strength and ultra-high strength concrete materials. The authors used the same hollow beam section presented in the study of **Lopes and Bernardo (2009)** as a reference to evaluate the impact of an opening on the beam behaviour subjected to loads (**Fig. 2.1)**. Flexural loading results showed that the hollow beam without opening (s) suffered from reductions by 24% and 42% in the ultimate loads of concrete with high-strength and ultra-high strength, respectively if compared with solid beams. Furthermore, the beams capacity for flexural loading decreased effectively by the opening (s) in the hollow beams. Moreover, the specimen with a square opening side of 16.6% from the height of the hollow specimen with 100 mm circular opening responded almost similarly with the hollow beam without an opening. Furthermore, for the hallow beams with openings depth (100 and 200 mm), the load-carrying capacity decreased up to up to 30% and 49%, respectively.

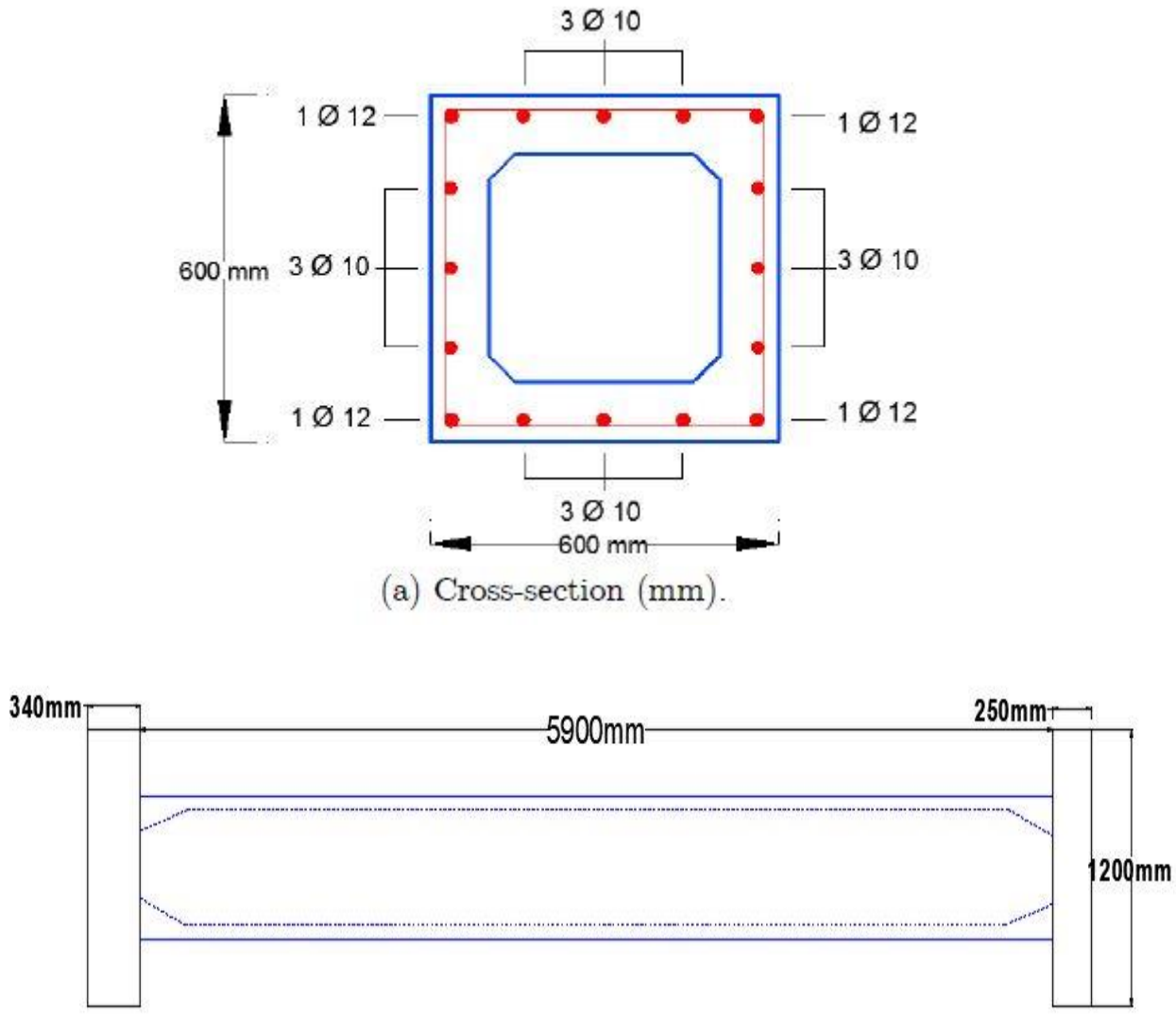

Fig. 2. 1: Reference RC beam used by Lopes and Bernardo, (2009)

Aziz, (**2016**) discussed the structural behaviour of reinforced concrete rectangular beams having a transverse opening in the web under the effect of single point loading. In this paper, the location of the openings was the primary variable adopted in his study (**Fig. 2.2)**. The experimental part included testing four beams with a dimension of (100×150×750 mm) with various locations of openings. The experimental results indicated that the ultimate strengths decreased by a ratio of 12%, 22% and 41% for beams containing opening at a distance (L/2), (L/3) and (L/6) from the edge, respectively. Moreover, the change in the locations of the openings from the centre toward the edge has led to a reduction in the carrying capacity by nearly 29%.To sum up, moving the location of the web opening toward the edges (supports) decreased the ultimate shear strength. In all tested beams, the crack path forced to pass through the weak locations (locations of openings), which is the reason behind adding individual details at these locations in the design.

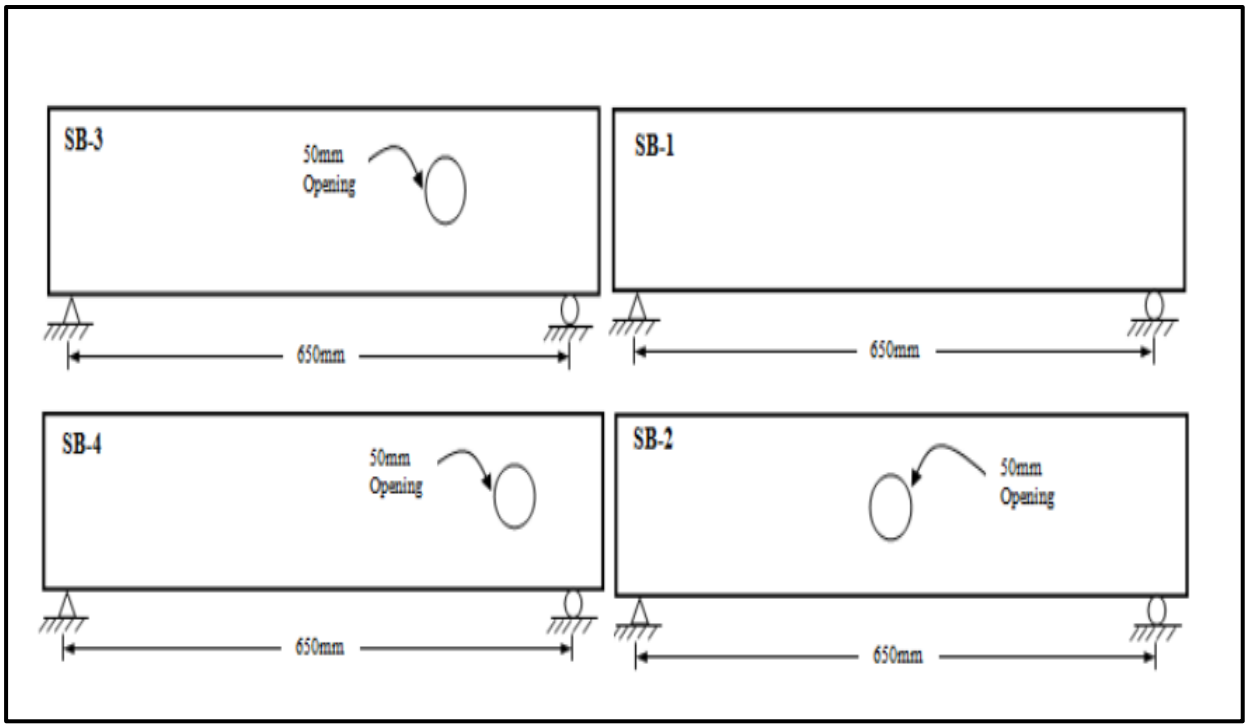

Fig. 2. 2: Location of openings in beams (Aziz, (2016)

To investigate and analyse the behaviour of high-strength Reinforced self –compacted concrete SCC (RSCC) deep beams with web opening, sixty-one deep beams were made by **Hassan et al., (2019).** The significant parameters were: the size of openings (50 mm and 75 mm), the shape of opening (circular, rhombus and square), openings location concerning the neutral axis and with respect to the load path (in the web centre, symmetrical and unsymmetrical openings). The test results indicated that the decreases in the cracking and

ultimate loads of the deep beam with web opening ranged between 5 to 55 % if compared with deep beam without opening. Besides, the shear failure was the primary mode of failure for all tested high-strength RSCC deep beams with web opening. Furthermore, the cracking and ultimate loads decreased owing to the increases in the size of the web opening as well as the overall ductility of the deep beam.

2.4 Strengthening of Openings in RC Beams

The effects of openings in beams can cause a decrease in the ultimate strength, a reduction in the stiffness and a tremendous deflection response. Therefore, to incorporate openings in RC beams either in the pre-design and construction stage or in the existing beams, an appropriate strengthening option is vital. In this section, the most relevant literature review of different strengthening methods for beams with various openings was reviewed.

Pimanmas (2010) studied the effectiveness of fibre-reinforced polymer (FRP) rods technique in strengthening RC beams with openings. Thirteen beams with circular and square openings have been tested, and two patterns of strengthening by FRP rods were investigated. The first pattern of strengthening was to place FRP rods enclosing to the opening, while the other was to place FRP rods diagonally throughout the entire depth of the beam in addition to internal strengthening by steel bars (**Fig. 2.3)**. Test result indicated that the strengthening by placing FRP rods with partial lengths was not fully effective, and the original performance cannot be reinstated. The diagonal crack was shown to be able to divert its propagation path to circumvent the FRP rod, which led to shear failure. When FRP rods are placed diagonally to the beam's axis alongside the opening throughout the entire beam's depth, the original performance was almost recovered. Furthermore, the essential behaviour of beams with circular and square openings was the same, except that the square opening tends to yield lower performance compared with the circular one.

The strengthening of reinforced concrete beams with a large square and circular openings positioned at the flexure zone by carbon fibre reinforced polymer (CFRP) sheets were examined by **Chin et al., (2011)**. The experimental program contained five specimens that were tested under four-point loading up to failure. The investigation included studying the structural behaviour in terms of crack patterns, failure mode, failure load, and the load-deflection response. The result showed that the large square opening caused a higher reduction in the structural capacity compared to the circular opening of the same size. Furthermore, the inclusion of a large square opening in the RC beam decreased the beam strength and stiffness

significantly by 19% and 48%, respectively. Using CFRP laminates for strengthening beams with a large circular opening at the mid-span could remarkably restore the beam original structural capacity. In contrast, an increase of 10% in the flexural strength was observed in the beam with a sizeable square opening. Moreover, the stiffness of strengthened beam with large circular and square openings has been increased by 33% and 17%, respectively when compared with the unstrengthened beams.

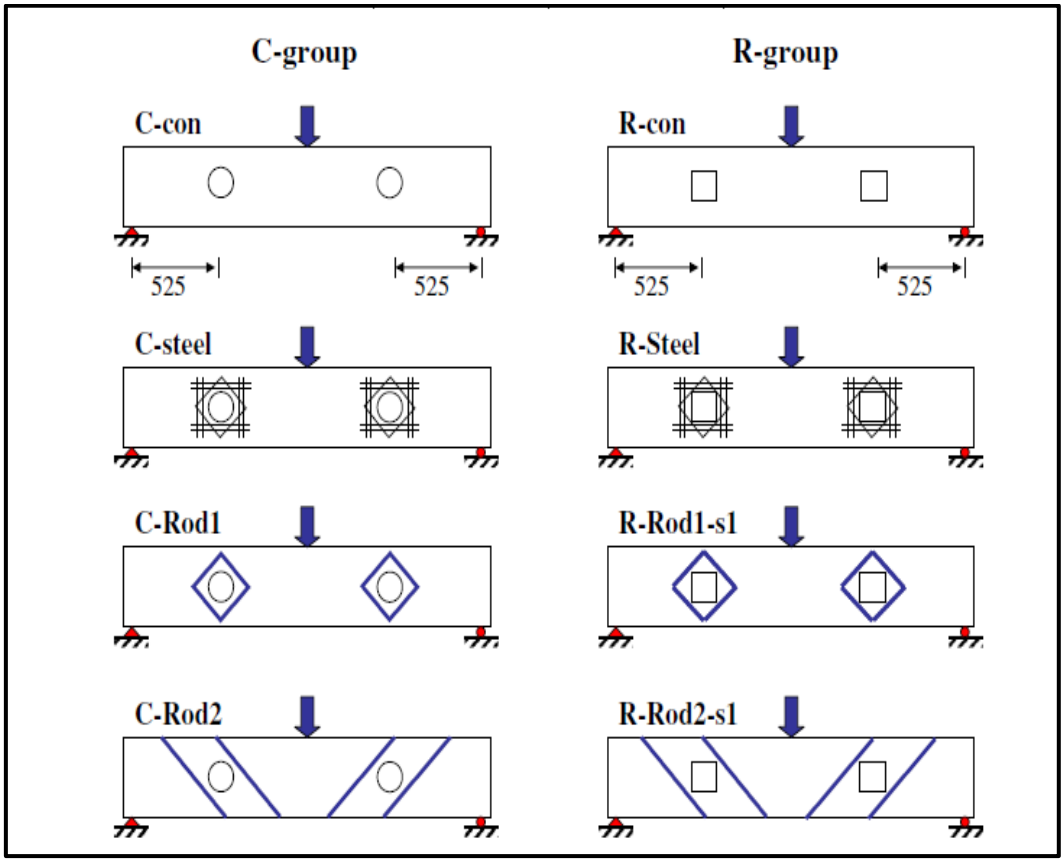

Fig. 2. 3: Specimens group of strengthening beams tested by Pimanmas, (2010)

Allam (2012) conducted a study to investigate the effect of strengthening RC beams with openings by carbon fibre reinforced polymer (CFRP). To validate the laboratory test results of six reinforced concrete beams, two-dimensional nonlinear FEA were utilized. All beams had the same rectangular cross-section geometry, and they were loaded under four-point bending. Test results showed that the simulation was capable of predicting the crack pattern and load-deflection relationship of beams. Moreover, the predicted crack pattern in FEA showed a good agreement with the crack pattern of the experimental beams, as shown in **Plate 2.3**. Meanwhile, the mid-span load-deflection curves of the finite element models exhibited a stiffer result compared to the experimental beams, owing to the assumption of the ideal bond utilized between the steel reinforcement and concrete.

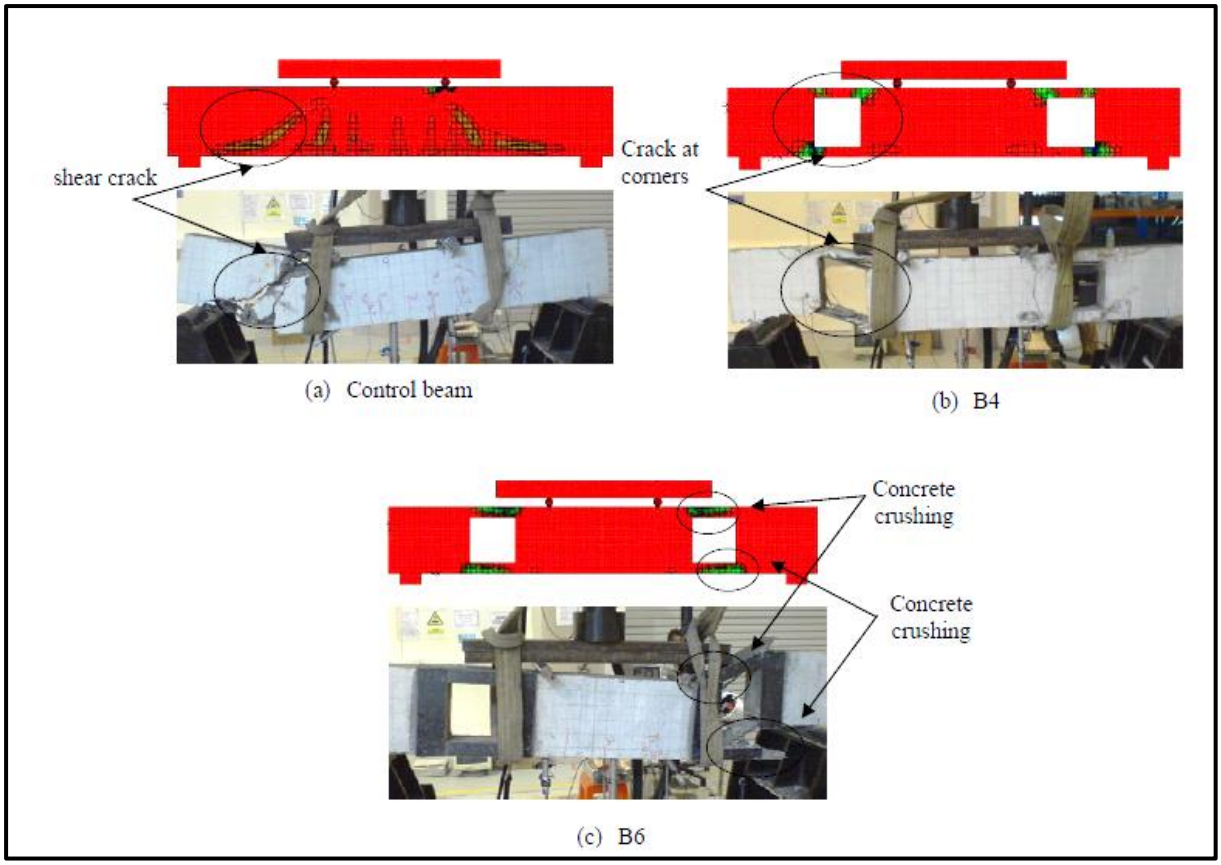

Plate 2. 3: Comparison between principal strain from FEM analysis and crack pattern from experiments Allam, (2012)

Hemzah (2014) investigated the behaviour of horizontally curved ring beams with and without openings that are non-strengthened and externally strengthened by CFRP sheets or internally by steel reinforcement. Four RC ring beams were fabricated and tested. The experimental variables that are considered in the test program included: the presence of opening, internal strengthening at the opening by reinforcing steel (stirrups), and external strengthening (confinement) by CFRP laminates for openings. The beams were tested under the action of four-point loading at the top face of mid-spans with four supports at the bottom face of the beams. Creating an opening in a circular beam near the utilized load led to a reduction in the capacity of the ultimate load by nearly 50% in comparison with the control specimen. In addition to that, the capacity of the ultimate load improved by 60% concerning the internal strengthening of the opening zone. Furthermore, the capacity of the ultimate load increased by about 75% when using CFRP sheets as external strengthening in beams with an opening near the utilized load. Moreover, the mode of failure changed from beam-type to frame-type failure when utilizing internal strengthening, while the failure mode retains to beam type failure when utilizing CFRP sheets.

The external prestressing technique for the strengthening of RC beams with an opening in the shear zone was used by **Atta and Khalil (2014)**. For that purpose, two unstrengthened and five strengthened rectangular beams with openings in the shear zone were experimentally tested. Reference specimens without opening were tested in which the details of the external prestressing bars location are illustrated in **Fig. 2.4**. The distribution impacts, shape and dimensions of the opening on the response of the deflection, patterns of crack, failure mode, ultimate loads and strains of steel were investigated. The strengthening technique by exterior prestressing was very functional in increasing the capacity of the shear load as the test results revealed, particularly for beams with rectangular and circular openings (the ratio of the opening height to the shear span length is not more than 0.2). External post-tensioning utilizing for shear domain strengthening of specimens with a circular opening decreased the shear cracks appearance and varied the failure mode to flexural failure, as shown in **Plate 2.4.**

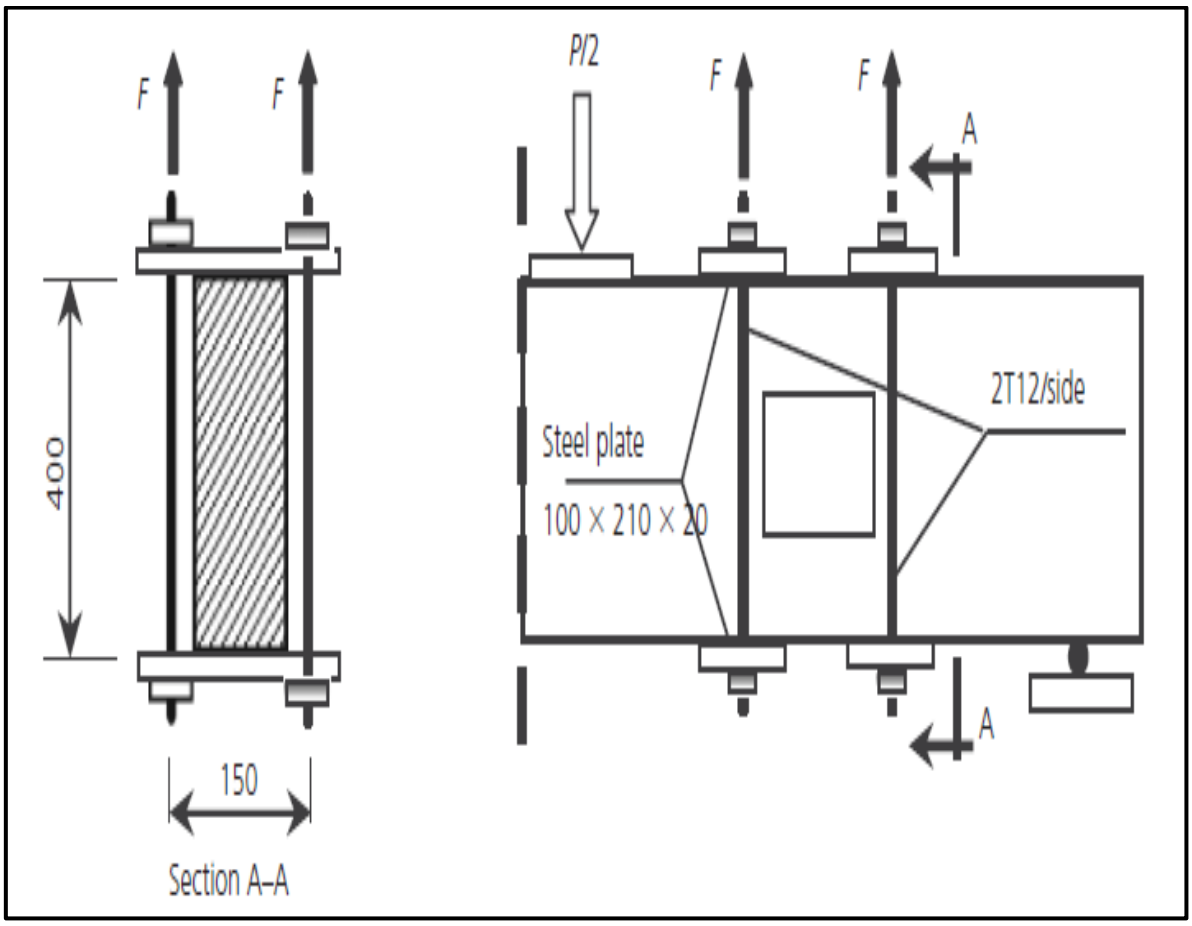

Fig. 2. 4: External prestressing bars location detail used by Atta and Khalil, (2014) (all dimensions in mm)

Plate 2. 4: Failure mode conversion from shear to flexural due to the use of external post-tensioning strengthen for beams tested by Atta and Khalil, (2014)

The flexure behaviour of beams with openings was examined under two-point load by **Kudatini (2016)** in which three types of beams with dimensions of (200 × 150 ×1700) mm were prepared. One beam was solid, and the other two beams had a transverse rectangular opening. One beam with a transverse opening was strengthened internally by addition of other four numbers of 8 mm diameter. The test result demonstrated that the ultimate strength of the unstrengthened beam decreased significantly by 8.9% compared with the solid beam. Furthermore, the load-carrying capacity of the beam with an opening that internally strengthened increased by 11.2% compared with the solid beam. Moreover, the ultimate load of the internally strengthened beam with opening increased by 22% compared with an unstrengthened beam with the opening.

Garg *et al.*, (**2017**) used lightweight FRP sheets (glass and aramid fibre sheets) for a strengthening purpose of beams with a circular opening. Fourteen beams were prepared within the experimental program in which twelve beams were strengthened by glass and aramid fibre sheets to examine the energy absorption flexural and ductility of the tested specimens. From the results, it has been concluded that utilizing both glass and aramid fibre sheets within and around the opening for strengthening increased the beams' ultimate load significantly. Moreover, the aramid fibre sheets acted better than the glass fibre sheets as the increase percentage in the ultimate load was 30% and 25%, respectively. **Plate 2.5 showed** the wrapping of aramid fibre sheets on the surface and inside the opening.

Plate 2. 5: Aramid fibre reinforced sheets wrapped around the opening of the tested beam used in the study of Garg *et al.*, (2017)

A detailed investigation was conducted by **Chin *et al.***, (**2016**) to examine the behaviour of RC beams with large openings externally confined by CFRP sheets. The experimental work included testing, under four-point load four beams with openings and two beams without. Besides, there was a massive opening located at the mid-span for each beam. The parameters used in this study were the dimension and shape of the opening as well as CFRP sheets strengthening configuration. The study was carried out experimentally and theoretically by utilizing FEA. The result of including a large opening at the mid-span showed a reduction in the beam capacity by half. FEA was used to analyze the effect of strengthening the openings

with the selected configurations. The results revealed that 80 to 90% of the lost capacity could be restored. The strengthening options from the FEA were verified using experimental testing, and almost similar results were obtained.

In a conducted study by **Nie *et al.***, (**2018**), eight reinforced concrete beams were tested under one point loading until failure. The experimental program included testing two solid beams without openings (T-section and rectangular section beams) and six T-section beams with a rectangular single web opening in the shear zone. From the six T-beams with openings, two specimens were not strengthened, and the remaining beams strengthened externally by CFRP laminates. Creating an opening in the web could effectively reduce the flexural capacity of the T-beam as revealed from the results. Furthermore, the strengthening system using CFRP laminates was required to avoid the failure in shear, and web chord confinement to guarantee a ductile response.

Congestion the service pipes in one place could produce several shortcomings. Thus, it is vital to use the longitudinal and transverse opening in beams, as shown in **Plate 2.6**, which can be considered as a creative solution to serve those pipes. **Abtan and AbdulJabbar**, (**2018**) conducted a study to investigate the behaviour of beams casting by using an SCC with longitudinal and transverse holes strengthened by CFRP laminates. The specimens comprised of testing thirteen RC beams divided into three groups. The first group had two hollow RC beams in addition to a solid one. The second and third groups consisted had five RC beams in each group that are strengthened or unstrengthened by CFRP, respectively, as shown in **Plate 2.7**. All beams were identical in geometry and reinforcement details but had a different location of web opening that arranged symmetrically without any special reinforcement around the openings. The result showed that the strengthening by CFRP enhanced the beam resistance by almost 29% due to the function of cracking delay. Moreover, the smallest value of the load capacity was observed in the strengthened beam with openings in the middle shear span and the beam centre, while the highest recorded value was in the strengthened beam with openings located near the supports, which considered as the optimum strengthening.

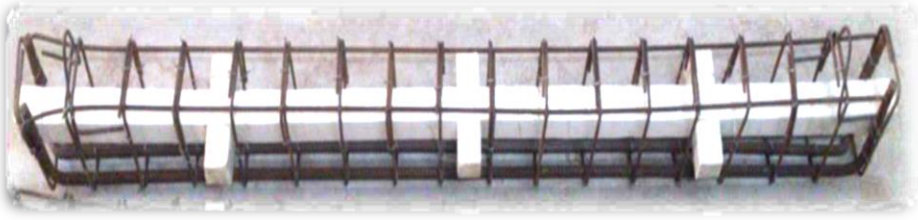

Plate 2. 6: Reinforcing Steel Cage Connected with Opening Molds Abtan and AbdulJabbar, (2018)

Plate 2. 7: Strengthening by CFRP at the Web Opening for Beams Tested by Abtan and AbdulJabbar, (2019)

Several strengthen techniques were investigated by **Elsepahy**, (**2018**) on the effect of creating an opening in RC beams prior and after casting by utilizing various reinforcement techniques (steel angles, mesh wire, beams reinforcement around the opening, straps of steel and system of stirrups), as shown in **Plate 2.8.** Thirteen rectangular RC beam specimens, subjected to two-point load were tested. The test results revealed that strengthening RC beams with openings could enhance the serviceability of beams and increase their stiffness. The strengthening of beams before casting by utilizing 4 stirrups as a rectangular shape with 8 mm diameter and 8 mm rods of steel was the more straightforward and best active technique.

Plate 2. 8: Different Strengthening techniques for RC Beams with Openings Elsepahy, (2018)

2.5 Summary and Remarks

The structural performance of self-compacting concrete from the above literature can be summarized by the following:

1. SCC performed structurally better than NVC in beams with congested reinforcement and complex frameworks.
2. The mix composition difference between SCC and NVC had no significant effect on the load-deflection response of beam before yielding.
3. In the process of flexural failure or shear failure under vertical load, there were no apparent differences between the behaviour of SCC and NVC beams.
4. For identical concrete strength and longitudinal bars rate, the yielding load of SCC beams was close to that of NVC beams, whereas the ultimate load of the former was higher. Besides, the shearing capacity was almost the same, and the crack load of SCC beams was slightly lower than that of the NVC beams.
5. Several numerical and experimental research have been implemented concerning the behaviour of various concrete beams with an opening (s). The majority of these studies dealt with simply supported beams, T-beams, deep beams, and horizontally curved beams with openings before and after casting.

Besides, various strengthening techniques were utilized for beams, as reported in the above, and the main findings can be summarized as follows:

1. The existence of an opening on the web led to a reduction in both cracking and ultimate load, as well as the post cracking stiffness of beams. Unless additional reinforcement provided to restrict the growth of cracks, the opening corners were liable to exhibit extensive cracking.
2. The increase in the opening size either by increasing the length or the depth of opening can decrease the strength as well as stiffness of the beam.

3. RC beams with circular openings were found to have higher load capacities and ductility's than beams with rectangular openings.
4. Specifying opening type whether it was small or large relied mainly on the structural response type of the specimen.
5. There were numerous strengthening techniques in the literature, and almost all the research showed that applying CFRP sheets around the opening was the most effective strengthening technique, which can generally reduce the beam deflection, control the cracks, increase the ultimate load capacity and change the beam mode failure.

Based on the literature review mentioned above, there was a lack in studies that used SCC hollow beams with an in-place circular opening, which will be under focus in the study. Moreover, the present work enriches the knowledge of the overall behaviour of SCC reinforced hollow concrete beams with and without in-place circular opening, strengthened and unstrengthened by external CFRP laminates. The work will be implemented experimentally and numerically using a three-dimensional finite element method (ABAQUS /CAE 2019).

CHAPTER THREE
EXPERIMENTAL WORK

3.1 Introduction

An experimental investigation is carried out in this study to investigate the structural behaviour of fourteen SCC reinforced hollow beams with and without in-place opening, strengthened and non-strengthened by CFRP strips under the effect of two-point load. In this chapter, the experimental work, which explains the primary variable, such as the location of the opening and the presence of external strengthening by CFRP laminates around the opening, will be described first. Then, the details of casting the specimens, the properties of steel reinforcement and concrete and the standard tests will be presented. Furthermore, the installation of CFRP strips, measuring tools and method of testing will be presented.

3.2 Specimens Description

The experimental work comprises casting fourteen SCC hollow reinforced beams; twelve of them were with drilled opening, and the remaining two beams were provided without opening (one for checking the test procedure and the other as a reference beam). The considered opening (s) were circular in shape, which can be easily created in an existing beam without affecting the integrity of the surrounding concrete by using a coring machine. All specimens have identical dimensions of (300 mm ×300 mm × 1500 mm) for width, height and length, respectively. A 100 mm was left from each end of all beams as a substantial part to avoid the crushing of the support. The flexural and shear reinforcement was designed based on the ACI design equation since the solid and the hollow reinforced concrete beams can be directly designed according to **(ACI 318-2014)**. The reinforcement details were the same for all beams (given in Appendix A). Each beam was reinforced by 2 Ø 10 mm bars at the top and 2 Ø 12 mm at the bottom, while the transverse reinforcement consists of Ø 10 @90 mm as stirrups at the edge quarters and Ø 10 @ 110 mm stirrups at the middle quarters, as shown in **Fig. 3.1**.

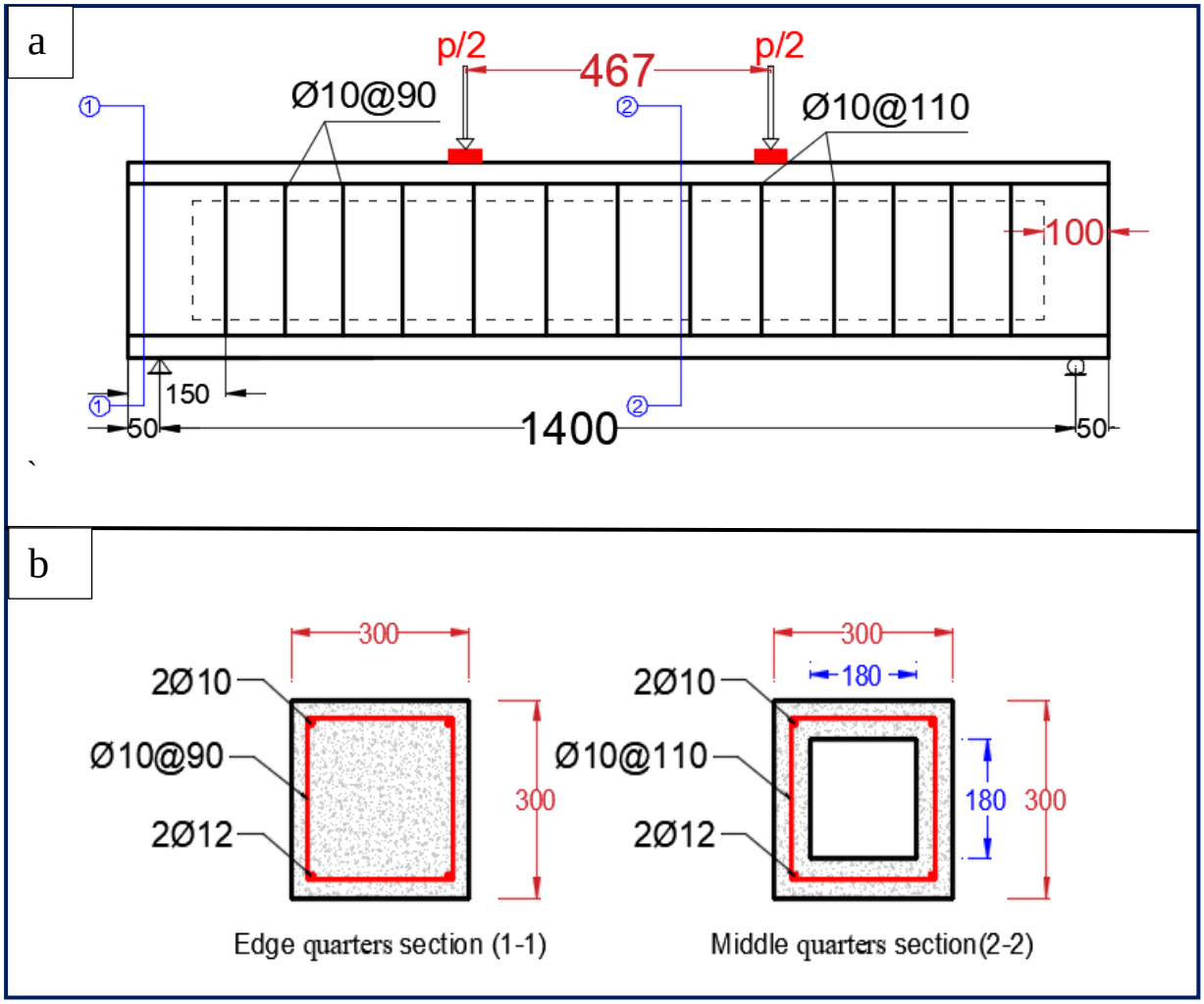

Fig. 3. 1: Reinforcement details for all the hollow beams (All dimensions in mm)
(a) Longitudinal view (b) Cross-section and reinforcement

It is worth to mention that each sample designed of a manner to refer to the type of the section (H= Hollow), (C=Control), the diameter of the opening (100 mm), and the location of the opening (S=near the support, M=middle of the beam). Besides, in case of opening's existence, in the front or the front and rear face of the beam (F=front, R=rear), or the bottom of the beam (B=bottom). For illustration, the H10SF specimen is a hollow beam with a 100mm diameter opening near the support in the front face of the beam. All beams' descriptions and details are shown in **Table 3.1**. The experimental specimens are divided into three groups according to the location of the opening, and the technique for strengthening.

Table 3. 1: Specimens description

Number of Group	Beam symbol	Number and Location of Openings	External CFRP Strips around Opening
	HC	-----	-----
Group 1	H10SF	Two symmetric openings at (250mm) from the support	-----
	H10MF	One opening at the middle of the web	-----
	H10SMF	Three openings: two symmetric at (250mm)from the support and the third one at the middle of the web	-----
	H10SFR	Two symmetric openings at (250mm) from the support	-----
	H10MFR	One opening at the middle of the web	-----
	H10SMFR	Three openings: two symmetric at (250mm) from the support and the third one in the middle	-----
Group 2	H10SB	Two symmetric openings at (250mm) from the support	-----
	H10MB	One opening at the middle of the bottom flange	-----
	H10SMB	Three openings two of them symmetric at (250mm) from the support and the third one in the middle	-----
Group 3	H10SFR-CFRP	Two symmetric openings at (250mm) from the support	2 vertical of 100mm width on each side
	H10MFR-CFRP	One opening at the middle of the web	2 vertical of 100mm width on each side
	H10SMFR-CFRP	Three openings two of them symmetric at (250mm) from the support and the third one in the middle	2 vertical of 100mm width on each side

3.2.1 Beams with Circular Opening in the Front and Rear (Group 1)

The first group contains six beams with a circular opening in the front or front and rear of the beams with a different combination for the opening location. The opening location was determined to be more than half the effective depth of the beam (0.5d) form the support, according to **Mansur *et al.***, (**1992**). For symmetry, one identical opening was created on each side of the beams, as shown in **Fig. 3.2**.

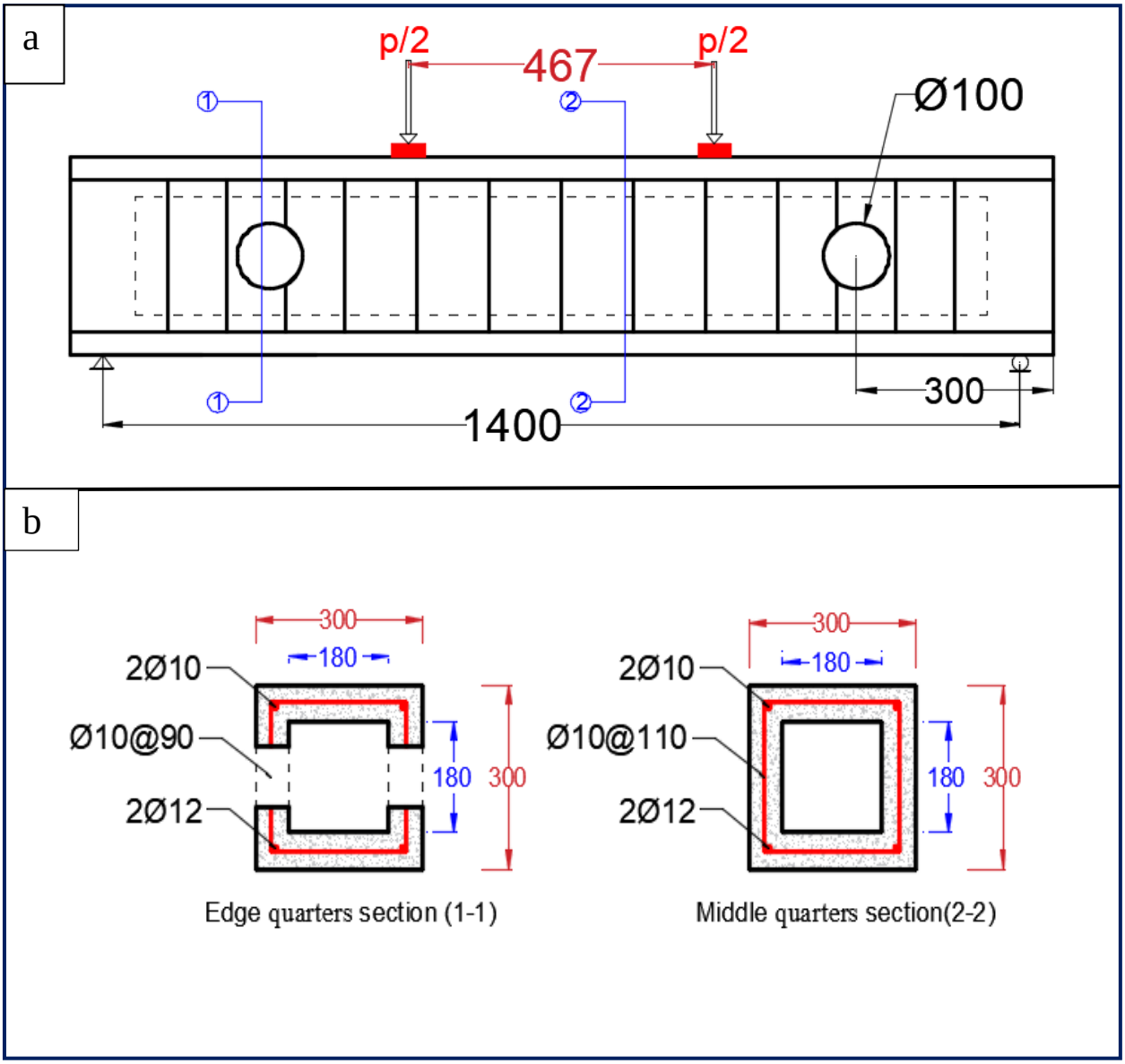

Fig. 3. 2: Reinforcement details for the beam H10SF (All dimensions in mm)
(a) Longitudinal view (b) Cross-section and reinforcement

3.2.2 Beams with Circular Opening in the Bottom Flange (Group 2)

The second group includes three beams with a circular opening in the bottom flange of the beams with a different combination for the opening location. According to **Mansur *et al.***, (**1992**), the opening location was determined to be more than half the effective depth of the beam (0.5d) form the support. One identical opening was created on each side of the beams for the symmetry, as shown in **Fig. 3.3.**

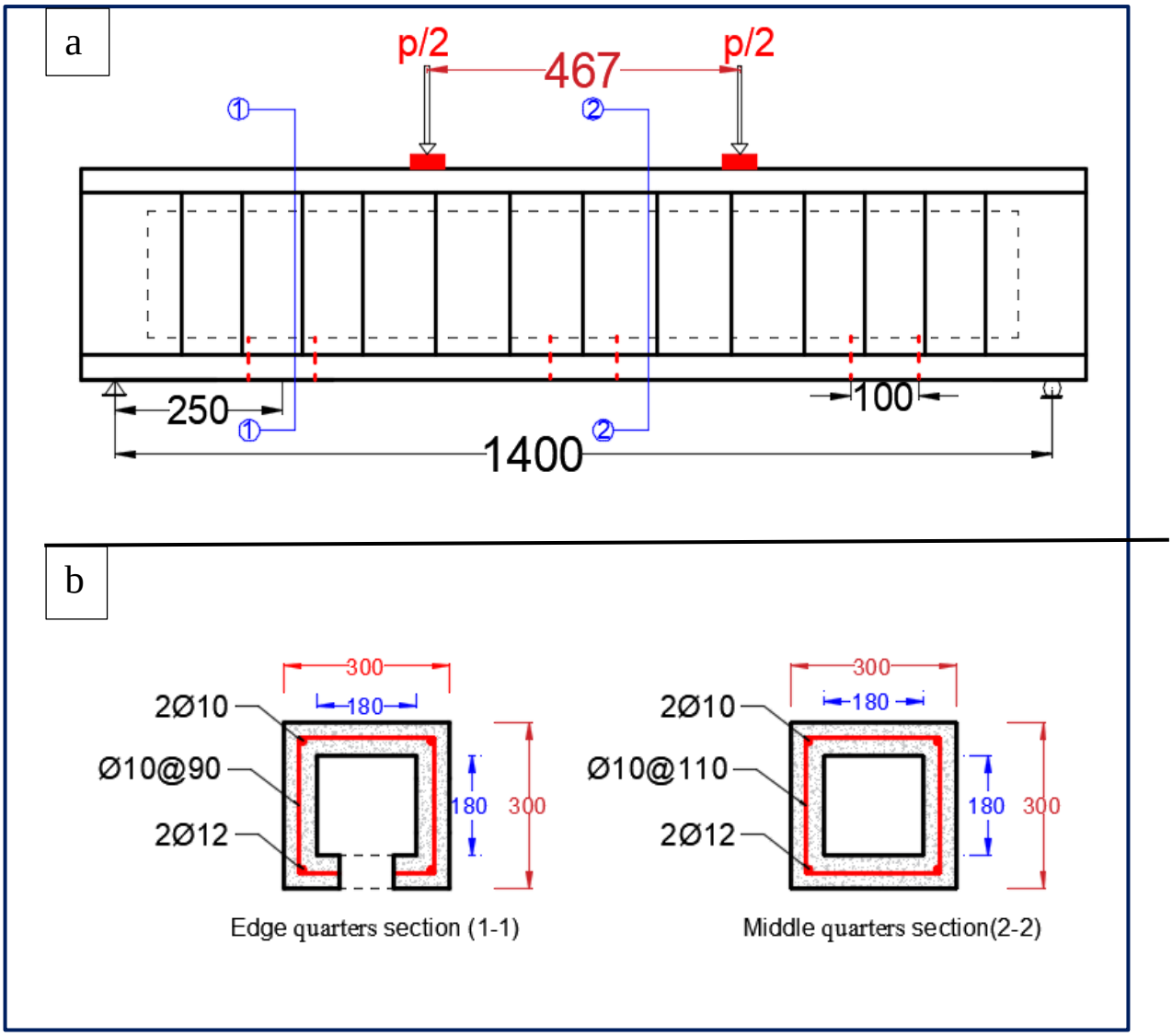

Fig. 3. 3: Reinforcement details for the beam H10SMB (All dimensions in mm)
(a) Longitudinal view (b) Cross-section and reinforcement

3.2.3 Beams with Circular Opening strengthened with CFRP (Group 3)

The third group comprises three specimens with a circular opening in the front and rear of the beam with a different combination for the opening location, as shown in **Table 3.1**. The specimens in this group have been chosen to be strengthened because they represent the critical beams among other beams. Location of opening, according to **Mansur *et al.***, (**1992**), was determined to be more than half the effective depth of the beam from the support. These beams were strengthened by two full wrap strips of CFRP laminates on the sides of the opening. Details of externally strengthening beams by CFRP laminates for the reinforced SCC hollow beams were illustrated in **Appendix (A)** and exhibited in **Fig. 3.4**.

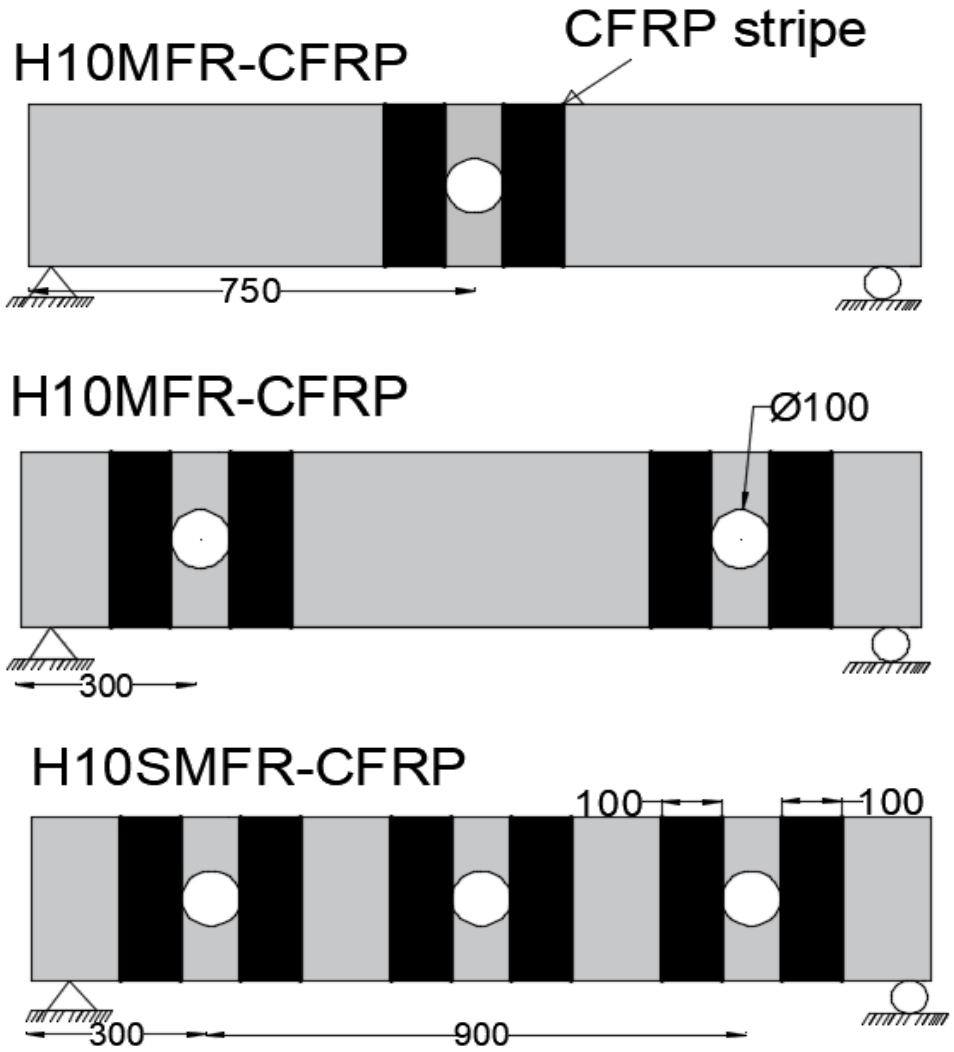

Fig. 3. 4: Full wrapping external strengthening around openings by CFRP laminates

3.3 Creating Opening in the Hollow beams

All openings were created using a core machine to simulate the real state of drilling a hole in an existing beam. The installation of the core machine requires some weights and continual water flow. After the installation of the core machine, the cutting process is starting until the required depth is reached, as shown in **Plate 3.1**.

Plate 3. 1: Coring process

3.4 External Strengthening by CFRP Laminates

Three specimens were selected to be strengthened by CFRP laminates (H10SFR-CFRP, H10MFR-CFRP, H10SMFR-CFRP). Such specimens were strengthened by two full wrap strips of CFRP laminates of 0.167 mm thickness and 100 mm width on the sides of the opening. Further details regarding the strengthening procedure of design for the specimens in group 3 are illustrated in **Appendix A**. The bond between the CFRP strips and the beam surfaces are the essential part in the efficiency of the strengthening system, as the weak bond that may result from inadequate preparation can render the strengthening application as useless. To ensure such proper bonding, the following steps were followed:

1. The surface of the specimen was grinded using an electric hand grinder to expose the aggregate and to obtain a clean sound surface, free of all contaminants such as cement laitance, and dirt. Specimens were cleaned by washing with water and allowed to dry

before the composite application. This procedure can remove loose particles and contaminations from the specimen's surface.

2. The corners of the specimens were rounded to avoid any stress concentration in the CFRP at corners of the beams. This stress concentration will lead to a rupture failure of CFRP at those corners before reaching their ultimate strength.
3. The mixed resin Sikadur-330 is applied to the prepared substrate using a special brush in an approximate quantity of (0.8 to 1.4 kg/m^2), depending on the roughness of the substrate.
4. The Sika Wrap®-300 C fabric was cut by scissors to strips for the required width and length for all specimens. The Sika Wrap®-300 fabric was placed onto the resin with a plastic roller until the resin is squeezed out between the roving.
5. As a covering layer, an additional resin layer of approximately (0.5kg/m^2) broadcast with the brush can be added, which will serve as a bonding coat for the following cementitious coatings.
6. After allowing the laminate to cure for several days, the specimens will be ready to test. **Plate 3.2** shows the procedure of application of CFRP sheet on the concrete element.

Plate 3. 2: CFRP system installation

Plate 3. 2: Continue

3.5 Self-Compacting Concrete (SCC) Mix

The EFNARC guidelines for self-compacting concrete **EFNARC**, (**2005**) were followed for mixing and testing. In this study, an SCC mix was designed according to the mix design procedure suggested by **Abo Dhaheer *et al.***, (**2016**) and **Alyhya *et al.***, (**2015**) to achieve a target 28 days concrete strength of 30 MPa. The amounts of ingredients by weight used to produce one cubic meter of SCC were presented in **Table 3.2**.

Table 3. 2: Ingredients' quantities for one cubic meter of SCC mix (kg)

Parameter	Weight	EFNARC Limitations
cement	380	380-600
Limestone powder	160	-------
water	190	150-210
Superplasticizer	4.5	-------
Fine Aggregate	800	(48-55)% of the total aggregate
Coarse Aggregate	800	750-1000
w/cm	0.5	-------

3.6 Material Properties

3.6.1.1

- **Cement**: Sulphate resisting Portland cement type **V** that produced in Iraq-Karbala was used, which is commercially known as (Lafarge-Iraq-BAZIAN / Al-Jasir) conforming

to the **Iraqi Standard Specification No. 5.** The chemical and physical properties of the cement used were given in **Tables B. 1 and B. 2** in **Appendix-B,** respectively.

- **Fine aggregate**: Natural sand from Karbala factory with a maximum size of 4.75 mm was utilized in this study. Before utilizing the sand, it was washed by water and cleaned to remove unwanted ingredients. Then, it lay out in the air and left to dry to avert the humidity saturation effect, which affects the water content of the designed mix. The grading test results conform to the **Iraqi Specification No. 45**, as shown in **Table B.3 in Appendix-B**.
- **Coarse aggregate**: Black crushed gravel with a maximum size of 19 mm from Al-Nibaey region was utilized in the current research. After cleaning the gravel by wash water, it was left in the air to dry. The sieve analysis of the coarse aggregate and the limits specified by the **Iraqi Specification No. 45** are given in **Table B. 4** in **Appendix-B.**
- **Water**: The water used in mixing and curing the SCC mixes should be clean and free from injurious amounts of oils, acids, alkalis, salts, organic materials. The tap water has been utilized for mixing and curing concrete in this research.
- **Limestone powder**: A local limestone powder, which is chemically known as $CaCO_3$ as the central component, was used. This material is locally known as Gubra, and it has been bought from a local market. It was used as a filler material with a max size of 0.125 mm in order to increase the viscosity of the SCC mixes. The chemical composition and physical properties of this material are given in **Tables B.5 and B.6** in **Appendix-B,** respectively.
- **Superplasticizer**: High range water reducing admixture was used in this research work, which is necessary to produce SCC. The admixture was supplied by Sika company, and it is commercially known as ViscoCrete-5930 (**Material sheet**, **2015**). It was the third generation of superplasticizers that are used in producing concrete and mortar. This type is suitable for producing many types of concrete, and it can be used in both cold and hot weather conditions. ViscoCrete-5930 can reduce the water content by up to 30 %, and it has several advantages besides reducing water content in the mixture such as; improve shrinkage and creep behaviour, increase high early strength and density. The characteristics of this type of superplasticizer are given in **Table B. 7 in Appendix-B.** It is worth to mention that such superplasticizer was conformed to the requirements of admixtures that are given by the **American Society of Testing Materials**, (**2013**).

3.6.1.2 Test of Fresh Properties

The standard fresh properties tests were carried out to ensure that the SCC mixes meet its functional requirements to determine the characteristics of a fresh SCC such as flowability, passing ability and resistance to segregation. Various tests were established in an attempt to characterize the properties of SCC, such as the slump flow, L-box, J-ring, and V-funnel …etc, **Da Silva and De Brito**, (**2015**). In this study, three standard tests were implemented to investigate the properties of SCC.

1. Slump Flow Test

The slump flow is a test to assess the flowability, and the flow rate of an SCC mix in the absence of obstructions, where the result is an indication of the flowability (**Ahmad *et al.***, (**2017**). The time from the start of lifting the cone upward until the SCC touches the 500 mm circle (***t_{500})*** is also a measure for the speed of flow, and hence how viscous the SCC mix is **EFNARC (2005)**. A truncated cone conforming to the **BS EN 12350-8**, (**2008**) is used in this test with a 100 mm diameter at the top, 200 mm at the bottom, and 300 mm height. Upon the test, the cone is placed on a one-meter square non-absorbing base plate, which is marked with three concentric circles: the first with 300 mm diameter, the second 500 mm diameter and the third one is 900 mm diameter. The cone is filled with SCC and left for a short period not more than 30 sec to be then lifted upward smoothly in one move, and the concrete begins to flow out under its own weight. After the SCC mix stops flowing, two perpendicular diameters should be taken across its spread, and the average value is reported. The preformed test is illustrated in **Plate 3.3**.

2. J-Ring Test

The target of the J-ring test is to investigate in the passing and the filling ability of SCC, as stated by **Ahmed**, (**2011**). Comparing the results of the test from two various segments of the sample can be utilized to examine the SCC segregation resistance. Three parameters are measured in the j-ring test: flow spread, time of flow t_{500J}, and blocking ratio. The former refers to the limited deformability of SCC owing to the blocking effect by reinforcement bars, while the flow time t_{500J} refers to the rate of deformation within a defined flow distance (**EFNARC**, (**2005**). The J-ring apparatus are shown in **Plate 3.4**. The test follows the following procedure. Firstly, placing the above- mentioned truncated cone on the base plate. Next, the J-ring will be positioned around the cone on the base plate. After that, SCC will be poured into the cone to fill it and left for a short period not more than 30 sec to be then lifted upward smoothly in one

move and let the concrete flow out under its own weight. When the SCC stops flowing, two perpendicular diameters should be measured, and the mean value is mentioned. The t_{500J} is measured by recording the time from the start of lifting the cone upward until the SCC touches a 500 mm diameter. To calculate the blocking ratio, a straight shaft is lied on the top of the J-ring with the flat part. After that, the altitude differences between the surface of concrete and the lower edge of the straight shaft will be measured at four locations outside the J-ring, two in the y-direction and two in the x-direction and at the central position, as shown in **Plate 3.4**.

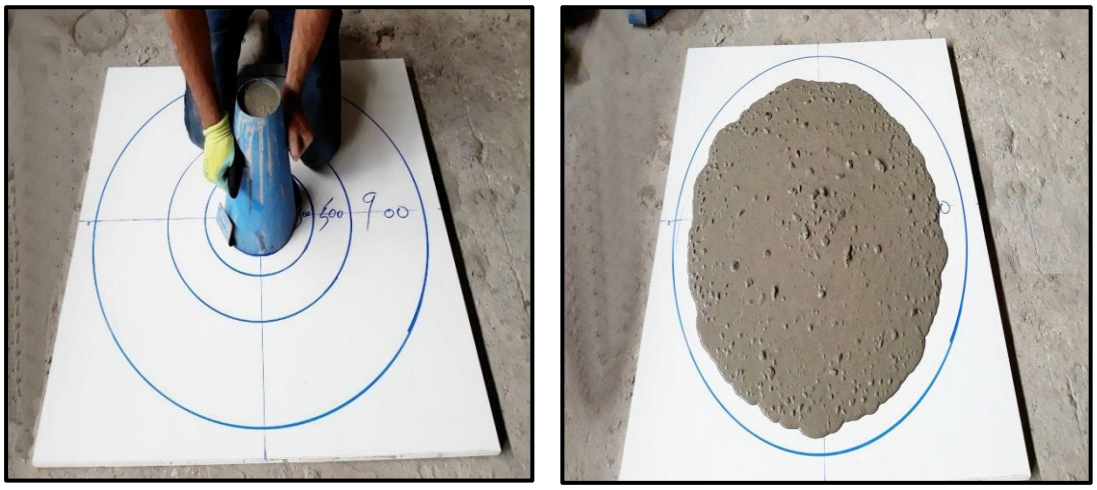

Plate 3. 3: Slump flow test for SCC

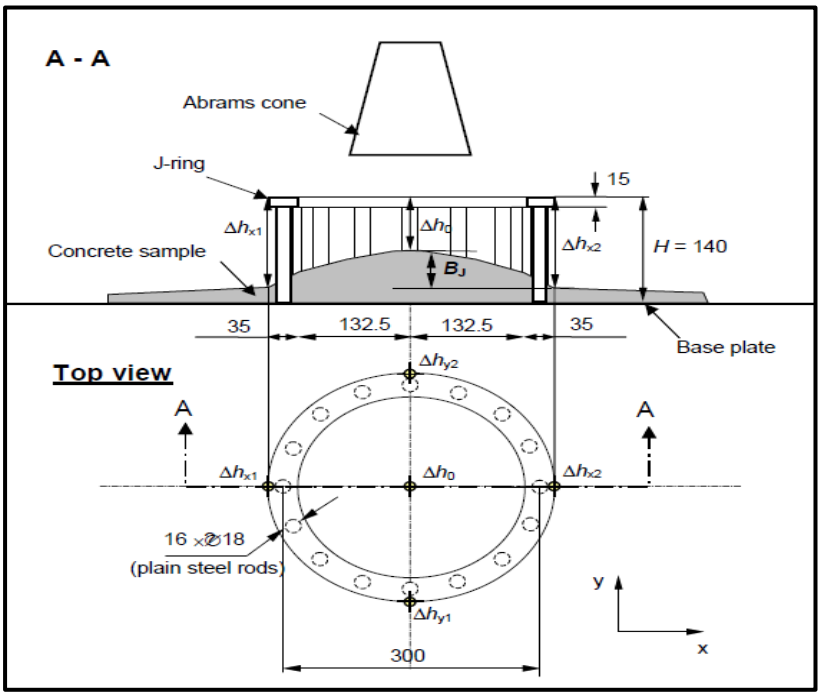

Plate 3. 4: J-Ring test for SCC

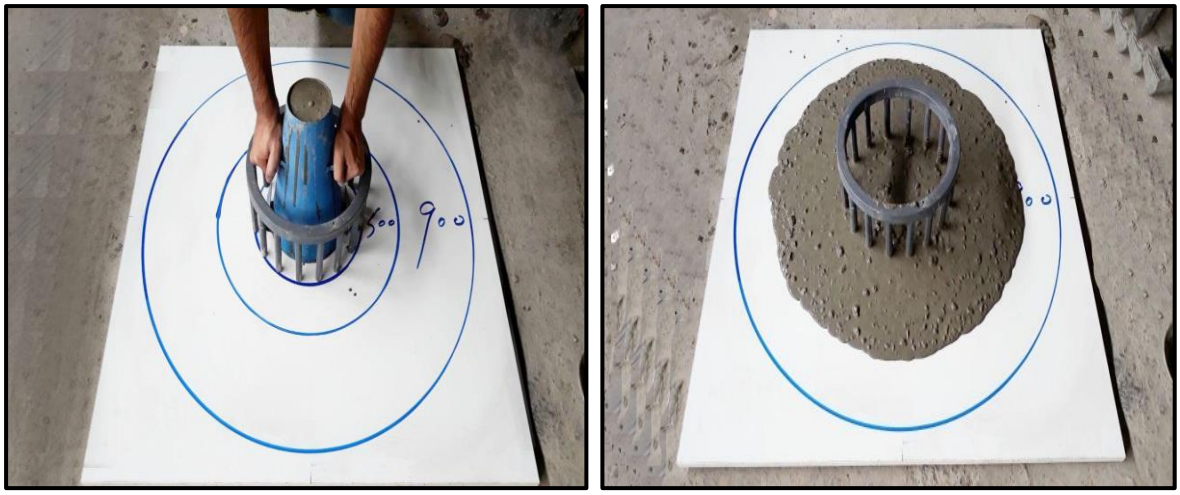

Plate 3. 4: Continue

3. L-box Test

The L-box test, which is shown in **Plate 3.3** is used to assess the filling and passing abilities of an SCC to flow through a tight opening, including spaces between reinforcing bars and other obstructions without segregation or blocking **(EFNARC**, (**2005**). A moveable gate, which is made from steel as well as two or three steel bars, will separate the vertical and horizontal channel. The vertical portion will be filled with SCC. By opening the gate, the concrete left to flow into the horizontal channel under its own weight, and the heights H_1 and H_2 are measured to determine the passing ability factor by dividing H_2/H_1. For all the above tests, the results are listed in **Table 3.5**.

Plate 3. 5: L-Box test for SCC

Table 3. 3: Fresh self –compacting concrete tests result

Test	Parameter	Measured Value
Slump flow	Spread diameter	810 mm
	t_{500}	2 sec
J-ring	Spread diameter	790 mm
	t_{500J}	3.5 sec
	Blocking ratio	0.35
L-box	Passing ratio	0.9

3.6.1.3 Mechanical Properties of Hardened SCC

1. Compressive Strength

The compressive strength test was conducted on (150×150×150) mm cubes according to the **BS 1881-116** (**1983**) using a digital compressive machine of 2000 kN capacity, as shown in **Plate 3.6**. The cubes have been tested on the same day of testing beams, and the static load was applied with a rate of loading 0.6 MPa/sec. The average compressive strength result of each mix exhibited in **Table 3.4**.

2. Splitting Tensile Strength

The splitting tensile strength was tested using cylinders of (100×200) mm according to the **ASTM C496/C496M-11**, (**2011**) using a testing machine of 2000 kN ultimate capacity, as shown in **Plate 3.6**. The cylinders have been tested on the same day of testing beams, and the results are listed in **Table 3.4**.

3. Flexural Strength

This test covers the determination of the flexural strength (modulus of rupture) of concrete specimens, according to **ASTM-C293**, (**2002**). Three prisms of (100×100×500) mm have been used for SCC. All prisms have been tested on the same day of testing the beams by using a hydraulic machine of 100 kN ultimate capacity, as shown in **Plate 3.7** results are presented

Plate 3. 6: Compression and Splitting Tensile Strength Machine

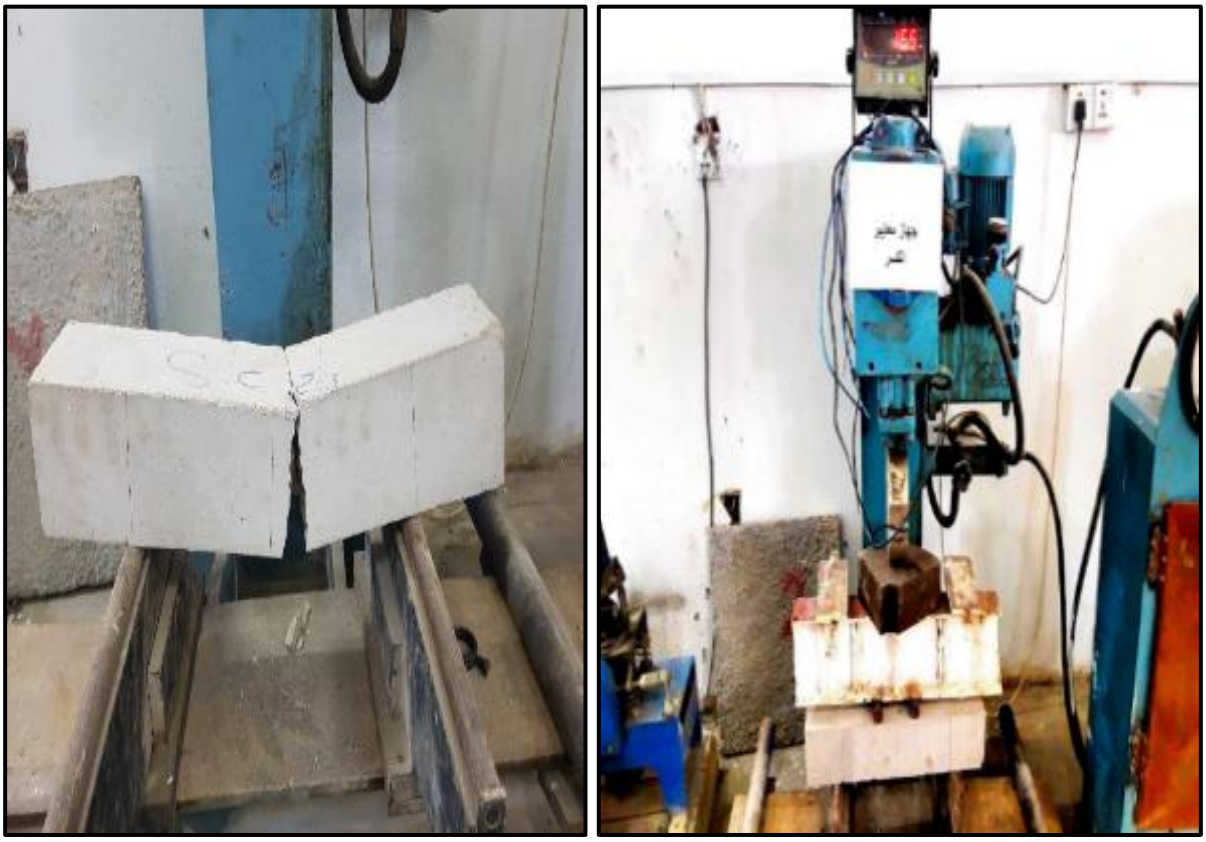

Plate 3. 7: Modulus of rupture (test specimen and machine)

Table 3. 4: Mechanical properties of SCC

Group	Specimen Symbol	Concrete Compressive Strength, f_{cu} MPa	Splitting Tensile Strength, f_{ct} MPa	Rupture Modulus, f_r MPa
Group 1	HC H10MF H10SF H10SMF H10MFR H10SFR H10SMFR	32.5	3.4	4.9
Group 2	H10MB H10SB H10MB	33.3	3.7	5.8
Group 3	H10MFR-CFRP H10SFR-CFRP H10SMFR-CFRP			

3.6.2 Carbon Fibre Reinforced Polymer (CFRB) Sheet and Epoxy

Carbon fibre fabric (Sika Wrap®-300) with 0.167mm thickness and Sikadur 330 epoxy-based impregnating resin (Sikadur 330) utilized for the strengthening technique, as shown in **Plate 3.8**. The major Sikadur-330 and CFRP properties were shown in **Appendix-B, Tables B-8 and B-9,** respectively.

Plate 3. 8: Materials used for strengthening by CFRP

3.6.3 Steel Reinforcement

Two diameters of steel reinforcement were utilized in the tested specimens in which 12 mm bar size was utilized as primary reinforcement in the bottom and 10 mm bar size was utilized in the top. Furthermore, as closed stirrups, the 10 mm bar size was also utilized. According to **ASTM A615**, (**2016**), the tensile test of steel reinforcement was carried out using at least three specimens to determine their tensile characteristics. Steel bars have been tested in the laboratory of the mechanical engineering department/Kerbala University using a tensile testing machine, as shown in **Plate 3.9.** The main characteristics of the steel bars are listed in **Table 3.5**.

Plate 3. 9: Tensile testing machine of steel reinforcement

Table 3. 5: Test results of steel reinforcing bar

Nominal Diameter mm	Measured Diameter mm	Yield Stress* (f_y) MPa	Ultimate Strength, f_u MPa	Elongation Ratio %
10	9.91	490	517	15.3
12	11.9	516	608	16.3

*** Each value is an average of three specimens (each 40 cm length).**

3.6.4 Compressed Cork

The compressed cork is used to make the hallowed part, which was bought from a local company, and it was cut with dimensions of (180×180×1300) mm that represents the dimension of the hallowed part of the beam. The density of the compressed cork equals 0.195 gm/cm^3. The cork was placed inside the reinforcement cage and fixed with spacers from all directions, as shown in **Plate 3.10**.

Plate 3. 10: Compressed cork inside the reinforcement cage

3.6 Wooden Mold

Fourteen wooden moulds with 18 mm thickness were prepared for casting the specimens. The wooden mould comprises four free sides and a bed in which the bed has been fixed to these sides by bolts. The dimensions were equalled to (300×300×1500) mm for height, width and length, respectively. All moulds were oiled prior to casting, and the compressed cork was put in the reinforcement cage, as shown in **Plate 3.11**.

Plate 3.11: Wooden mould

3.8 Mixing procedure

The concrete was mixed using a central mixer, and the following points summarize the procedure of mixing:

1. All quantities were weighed before mixing and packed in a clean container.
2. The aggregate (coarse and fine), cement, and the limestone powder were added and mixed in its dry condition for two minutes in the central mixer to be mixed later with three quarters of the required water and superplasticizer.
3. The remaining water and superplasticizer were added for the mixer and mixed for three to five minutes.
4. The concrete surface was levelled and finished by a trowel after the concrete was cast into the wooden moulds, as shown in **Plate 3.12**. Furthermore, to avoid the water evaporation, the specimens were wrapped with nylon sheets.
5. After 24 hours from casting, the beams were extracted from the moulds, and they were covered by burlap sacks to keep moistness for 28 days. The same procedure was followed for the cubes, cylinders and prisms. The specimens were tested following the standard specifications after taken out from the curing tank after 28 days.

Plate 3. 12: specimens ready to cast

Plate 3.12: Continue

3.9 Instrumentation and Test Procedure

After completing the curing process for all samples, an in-place opening (s) was created in the beams, and they were cleaned and painted in white to clarify cracks and distinguish failure modes, as shown in **Plate 3.14**. The test was carried out on all beams up to failure by using a hydraulic testing machine with an ultimate capacity of 2000 kN. This machine is available in the concrete laboratory of the Civil Engineering Department / Engineering College / University of Kerbela, as shown in **Plate 3.13**. The load was applied progressively up to the failure of the girder or when the deflection increases at constant load. The increment of the load was about 5 kN, and the load was recorded by using a load cell with a capacity of 1000 kN linked to a computer,. The significant properties of the beam (i.e. structural behaviour were recorded at each loading stage throughout testing. The deflection was measured by using LVDTs of 20 mm settlement capacity, which was linked to a computer as presented in **Fig 3.5**.

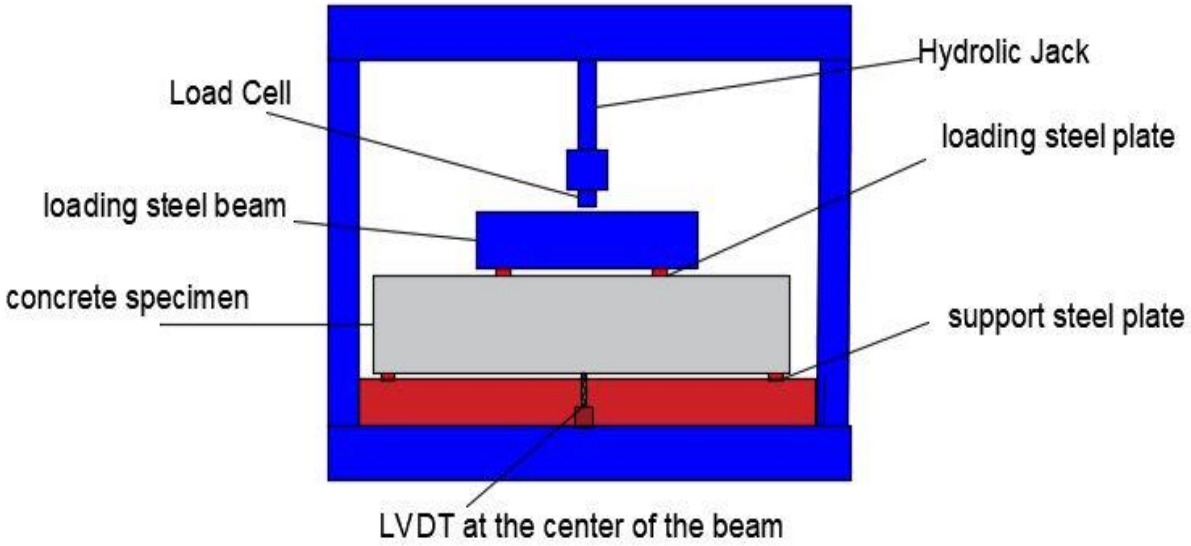

Fig. 3.5: Instruments details of hydraulic testing machine

Plate 3. 13: Hydraulic testing machine & the load cell attached with the hydraulic machine

Plate 3. 14: Beams after painting

3.10 Support and Loading Conditions

The system of support was hinged at the first and roller at the other support. The hinged end consists of a smooth steel shaft of 25mm diameter connected to the base plate with welding, and two shafts of 25mm as diameter and welded to steel beam (to make grove). The roller support made of one steel shaft of diameter 25mm free. All the hollow beams were tested under two-point loading. **Figure 3.6** shows the details of support conditions.

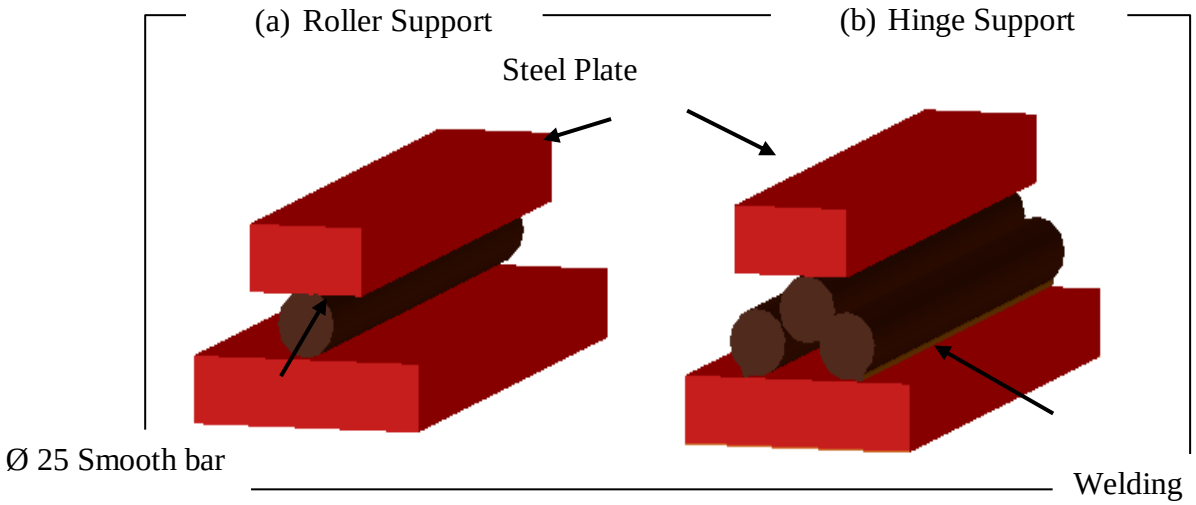

Fig. 3.6: Details of the typical support condition

CHAPTER FOUR

EXPERIMENTAL RESULTS AND DISCUSSION

4.1 Introduction

The results and discussions from testing fourteen SCC hollow beams that are labelled in chapter three are presented in this chapter, which are tested under two-point load and divided into three groups. The first group contains six beams with a circular opening in the front or the front and rear of the web with various openings' locations. The second group comprises three beams with a circular opening in the bottom flange of the beam, while the third group includes three beams that are strengthened with CFRP laminates around the openings. The three groups were tested to examine the influence of different considered variables such as various locations of openings, number of openings and the effect of external strengthening by CFRP strips. Moreover, the test results were discussed to include cracks propagation and the mode of failure, the ultimate strength, stiffness of the beams at service load (70% of the ultimate load), which was calculated using the formula (k=F/**Δ)**, load mid-span deflection curves, (service deflection at 70% of the ultimate load) and ductility of the tested beams that was calculated by dividing the ultimate deflection by the service deflection (**Δu/ Δy)**.

4.2 Experimental Result for Tested Beams

This section deals with the overall behaviour of fourteen SCC hollow beams without and with in-place circular opening non-strengthened and strengthened with CFRP strips.

4.2.1 Pilot and Hollow Control Beams (Without Opening)

Two beams without opening were cast in which the first beam was a pilot beam, and the other was a control beam. The pilot beam was used to check the validity of the test process, support, load positions, location of the LVDT, and the overall test incremental load applications. The device was found to be worked properly and could be used to test all other beams. The control beam (HC) is a hollow SCC beam without opening loaded gradually until the first crack was evident in its mid-span, at a load equals nearly to 55 kN. Beyond the first crack load, cracks started to propagate with the increase in the load at the maximum bending moment zone and reached the neutral axis. HC failed at about

155 kN load, and the mode of failure was a flexural failure as it designed to fail, as shown in **Plate 4.1**. The mid-span load-deflection curve for HC is shown in **Fig. 4.1**, where the elastic stage exhibited a linear behaviour until the first change in the slope of the load-deflection curve occurred due to the first crack load. With the increase in the applied load, a smooth increase in the deflection of HC occurred until the ultimate failure of the beam occurs.

Plate 4. 1: Mode of failure and cracks pattern for (HC)

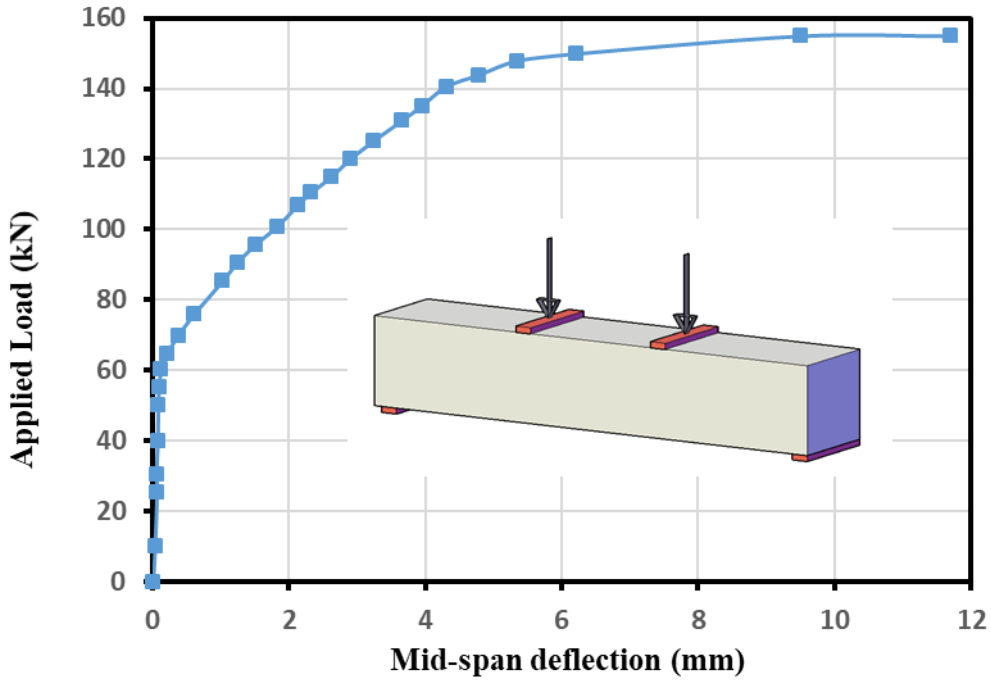

Fig. 4. 1: Load mid-span deflection curve for (HC)

4.2.2 Hollow Beams with Opening in the Web (Group1)

4.2.2.1 Hollow Beam with in Front Opening at the Mid-Span (H10MF)

This specimen contained an opening at the middle of the web in the front side of the beam. Results showed that a small vertical deflection has initiated at the mid-span of the tested specimen at the early stage of loading. As the load increases gradually, the first crack started to appear at a load equals nearly to 50 kN below the opening, which is

located at the maximum moment zone. With the progress of the loading process, the cracks started to widen and move up towards the neutral axis, near the opening (or under the applied load). Finally, a flexural failure at an ultimate load of about 147 kN occurs. Thus, a reduction ratio in the load-carrying capacity by 5.2% is recorded in comparison to HC. Moreover, the mid-span load-deflection curve for H10MF showed a linear behaviour at the first stage of the loading until the first crack appeared. After the elastic stage, the load-deflection curve exhibited a smooth increase in the deflection at service load by 20% owing to the reduction in the beam stiffness by 16%, which is due to the presence of the opening. Furthermore, the ductility index value of H10MF was nearly equalled to 2.8 if compared with the ductility index value of HC, which was 5. **Plate 4.2** shows the mode of failure and cracks pattern, while **Fig. 4.2** exhibited the load mid-span deflection curve.

Plate 4. 2: Mode of failure and cracks pattern for (H10MF)

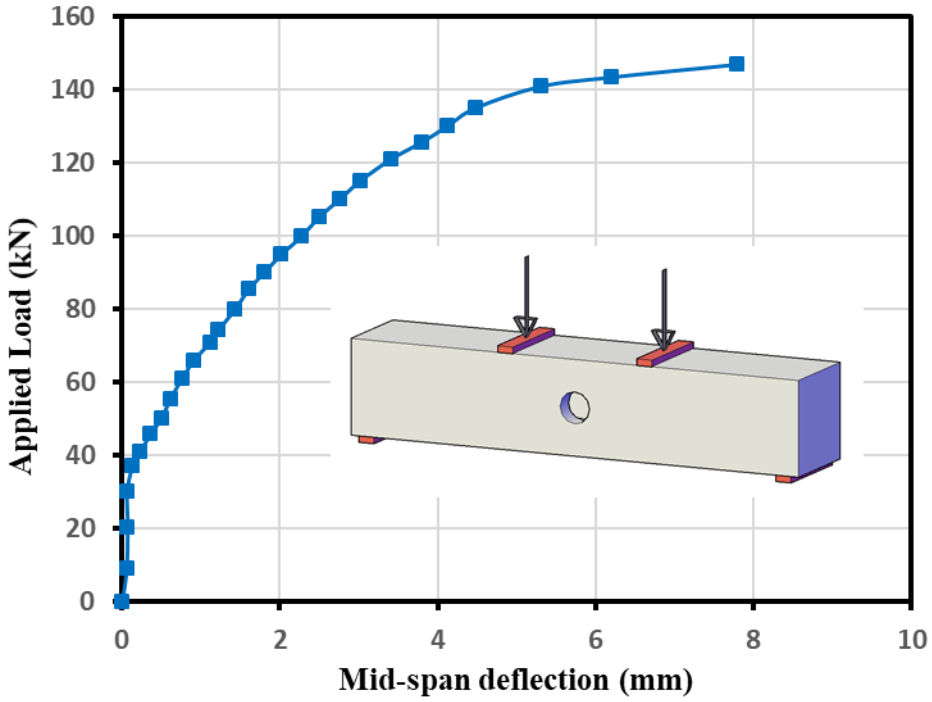

Fig. 4. 2: Load mid-span deflection curve for (H10MF)

4.2.2.2 Hollow Beam with Front Openings Near Supports (H10SF)

This beam consisted of two openings located at the shear span at a distance of 250 mm from the support in the frontal side of the beam. The load was applied gradually until the first visible crack appeared at a load of 40 kN in the tension zone. Besides, the diagonal crack began to appear and spread in both sides of the specimen owing to the presence of the openings in the zone of shear. Meanwhile, many vertical cracks were also developed with the progress of the loading process, and the first visible crack started to expand. Furthermore, the cracks propagated and moved towards the neutral axis, as shown in **Plate 4.3**. Finally, the beam exhibited a sudden shear failure at a load 144.5 kN, recording a reduction ratio in the ultimate strength by about 6.8% if compared with HC. **Figure 4.3** exhibited the load mid-span deflection curve, which revealed a linear behaviour at the early stage of the loading until the first hair crack occurs. As the load increases further, the non-linear behaviour stage began. The figure also showed an observed reduction in the stiffness by about 28% due to the change in the section geometry owing to openings, which led to an increase in the deflection at service load by 39%. Moreover, the ductility index value of the beam was about 2.37 if compared with HC.

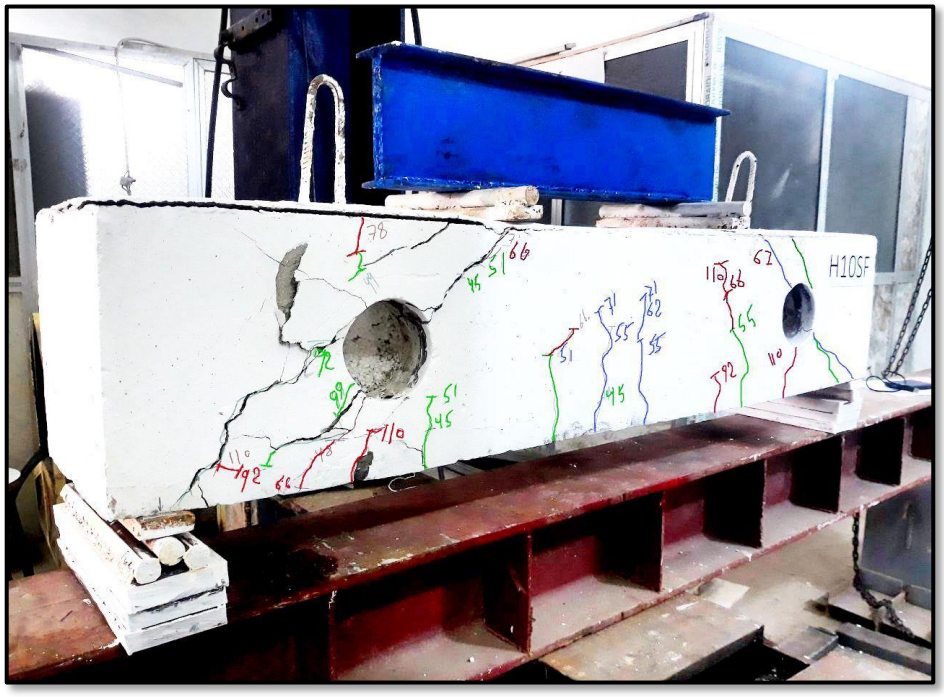

Plate 4. 3: Mode of failure and cracks pattern for (H10SF)

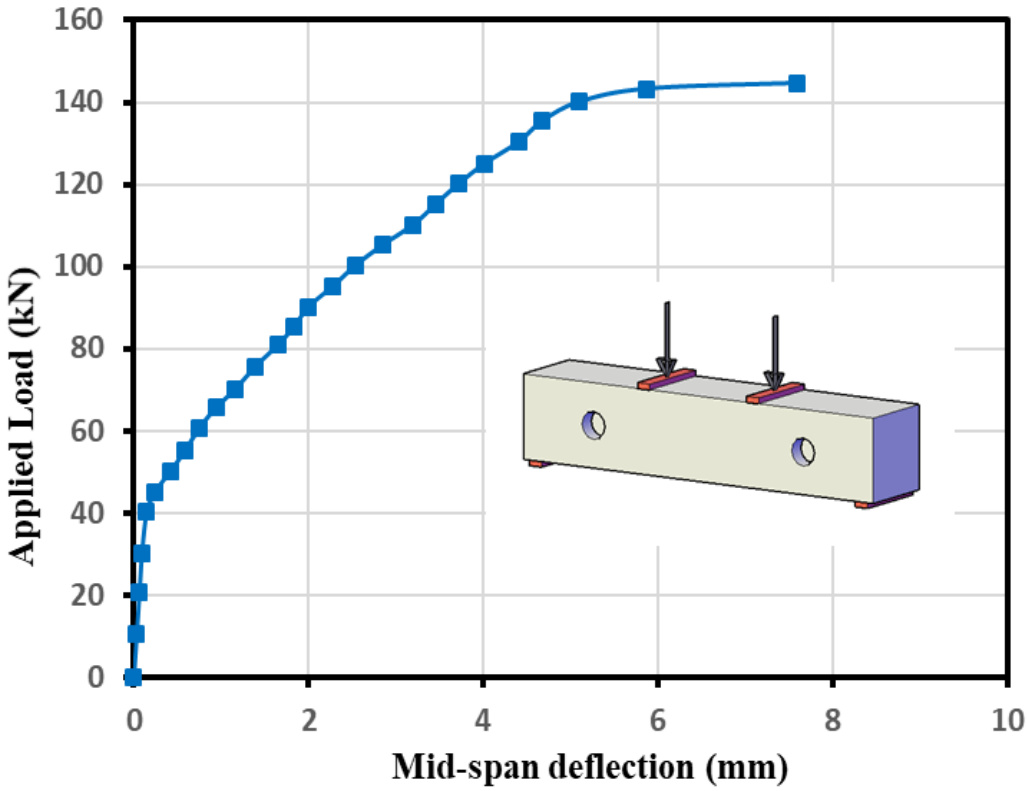

Fig. 4. 3: Load mid-span deflection curve for (H10SF)

4.2.2.3 Hollow Beam with Front Openings in the Mid-Span and Near the Supports (H10SMF)

This beam included three openings: two of them are located near the support at a distance 250 mm, and the third one is located at the middle of the web, as shown in **Plate 4.4**. At 37 kN load, the first visible crack was noticed at the flexural zone below the opening. With the progress of the loading process, an inclined crack began to appear and propagate in both sides of the beam. Furthermore, the cracks started to propagate and moved towards the neutral axis as the load increased further. Finally, the beam failed with flexural-shear failure at a load of about 143 kN recording a reduction ratio in the ultimate strength by nearly 7.7 % if compared with HC. **Figure 4.4** exhibited the load-mid-span deflection curve, which revealed a linear behaviour in the first stage of loading. After exceeding the elastic stage of loading, the non-linear stage began, which showed a significant reduction in the stiffness by about 34% due to the unforeseen changes in the section geometry due to the presence of three openings in the beam that increased the deflection at service load by 52%. In addition to that, the ductility index value of H10SMF was 2.14 if compared to the ductility index of HC, which indicated a more brittle behaviour.

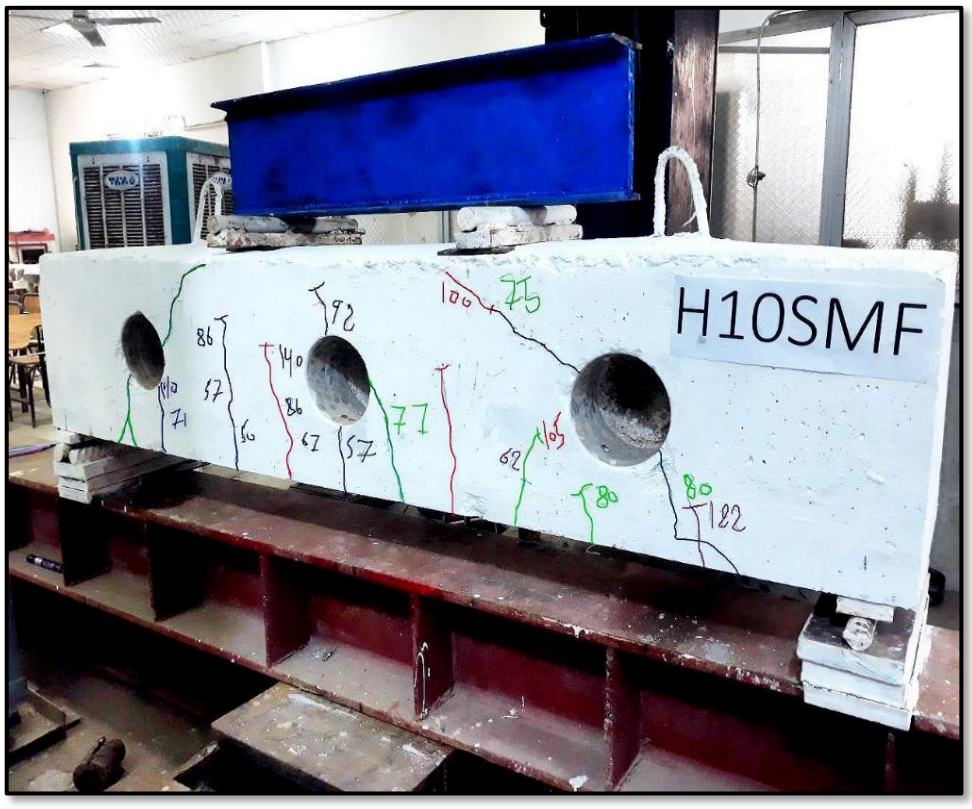

Plate 4. 4: Mode of failure and cracks pattern for (H10SMF)

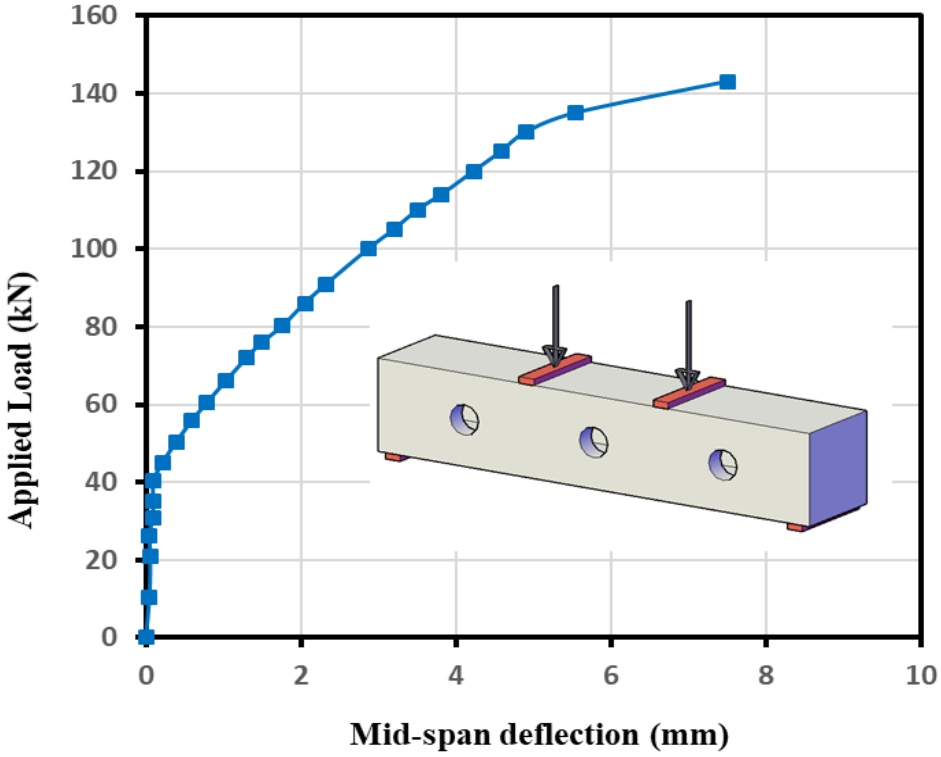

Fig. 4. 4: Load mid-span deflection curve for (H10SMF)

4.2.2.4 Hollow Beam with Front and Rear Openings at the Mid-Span (H10MFR)

The specimen H10MFR consisted of an opening at the mid-span in the front and rear of the web. The beam was loaded progressively until the first visible crack was remarked at the maximum moment zone at a load of about 45 kN below the opening. Some inclined cracks start to appear as the load increased further, and the first cracks start to widen. Furthermore, the cracks propagated and moved up towards as the applied load increases, as shown in **Plate 4.5**. Finally, a flexural failure at a load of about of 140.3 kN has been occurred recording a reduction ratio in the ultimate strength by about 9.9 % if compared with HC. The load-mid-span deflection curve exhibited a linear behaviour in the first stages of loading, as shown in **Fig. 4.5**. After exceeding the elastic stage, the first change in the slope has occurred, and the non-linear behaviour stage began, which revealed a significant reduction in the stiffness by 19% due to the presence of the opening in the front and rear parts of the web. This has also caused changes in the section geometry of the beam, which led to an increase in the deflection at service load by

24% on the other hand, the ductility index decreased, and its value was about 2 if compared with the control beam.

Plate 4. 5: Mode of failure and cracks pattern for (H10MFR)

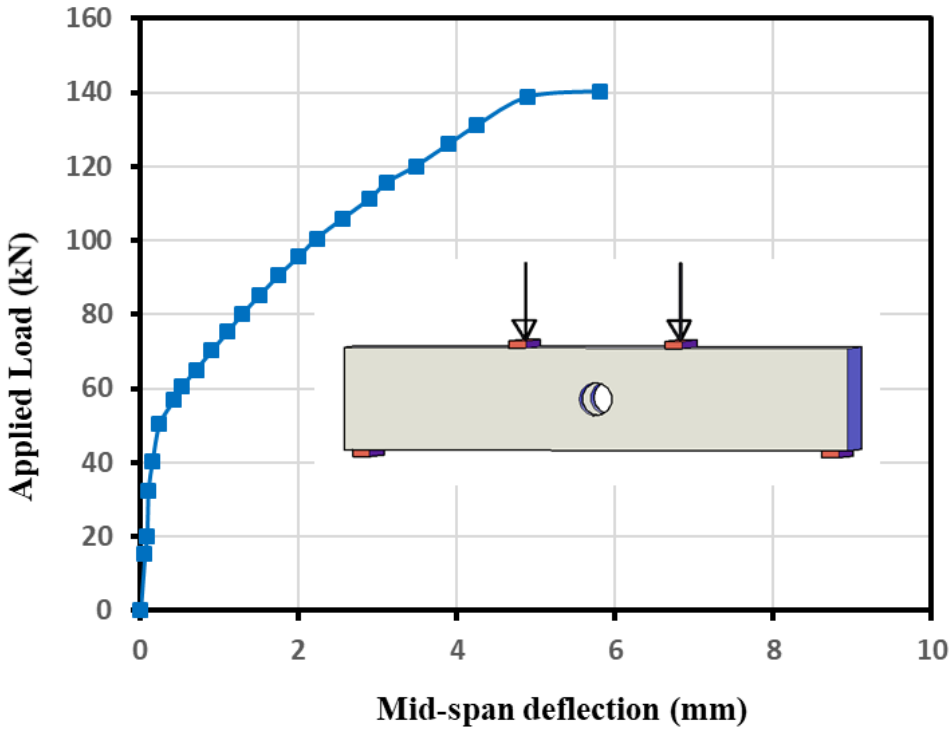

Fig. 4. 5: Load mid-span deflection curve for (H10MFR)

4.2.2.5 Hollow Beam with Front and Rear Openings Near Supports (H10SFR)

H10SFR specimen contained two openings located near the support in front and rear of the beam at a distance of 250 mm from the support. The specimen was loaded progressively until the first hair crack observed at a load about 40 kN in the maximum moment zone. Many diagonal cracks start to appear in the shear span due to the presence of the openings. Beyond the first crack loading stage, the cracks propagated and started to move up and reached the neutral axis near the applied load or opening, as shown in **Plate 4.6**. H10SFR exhibited a sudden shear failure at a load about 138.8 kN, recording a reduction ratio of about 10.5% if compared with HC. This might be due to the reason that two stirrups were intercepted by the openings that made it inefficient to carry any significant applied shear. The load-mid-span deflection exhibited in **Fig. 4.6** revealed that the relationship is a linear behaviour, as it is evident in the early stages of loading. After the first hair crack was noticed, the first variation in the slope of the load-deflection curves took place. Beyond the elastic phase, the beam suffered from a higher deflection at service load up 61% due to the reduction in its stiffness by 38% Meanwhile, the ductility index exhibited a noticeable decrease, and its value was 1.92 if compared to HC ductility index.

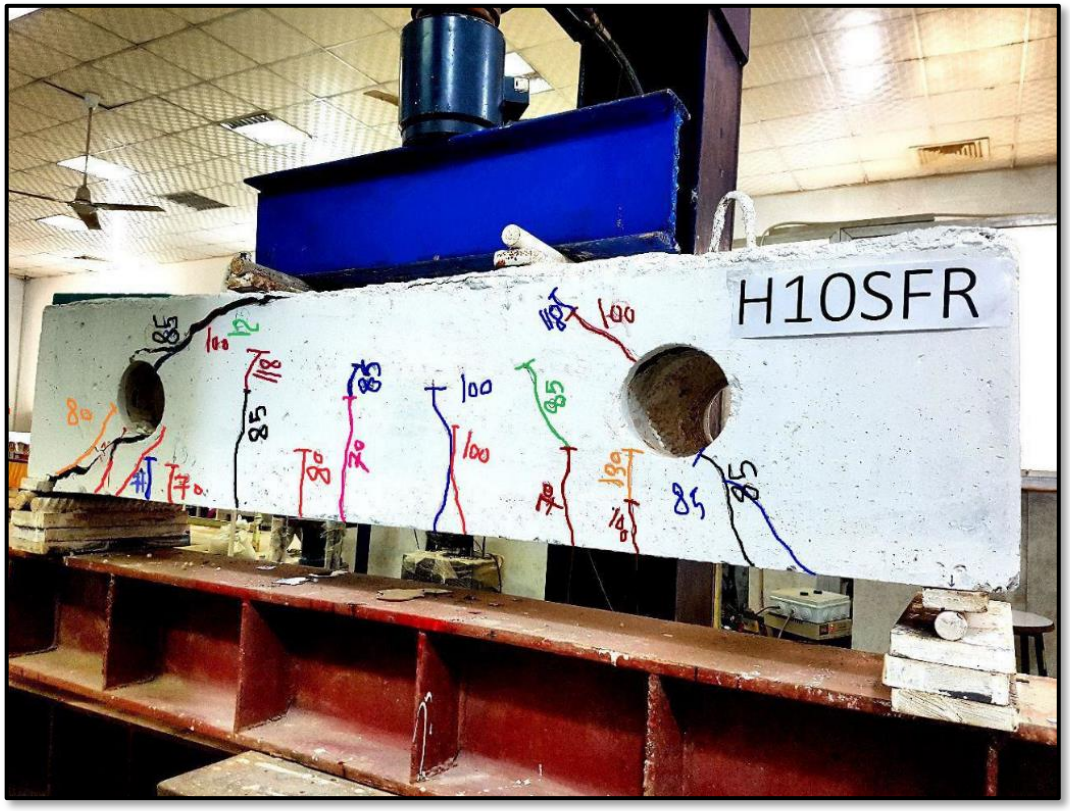

Plate 4. 6: Mode of failure and cracks pattern for (H10SFR)

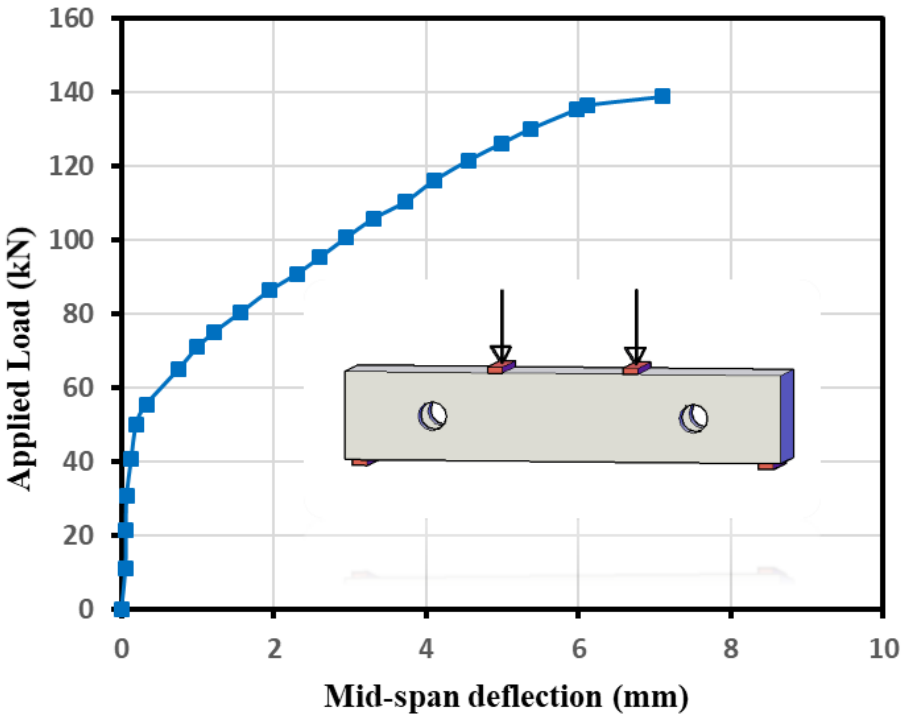

Fig. 4. 6: Load mid-span deflection curve for (H10SFR)

4.2.2.6 Hollow Beam with Front and Rear Openings in Mid-Span and Near the Supports (H10SMFR)

H10SMFR contained three openings in which the first one is located in the middle of the beam at the flexural zone while the other two are located at the shear zone at a distance equals to 250 mm from the support. The specimen was loaded gradually until the first hair crack noticed at about 35 kN load at tension zone, with loading process development, many diagonal cracks appeared near the support, and the first hair crack started to expand. With further load, the cracks propagated and moved up towards the applied load or openings and reached the neutral axis, as shown in **Plate 4.7**. Finally, a flexural-shear failure at a load about 130.2 kN has occurred, which cause a reduction ratio in the ultimate strength by about 16% if compared with HC. The load-mid-span deflection curve showed a linear behaviour as it is evident in the elastic phase of loading, which is shown in **Fig. 4.7**. After exceeding the elastic phase, the slope of the curve started to variate, and a remarkable increase in the deflection at service load by about 68% has been occurred, due to the reduction in the beam stiffness by 41% meanwhile, the ductility index reduced markedly, and its new value was about 1.53 .H10SMFR considered as the worst case in-group 1 because it exhibited a considerable reduction in the ultimate load in comparison

with other beams in the group, the results of this beam might be due to the fact that two stirrups were cut off by the openings, which made it unable to carry any significant applied shear, in addition to the variation in the section geometry

Plate 4. 7: Mode of failure and cracks pattern for (H10SMFR)

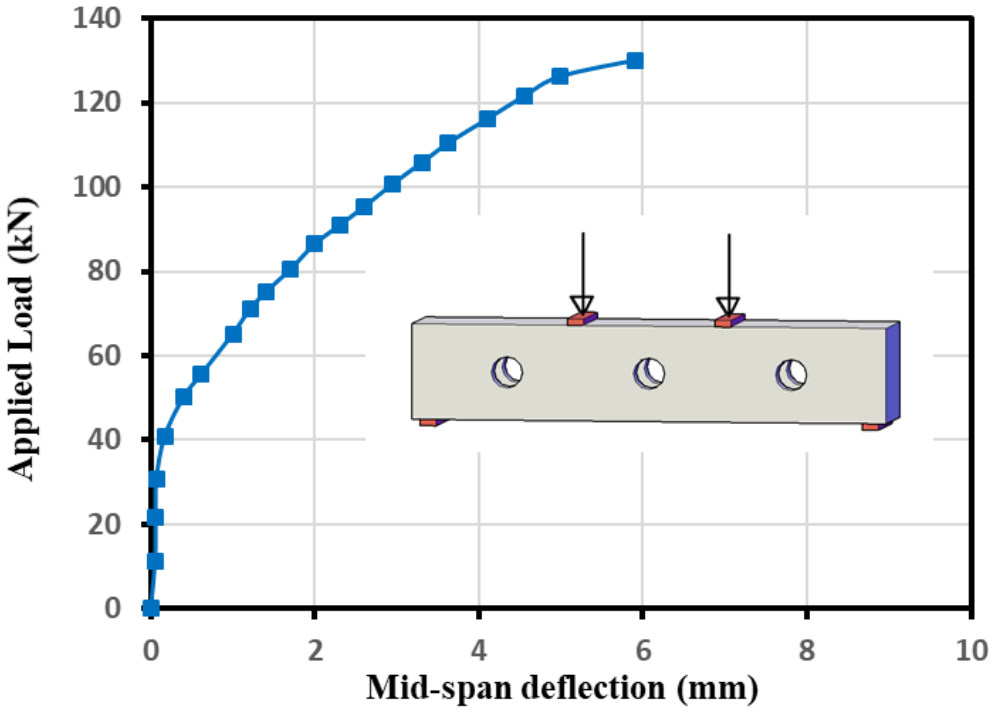

Fig. 4. 7: Load mid-span deflection curve for (H10SMFR)

4.2.3 Hollow Beams with Opening in the Bottom Flange (Group2)

4.2.3.1 Hollow Beams with Opening in the Mid-span at the Bottom Flange (H10MB)

This beam comprised one opening located in the middle of the bottom flange. H10MB was loaded gradually, and the first vertical crack appeared at a load about 52 kN at the flexure zone. As the load increased further, new cracks were developed in shear span, and it should be noted that the shear cracks had a little effect compared to the flexure cracks, which considered as significant cracks in this beam as shown in **Plate 4.8.** Finally, a flexure failure has been occurred at a load 146.4 kN owing to the presence of the opening in the maximum bending moment zone, which reduced the load-load-carrying capacity by 5.5% if compared to HC. The load-deflection curves for H10MB shown in **Fig. 4.8** revealed a linear behaviour at the first phase of loading, similar to HC. Beyond the elastic stage, the curve exhibited a slight increase in the deflection at service load by 28% owing to the reduction in stiffness by 22%. Furthermore, the deflection ductility index value reduced to a value of 2.5 if compared to HC, due to the presence of the opening that caused changes in the section geometry and decreases in the specimen's stiffness.

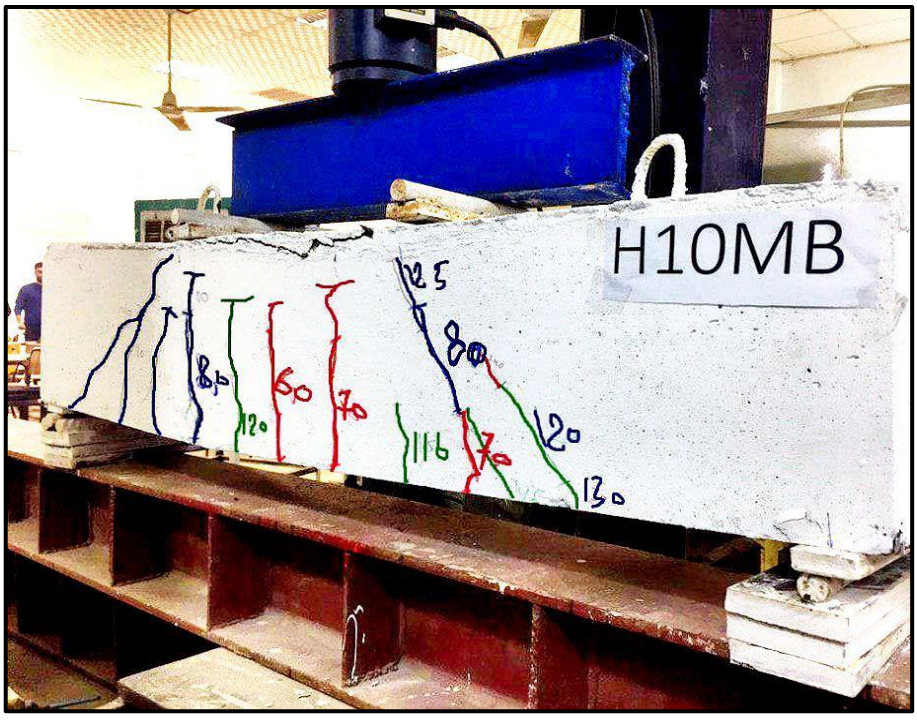

Plate 4. 8: Mode of failure and cracks pattern for (H10MB)

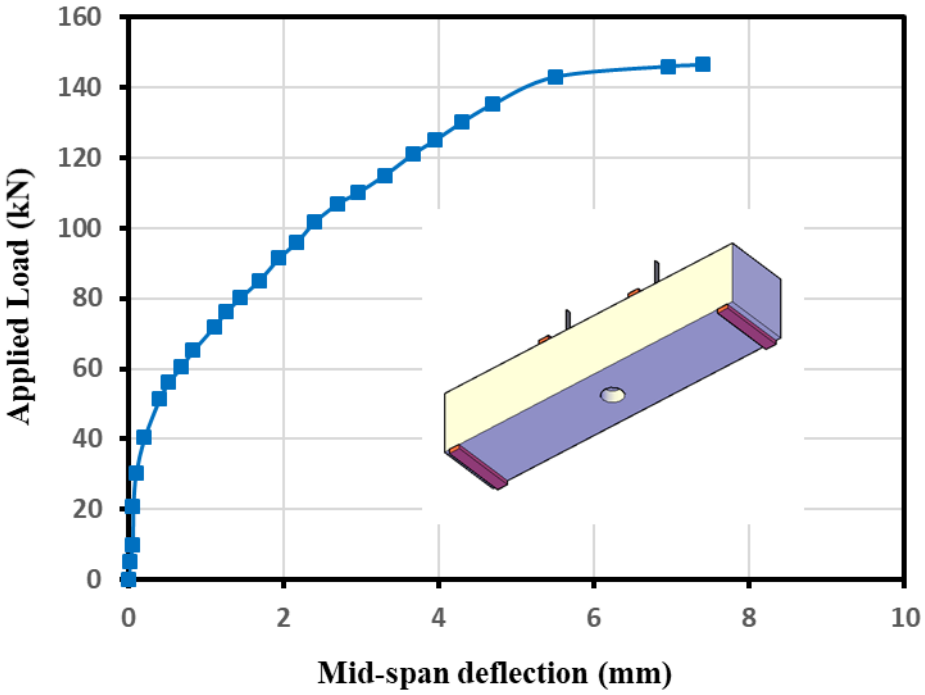

Fig. 4. 8: Load mid-span deflection curve for (H10MB)

4.2.3.2 Hollow Beams with Opening Near Supports at Bottom Flange (H10SB)

H10SB included two openings located at a distance 250 mm from the supports at the bottom flange. At 46 kN load, the first visible crack was observed within maximum bending moment zone. With increasing the load, inclined cracks started to appear on both side of the beam, and the first crack started to widen. With the development of the loading procedure, the cracks propagated and moved towards the compression zone and reached the neutral axis, as shown in **Plate 4.9**. At a load of about 145.5 kN, the beam had exposed to flexure failure that causes a reduction ratio in its ultimate strength by about 6.1% if compared to HC. The load-mid-span deflection for H10SB is shown in **Fig. 4.9**, which exhibited a linear behaviour at the elastic stage similar to control beam until the first change in the slope occurred at the first crack load. Beyond the elastic phase, the non-linear behaviour stage began, and the slope of the curve started to decrease if compared to HC owing to the reduction in the stiffness by 23%. Meanwhile, the deflection at service load displayed a smooth increase by 30% if compared to HC. In contrast, the deflection ductility index value became about 2.33, which means that the specimen became more brittle if compared to HC.

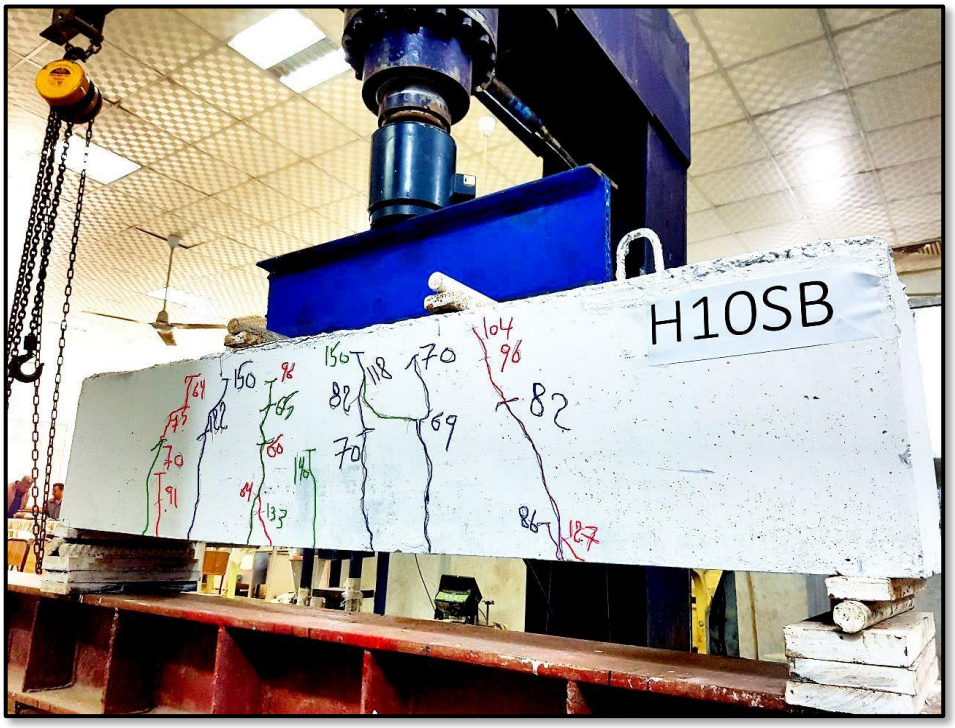

Plate 4. 9: Mode of failure and cracks pattern for (H10SB)

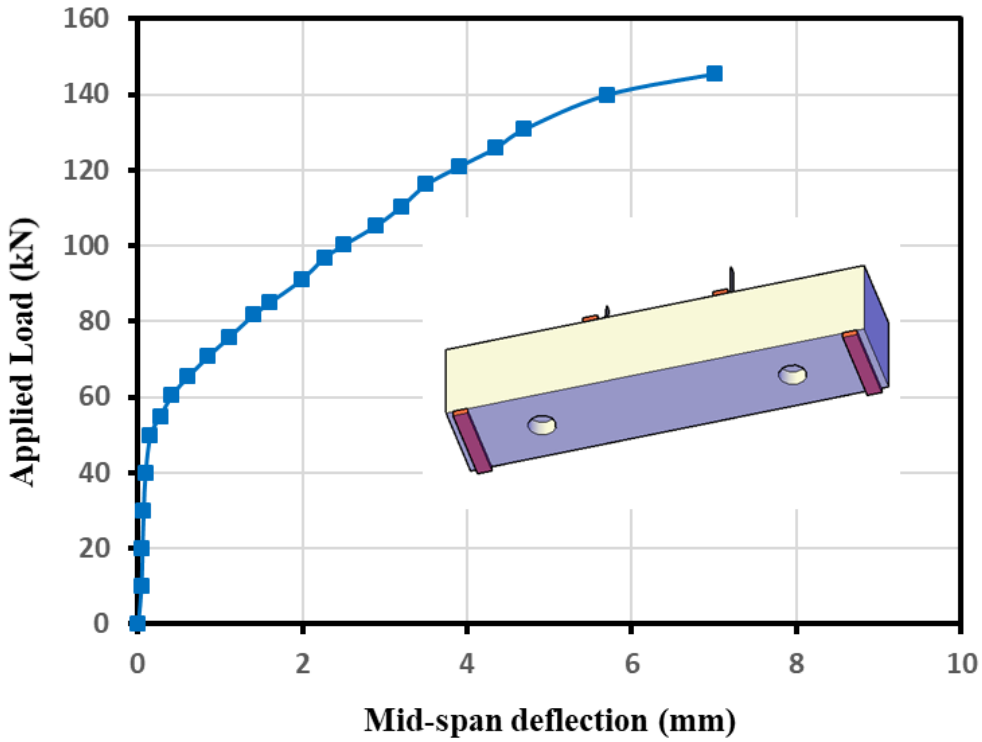

Fig. 4. 9: Load mid-span deflection curve for (H10SB)

4.2.3.3 Hollow Beams with Opening in the Mid-Span and Near the Supports at the Bottom Flange (H10SMB)

This specimen included three openings at the bottom flange; two of them are located at 250 mm from the supports, while the third one is situated at the mid-span. The first visible hair crack for H10SMB was noted at a load about 40 kN at the tension zone. After that, the first crack began to widen, and many diagonal cracks started to appear on both sides of the beam. As the load increases, the cracks developed and moved towards the utilized load and openings, as shown in **Plate 4.10**. Finally, flexure-shear failure has occurred at a load of 141 kN, which caused a reduction ratio in the load-carrying capacity by 9% if compared to HC. The load-mid-span deflection curve shown in **Fig. 4.10** revealed a linear behaviour similar to the HC at the first phase of loading. Beyond the elastic stage, the slope of the deflection curve decreased significantly due to the reduction in the stiffness by 39%, which caused an increase in the deflection at service load by 63%. The deflection ductility index value reduced markedly, and its value was 2.16. Moreover, H10SMB considered as the worst case among the beams in group 2 due to the substantial reduction in its ultimate strength, stiffness, and deflection ductility index compared with other beams within the same group.

Plate 4. 10: Mode of failure and cracks pattern for (H10SMB)

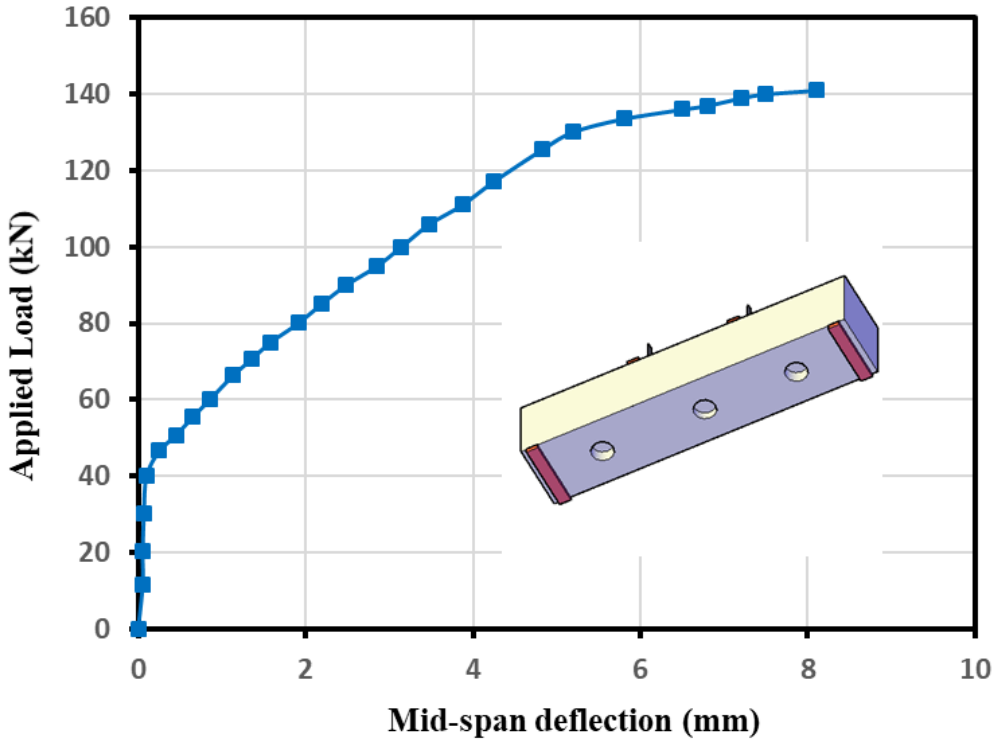

Fig. 4. 10: Load mid-span deflection curve for (H10SMB)

4.2.4 Hollow Beams with Opening Externally strengthened with CFRP Laminates

4.2.4.1 Hollow Beams Externally Strengthened with Front and Rear Opening in the Mid-Span (H10MFR-CFRP)

H10MFR-CFRP included an opening in the mid-span of the web that is externally strengthened by a full wrap of CFRP laminates of (0.167 mm) thickness on each side of the opening. The load was applied gradually, and the deformation was initially within the elastic phase at the first phase of loading. At 55 kN load in the maximum moment section, the first visible crack observed. The flexure cracks started to propagate as the load increases, and inclined cracks started to appear, which has less effect compared to flexure cracks and some of them were not visible due to the wrapped area by CFRP, as shown in **Plate 4.11**. Finally, a flexure failure at a load of 152 kN occurs. Moreover, the strengthened beam exhibited an enhancement in the ultimate failure load in which the reduction ratio was decreased to reach 1.94% if compared with HC. The load-mid-span deflection curve for H10MFR-CFRP shown in **Figure (4.11)** revealed a linear behaviour identical to the HC. The load-mid-span deflection curve for H10MFR-CFRP shown in **Fig. 4.11** displayed a linear behaviour identical to the HC. On the other hand, the stiffness

for the strengthened beam reduced by 18% that led to an increase in the deflection at service load by 22%. Meanwhile, the deflection ductility index reduced and its value was 3.17 if compared to HC.

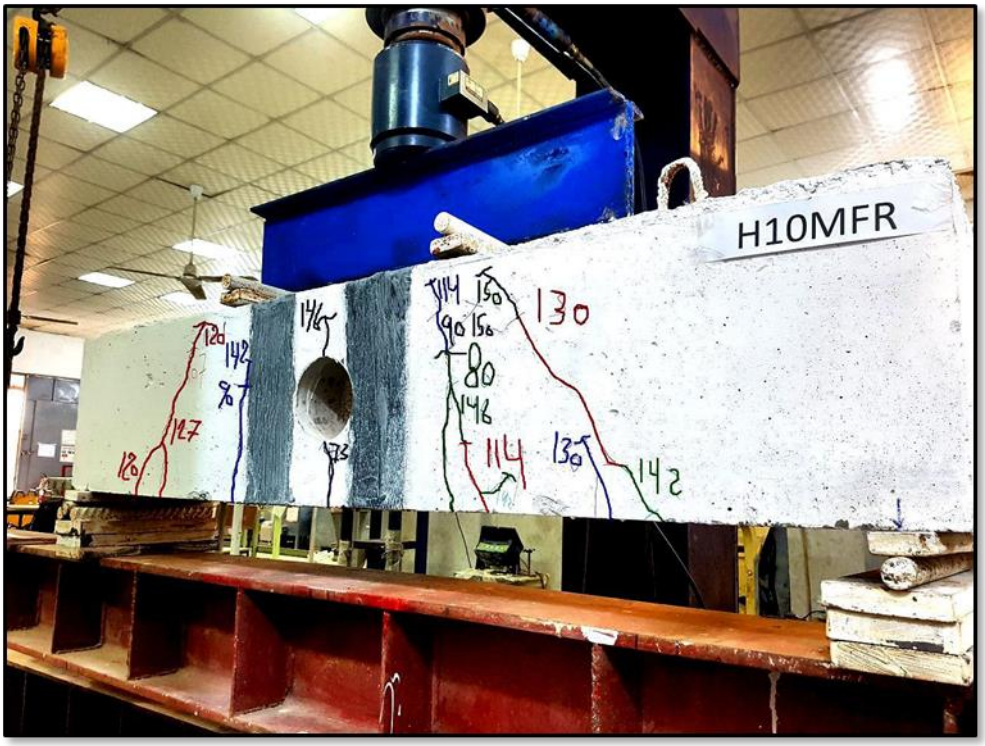

Plate 4. 11: Mode of failure and cracks pattern for (H10MFR-CFRP)

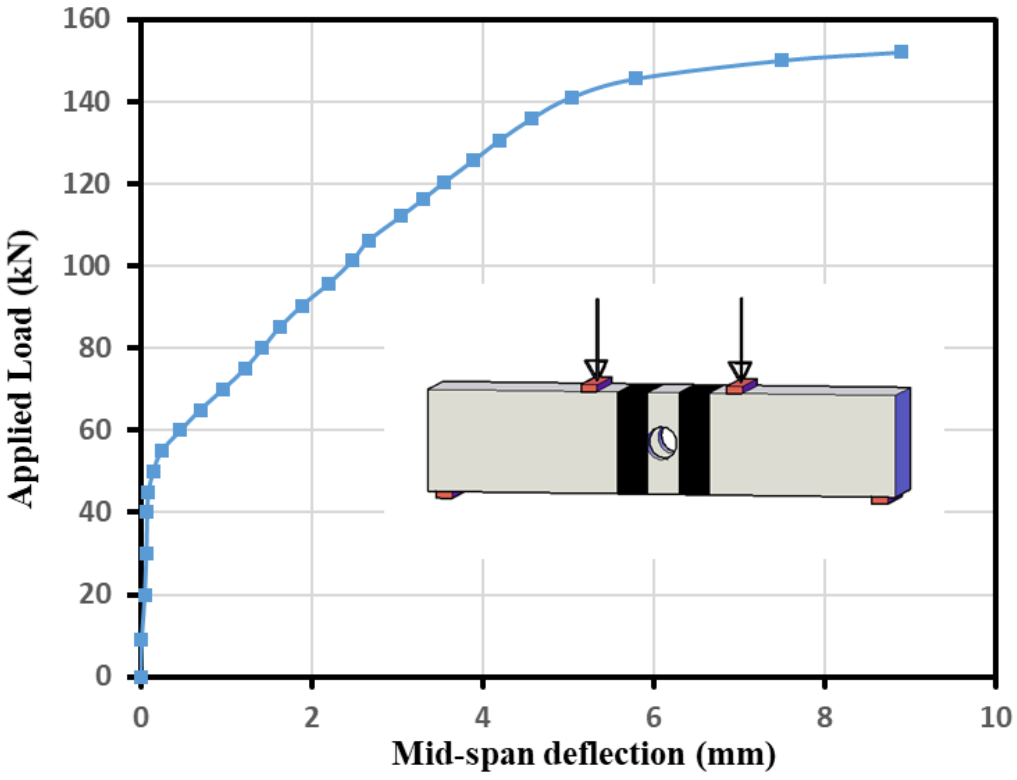

Fig. 4. 11: Load mid-span deflection curve for (H10MFR-CFRP)

4.2.4.2 Hollow Beams with Front and Rear Openings Near Supports Externally Strengthened (H10SFR-CFRP)

H10SFR-CFRP comprised two openings located at a distance 250 mm from the supports and are externally strengthened by a full wrap of CFRP laminates of (0.167 mm) thickness on each side of the openings, as shown in **Plate 4.12**. At 50 kN load, the first visible crack was noticed at the tension zone. Numerous diagonal cracks began to appear with the development of loading procedure, separated on both sides of the beam, and the flexure cracks propagated rapidly and moved towards the neutral axis. It can be noticed that inclined cracks propagation did not invade CFRP laminates and the cracks deeply permeate through the cross-section and caused failure at a load of 151 kN. Moreover, shear failure has been occurred, which led to a reduction in the ultimate strength ratio by about 2.6 if compared with HC due to the presence of openings in the shear span. The load mid-span deflection curve of H10SFR-CFRP exhibited in **Fig. 4.12** presented, in the first stage of loading, a linear behaviour similar to HC. With further load increment, the slope of the beam reduced compared to HC, and a reduction in the stiffness by 30% is occurred, which led to an increase in the deflection at service load by 43%. On the other hand, the deflection ductility index value was 2.89 if compared with HC, which evidence to more brittle behaviour.

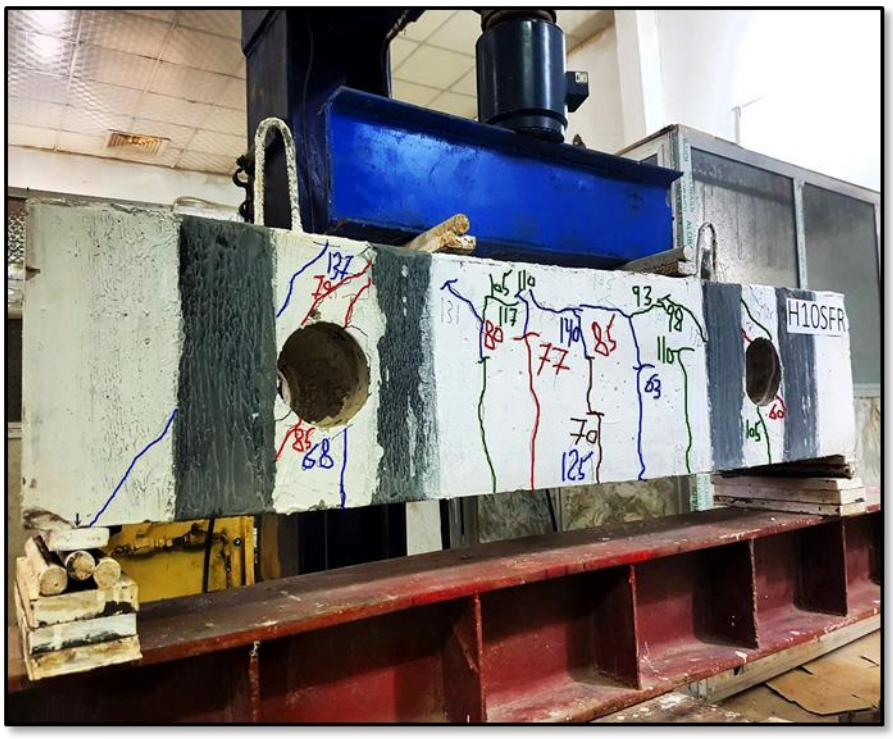

Plate 4. 12:Mode of failure and cracks pattern for (H10SFR-CFRP)

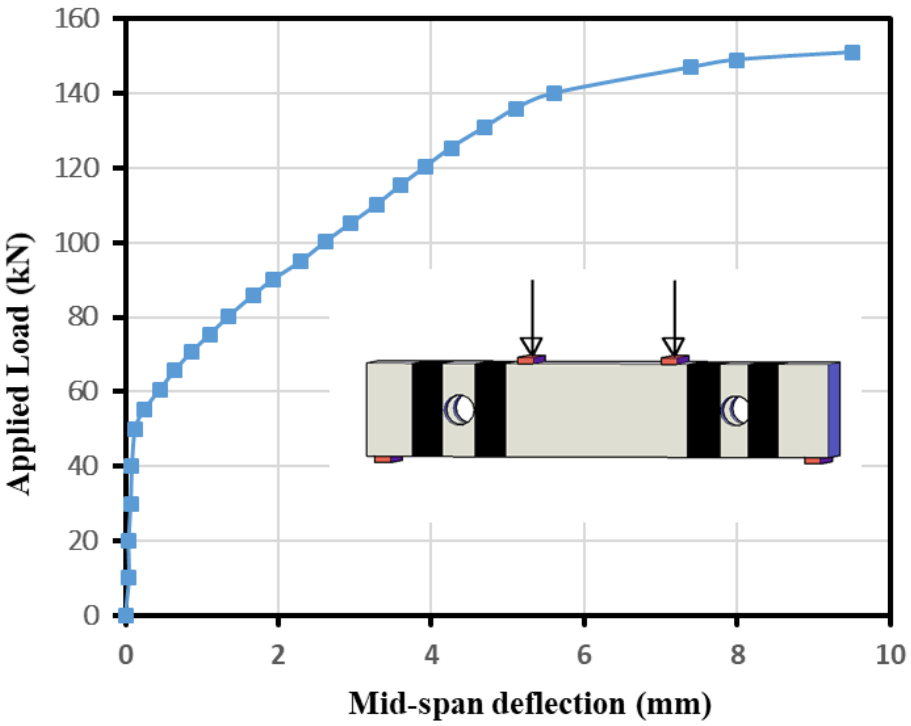

Fig. 4. 12: Load mid-span deflection curve for (H10SFR-CFRP)

4.2.4.3 Hollow Beams with Front and Rear Openings in the Mid-Span and Near the Supports Externally Strengthened (H10SMFR-CFRP)

This beam involved three openings in which two of them are located at a distance 250 mm from the supports, and the third one is located in the middle of the web. This beam was externally strengthened by a full wrap of CFRP laminates of (0.167 mm) thickness on each side of the opening. The first hair cracks were observed in the maximum bending moment section at 45 kN load. With the development of the loading procedure, numerous inclined cracks started to appear and propagated rapidly on both sides of the specimen, and stopped at the wrapping of the CFRP strips, as shown in **Plate 4.13**. Finally, flexure-shear failure has been occurred due to the combined effect of flexure and shear, at a load of about 142 kN, that cause a reduction ratio in the ultimate strength by about 8.4 % if compared to (HC). The load-mid-span deflection curve for the beam shown in **Fig. 4.13**, demonstrated a linear behaviour in the first stage of loading. After exceeding the elastic stage, the slope of the deflection curve decreased, and an increase in the deflection at service load by 29% has been occurred, due to the presence of the openings that caused

a reduction in the stiffness by 23%. Furthermore, the deflection ductility index value was 2.35 if compared to HC, which refers to brittle behaviour.

Plate 4. 13: Mode of failure and cracks pattern for (H10SMFR-CFRP)

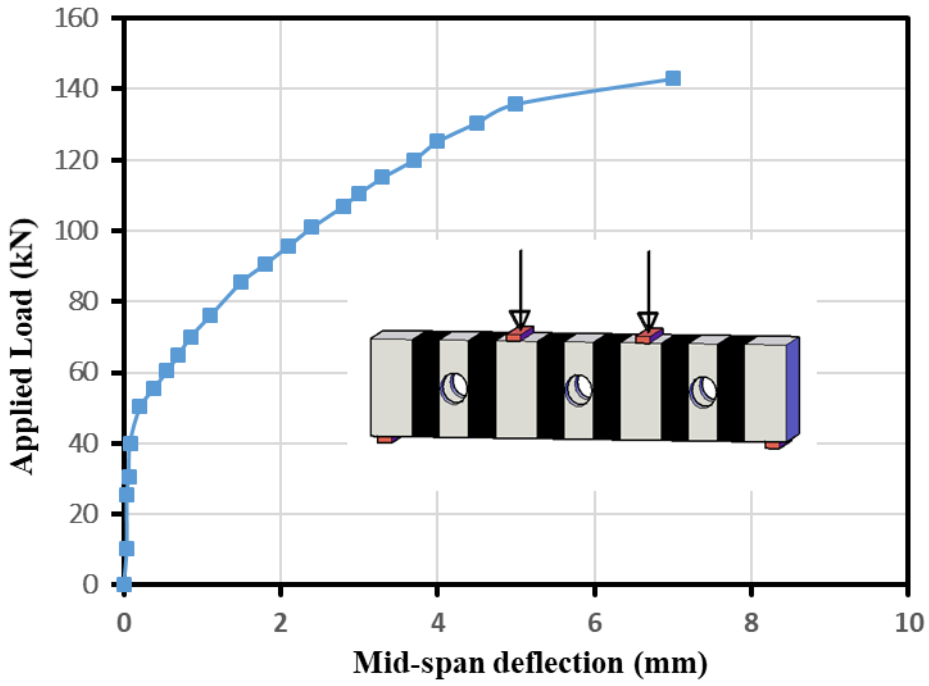

Fig. 4. 13: Load mid-span deflection curve for (H10SMFR-CFRP)

4.2.5 Summary of Test Results

The following notes were obtained as a summary for the results of the hollow reinforced SCC beams with an in-place circular opening that are strengthened or unstrengthened:

1. The first cracking load appeared in the flexure zone at a load range between (35-55) kN, as given in **Table 4.1**.
2. For group 1, it can be noticed that creating an opening in an existing hollow SCC beam caused a reduction in the ultimate load in which H10MF showed the smallest reduction with ratio of 5.2% while H10SMFR showed the most considerable reduction with a ratio of 16% if compared with HC, as shown in Table **4.1**.
3. For group 2, the smallest reduction in the ultimate load was noticed in H10MB with a ratio of 5.5% against the most substantial reduction in H10SMB with a ratio of 9% if compared with HC, as shown in Table **4.1**.
4. Most of the beams results indicated in **Table 4.1** displayed a flexural or flexural-shear failure, while three specimens exposed to sudden shear failure. This might be because of two of the stirrups intercepted by the openings, which made them inefficient to carry any significant applied shear existing by the opening in the shear span, or due to change in the section geometry that occurred by the opening.
5. Creating an opening in an existing beam decreased the deflection ductility index value, as shown in **Table 4.2** if compared with HC.
6. The external strengthening by CFRP laminates for the hollow SCC beams in group 3 enhanced the post-cracking behaviour of specimens and delayed the appearing of cracks compared to the unstrengthened beams due to redistributing stresses during loading process by CFRP laminates, which enable the specimen to resist more applied stresses, as exhibited in **Table 4.2**.
7. The external strengthening by CFRP laminates increased the ultimate failure load for H10MFR-CFRP, H10SFR-CFRP, and H10SMFR-CFRP in which the enhancement ratios were (8.3%, 8.8%, 9%), respectively if compared with the unstrengthened beams (H10MFR, H10SFR, and H10AMFR).
8. Strengthening beams by CFRP laminates increased the stiffness's of the beams (see **Table 4.2)**, which led to a reduction in the deflection of these specimens.

9. The strengthening by CFRP laminates enhanced the deflection ductility index for H10MFR-CFRP, H10SFR-CFRP, and H10SMFR-CFRP, as the values were (3.17, 2.89, 2.35) respectively if compared with the unstrengthened specimens (H10MFR, H10SFR, H10AMFR) where the values were (2, 1.92, 1.53), respectively.

Table 4. 1: Summary Results of Tested specimens

Group	Specimen Designation	First Crack P_{cr} (kN)	Ultimate Load Pu(kN)	Reduction Ratio% $\frac{(Pu_{(HC)} - Pu(specimen))*100}{Pu_{(HC)}}$	Failure Mode
	HC	55	155	-	Flexure
Group 1	H10MF	50	147.0	5.20	Flexure
	H10SF	40	144.5	6.80	Shear
	H10SMF	37	143.0	7.70	Flexure + Shear
	H10MFR	45	140.3	9.50	Flexure
	H10SFR	40	138.8	10.5	Shear
	H10SMFR	35	130.2	16.0	Flexure + Shear
Group 2	H10MB	52	146.4	5.50	Flexure
	H10SB	46	145.5	6.10	Flexure
	H10SMB	40	141.0	9.00	Flexure + Shear
Group 3	H10MFR-CFRP	55	152.0	1.94	Flexure
	H10SFR-CFRP	50	151.0	2.60	Shear
	H10SMFR-CFRP	45	142.0	8.40	Flexure + Shear

Table 4. 2: Stiffenesses and ductility indices of Tested specimens

Group	Specimen Designation	Stiffens at service load (FS= 0.7 Fu) K= FS / Δy	Reduction ratio for service Stiffens % $\frac{(k_{(HC)} - k(specimen))*100}{k_{(HC)}}$	Deflection at service load Δy= 0.7 Fu (mm)	Increasing ratio for service deflection % $\frac{(\Delta y_{(HC)} - \Delta y(specimen))*100}{\Delta y_{(HC)}}$	Maximum Deflection (Δu mm)	Ductility index (Δu/ Δy)
	HC	47.8		2.3		11.7	5
G1	H10MF	40.0	16	2.75	20	7.8	2.80
	H10SF	34.4	28	3.20	39	7.6	2.37
	H10SMF	31.4	34	3.50	52	7.5	2.14
	H10MFR	38.6	19	2.85	24	5.8	2.00
	H10SFR	29.7	38	3.70	61	7.1	1.92
	H10SMFR	28.4	41	3.87	68	5.9	1.53
G2	H10MB	37.3	22	2.95	28	7.4	2.50
	H10SB	36.7	23	3.00	30	7.0	2.33
	H10SMB	29.3	39	3.75	63	8.1	2.16
G3	H10MFR-CFRP	39.3	18	2.80	22	8.9	3.17
	H10SFR-CFRP	33.5	30	3.28	43	9.5	2.89
	H10SMFR-CFRP	37.0	23	2.97	29	7.0	2.35

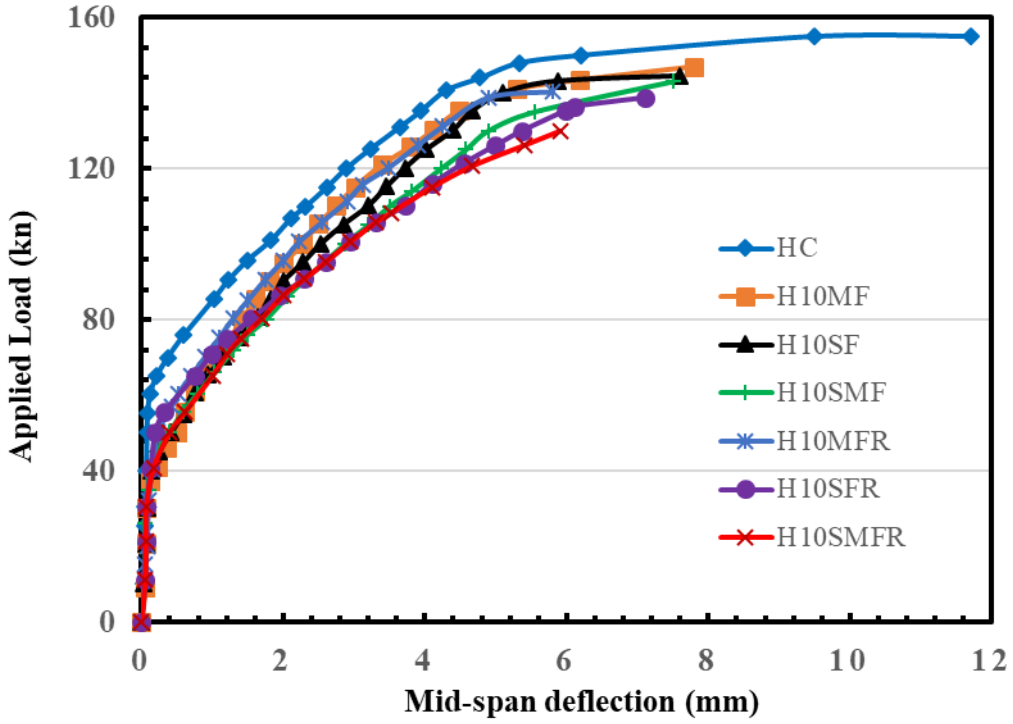

Fig. 4. 14: Load mid-span deflection curve for beams of group 1

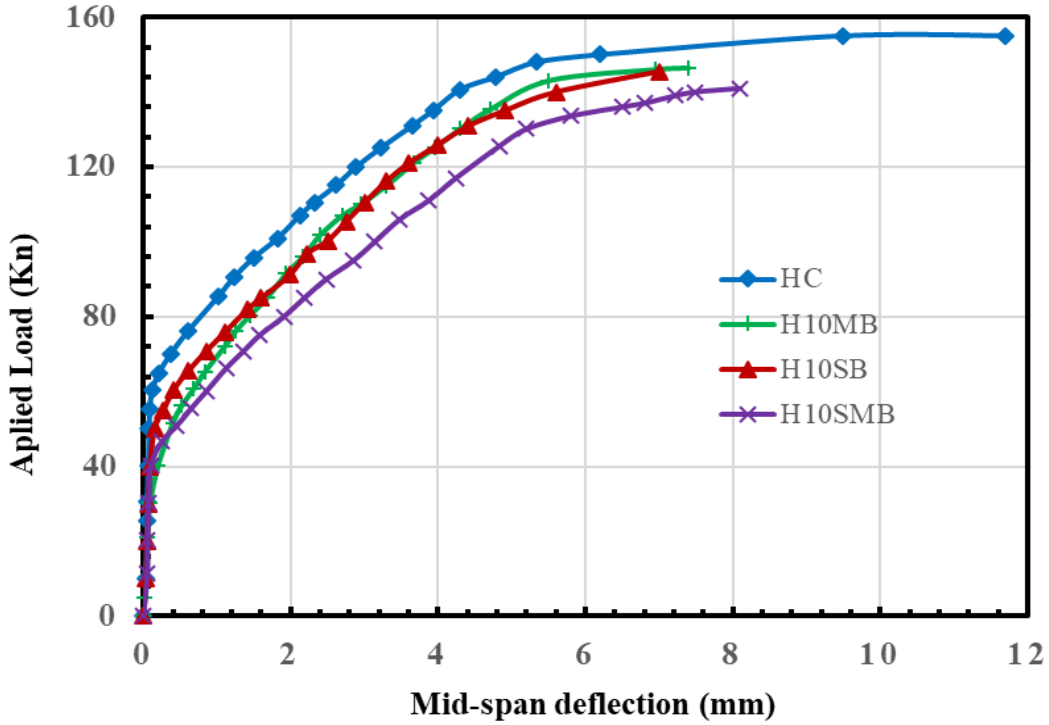

Fig. 4. 15: Load mid-span deflection curve for beams of group 2

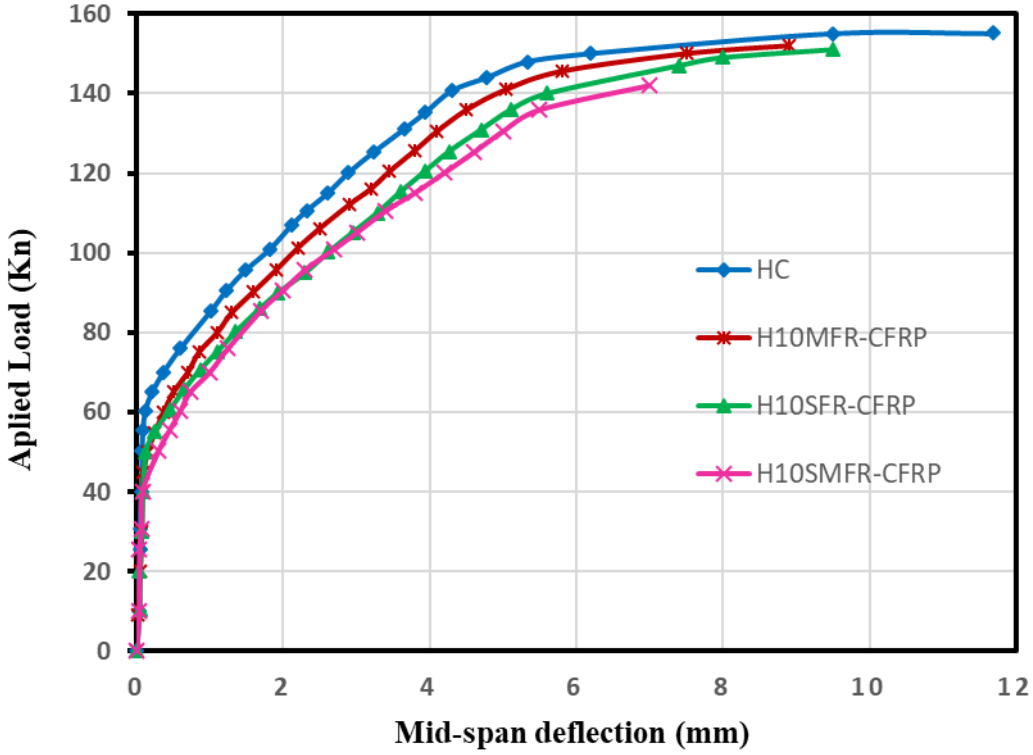

Fig. 4. 16: Load mid-span deflection curve for tested beams of group 3

CHAPTER FIVE

FINITE ELEMENT ANALYSIS

5.1 Introduction

The present chapter aims to make a comparison between the results of the experimental analysis, and the finite element analysis, to ensure the appropriateness of materials properties, elements type, and convergence criteria. This can help in modelling the response of hollow reinforced SCC beams with and without an opening (s) strengthened and non-strengthened with CFRP strips. Thus, a nonlinear finite element analysis has been carried out in this chapter to analyse the tested specimens in chapter four, and to study new important variables by using powerful nonlinear finite element method package (ABAQUS/Standard 2019).

5.2 Description of Finite Element Modelling

This section presents a description to the geometry of the tested beams, loading and boundary condition used in the current study.

5.2.1 Modelling of SCC Hollow Beam

To simulate the reinforced hollow SCC beam, the same geometry, material properties, loading and boundary condition used in the experimental work were utilised in the finite element modelling. In general, five parts were involved in the modelling of the thirteen SCC hollow beams. These parts were concrete properties, flexural reinforcement, shear reinforcement, steel plates, and CFRP sheets. Every part was drawn alone, and then they were assembled to form the specimen model. After the assembly step, parts must bond with each other, where the steel was embedded inside the concrete by embedded region constrain to form one mass. On the other hand, tie constraint was used to connect the concrete with steel plates. To achieve an appropriate stress distribution in the 3D finite element analysis, concrete and steel plates have meshed into linear solid brick element with reduced integration (C3D8R), while steel reinforcement has meshed into linear truss element (T3D2), as shown in **Fig. 5.1**.

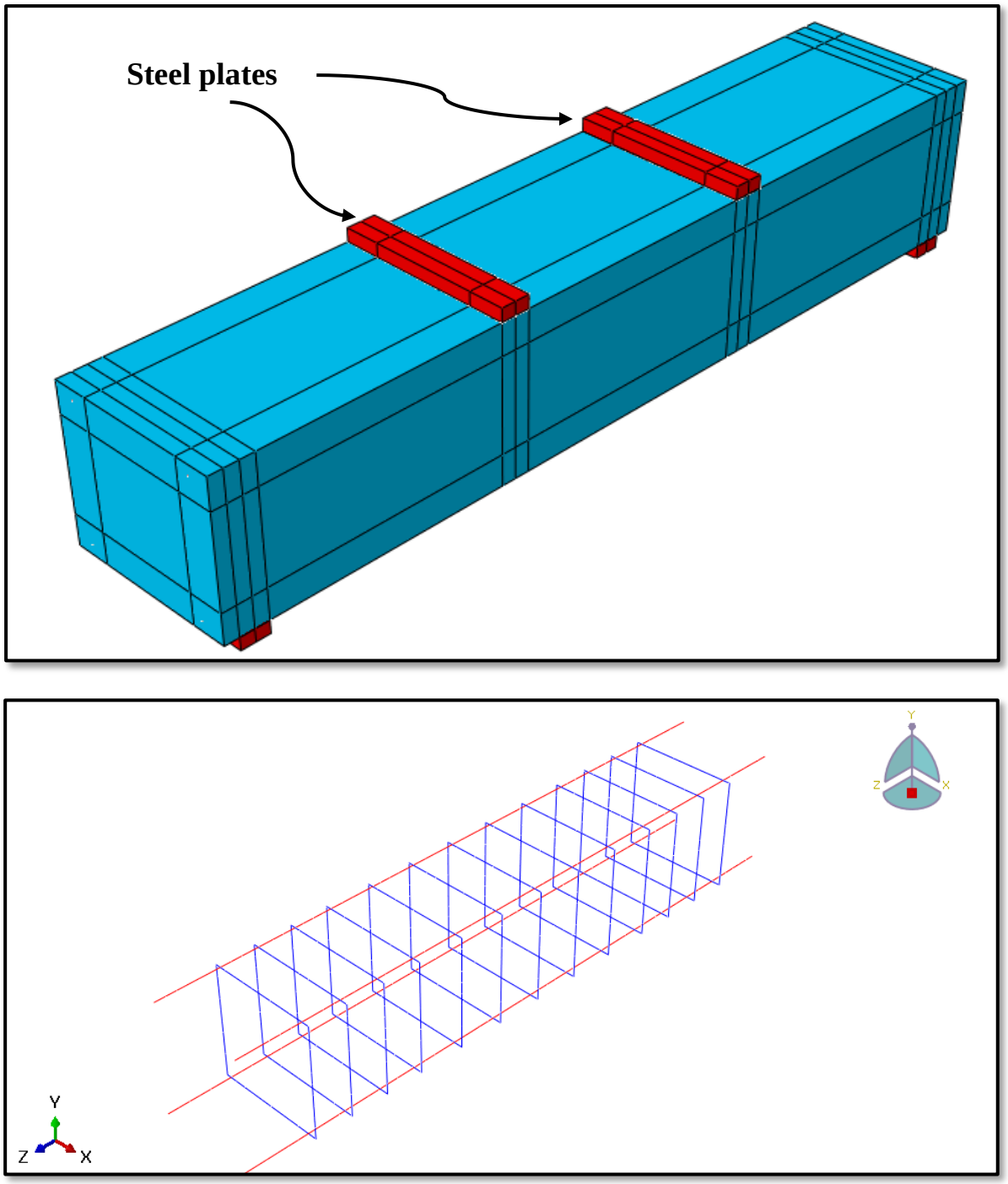

Fig. 5. 1: Assembled parts of the SCC hollow beam model

In the beams that are externally strengthened (group 3), the lamina option for the elastic behaviour of the CFRP laminate, which has been treated as a linearly elastic material was selected. The CFRP lamina was modelled using shell element, and a tie constraint was used to bond the CFRP and the concrete. After that, it meshed by using S4R (a 4-node thin shell with reduced integration). **Figure 5.2** shows the CFRP arrangement for the tested beams. The

modelling of material properties for concrete, steel reinforcement, CFRP laminate are presented in **Appendix-B**.

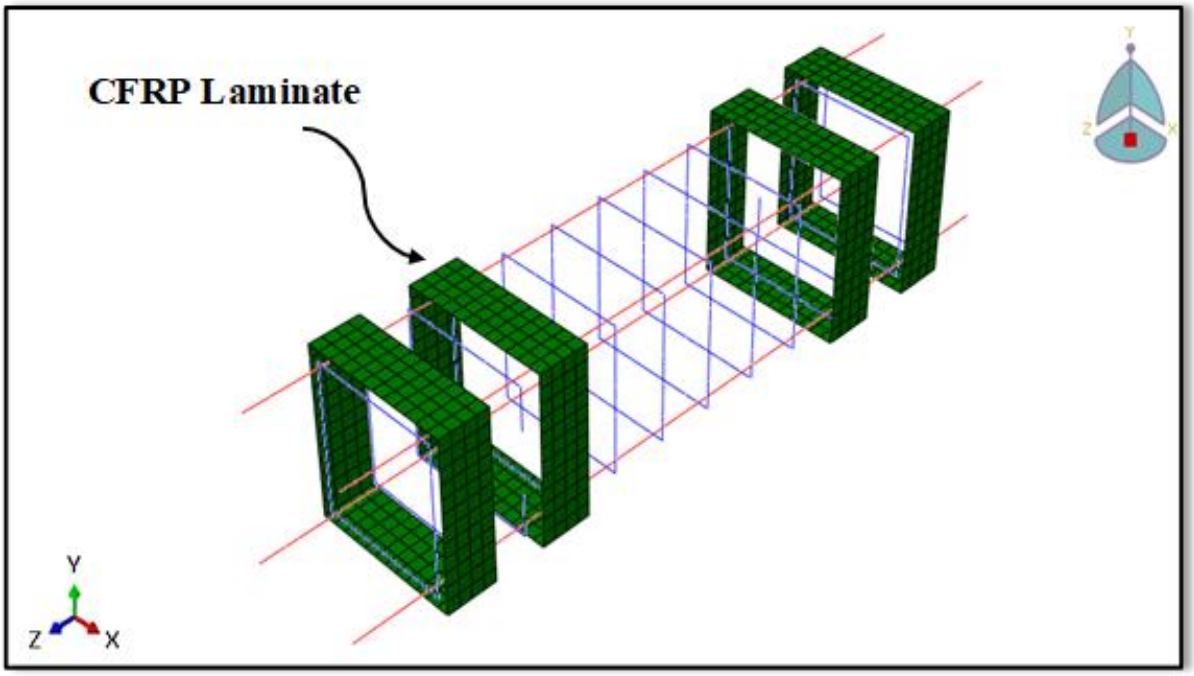

Fig. 5. 2: CFRP Laminates arrangement of the tested beams

5.3.2 Loading and Boundary Conditions

In the experimental work, the loads were applied on each tested beam by two points. Two steel plates have performed these loads with dimensions (50×25×300) mm located at the top face to transform the loads to the tested beam, as illustrated in **Fig. 5.3**.

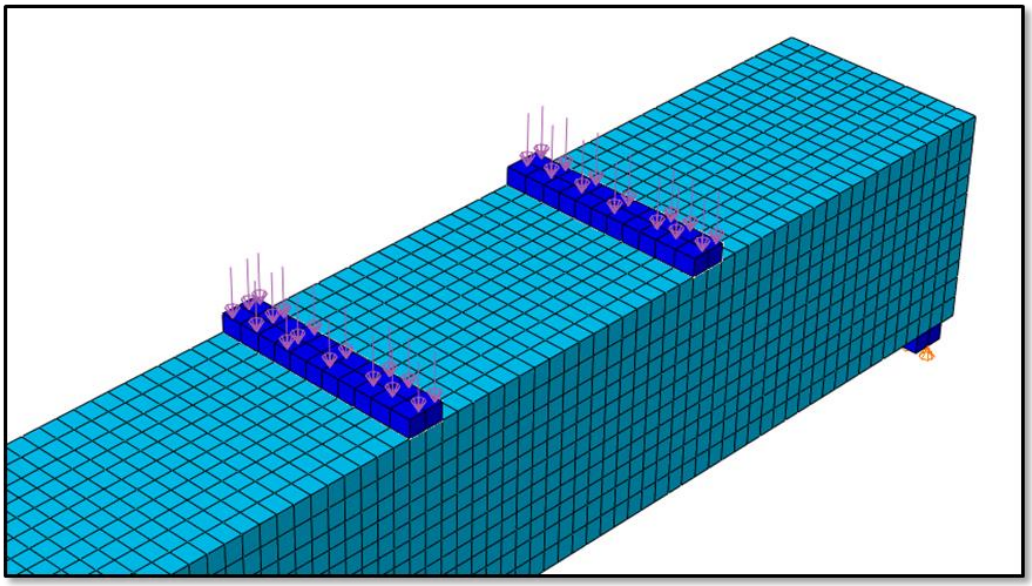

Fig. 5. 3: Distribution of applied load on steel plates

Displacements at the boundaries was used to constrain all reinforced concrete specimens models to get the appropriate solution. All models were constrained in the z-direction, and y-direction (Uz=Uy=Ux= 0) at the hinge support, while constrained in the y-direction and x-direction (Uy= Ux=0) at the roller support, as illustrated in **Fig. 5.4**.

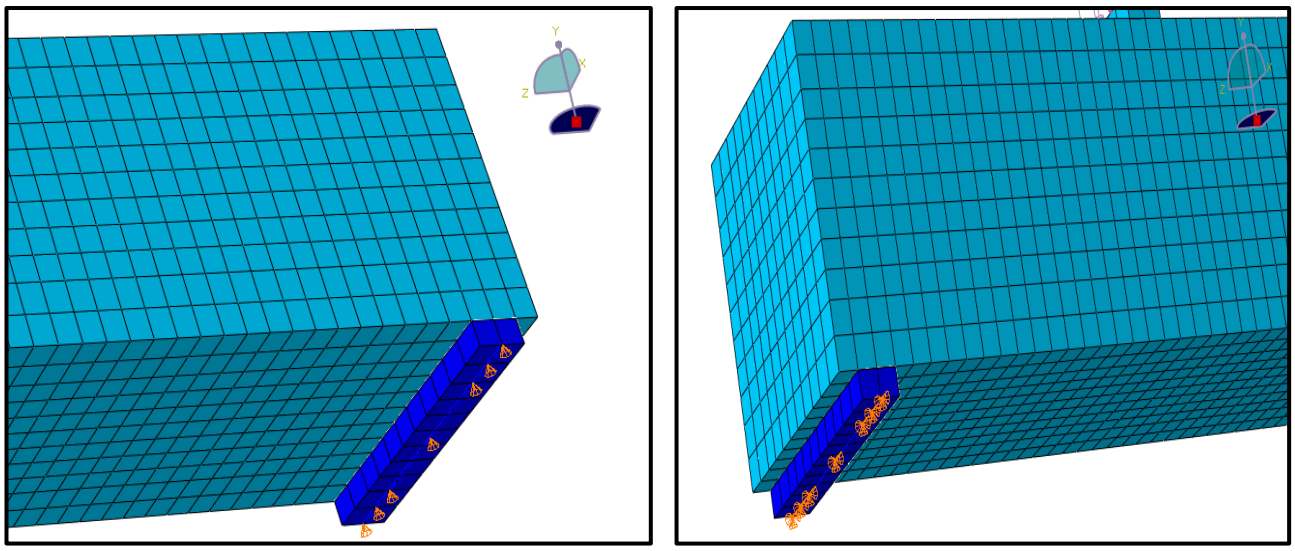

(a) **(b)**

Fig. 5. 4: Boundary conditions of the hinge and roller supports
(a) roller Support, (b) hinge Support

5.2 Convergence Study

The mesh size selection is an essential step in finite element modelling. Adequate pre-analysis for different mesh densities was carried out to decide the best density that gives the desired precision. Good convergence is achieved in the result when the beam is divided into an adequate number of elements, and it becomes visible when the decrease in the mesh size has a small effect on the result. For this purpose, and in the current FEA, a convergence study was made to get the suitable mesh size. The convergence study was done by choosing the element size of the model (HC) (50, 40, 30, 25, 20, and 15 mm), as shown in **Fig. 5.6**. From the convergence study, it can be noticed that the change in the ultimate load can be neglected when the mesh size decreased from 25 to 20. Furthermore, the deflection value becomes more accurate when compared with the experimental result for the control beam, as shown in **Table 6.1**. For that purpose, a (25 mm) mesh size was selected for all the tested beam. **Fig. 5.5** shows the changes in the load-mid-span deflection with varying mesh sizes.

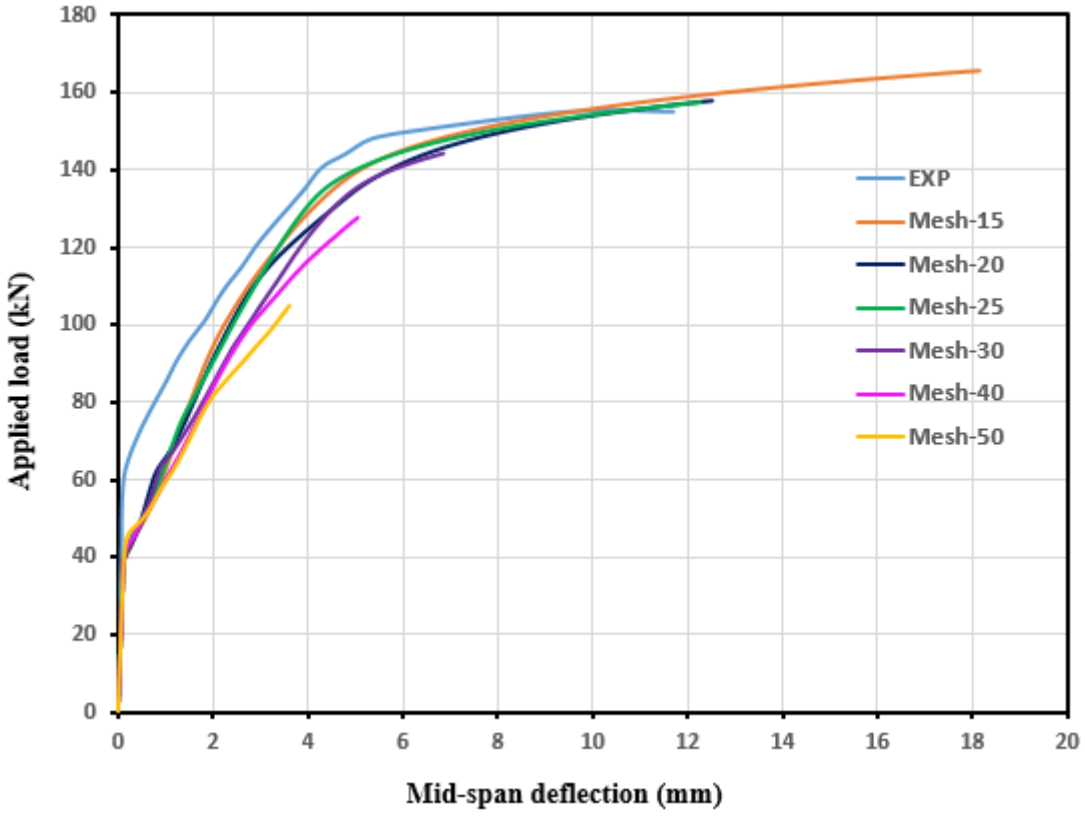

Fig. 5. 5: Mesh size effect of on mid-span load-deflection curve

Table 5. 1: Effect of mesh size on ultimate load and deflection

Mesh size		Ultimate load, kN	Maximum Deflection, mm
15	Exp.	155.0	11.7
	FEA.	165.6	18.2
20	Exp.	155.0	11.7
	FEA	157.8	12.5
25	Exp.	155.0	11.7
	FEA	157.4	12.2
30	Exp.	155.0	11.7
	FEA	144.2	6.90
40	Exp.	155.0	11.7
	FEA	127.7	5.00
50	Exp.	155.0	11.7
	FEA	`104.9	3.60

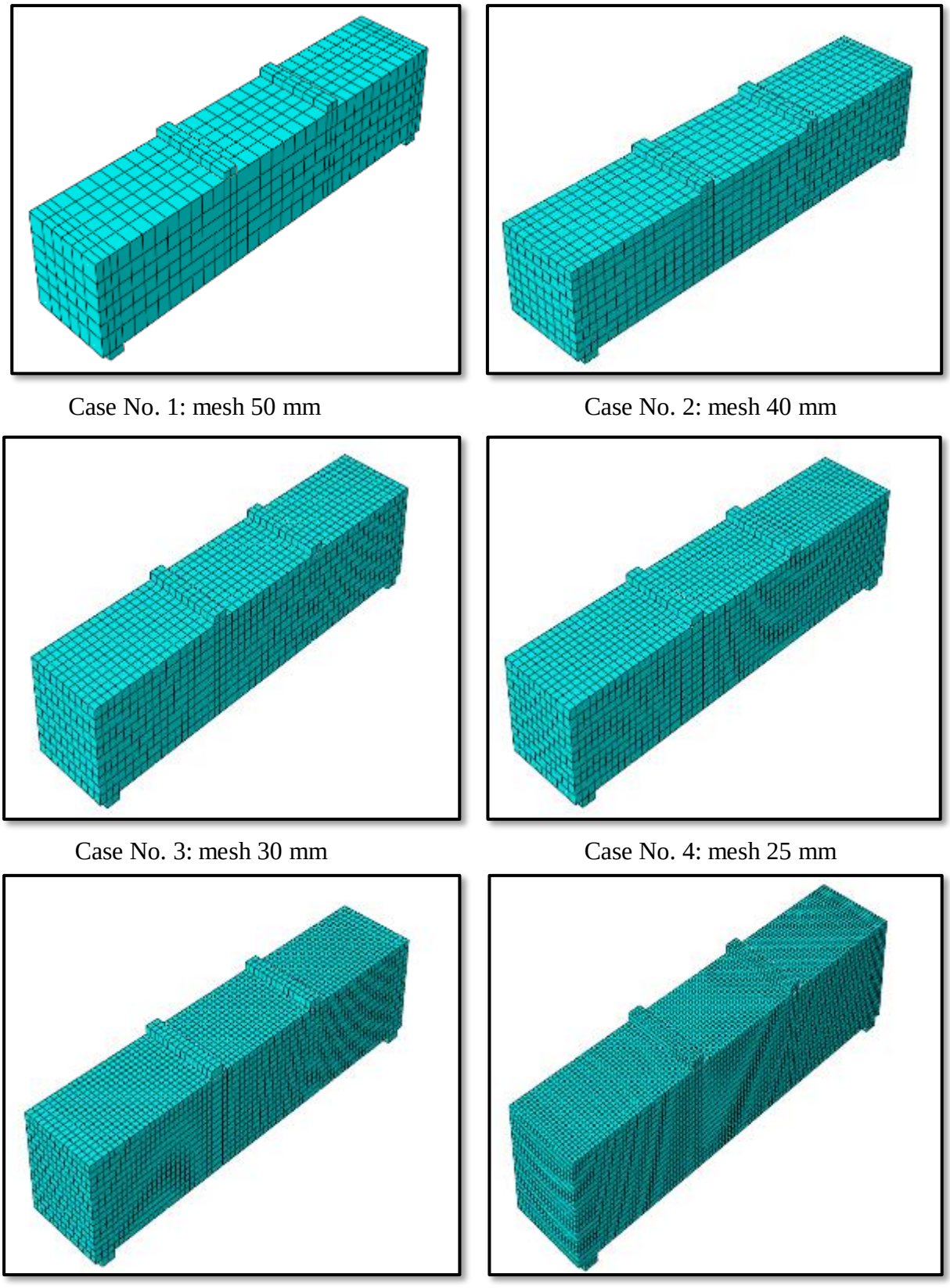

Case No. 1: mesh 50 mm

Case No. 2: mesh 40 mm

Case No. 3: mesh 30 mm

Case No. 4: mesh 25 mm

Case No. 5: mesh 20 mm

Case No. 6: mesh 15 mm

Fig. 5. 6: Finite element mesh density

5.4 Comparison between FEA and Experimental Results

In this section, the results of the experimental work are compared with that of the finite element. The comparison is made in terms of the ultimate load, maximum deflection, cracks pattern at failure, and load-deflection curve.

5.4.1 Load Deflection Behaviour

Figures 5.7 to 5.19 present a comparison between the numerical and experimental load-deflection curves in which the deflections are measured at the mid-span point for all tested specimens in the experimental work. The comparison revealed the validity of the numerical results obtained from the ABAQUS program by showing a good convergence with the experimental results that were previously discussed in chapter four.

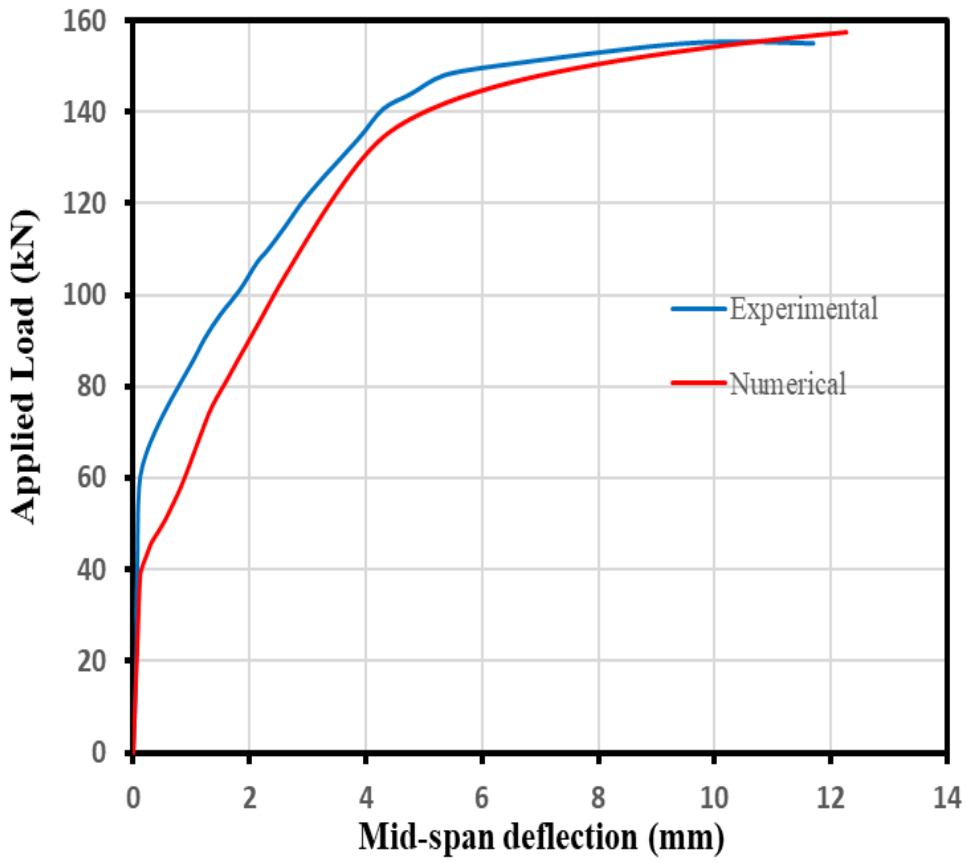

Fig. 5. 7: Experimental and numerical load-deflection curves for (HC)

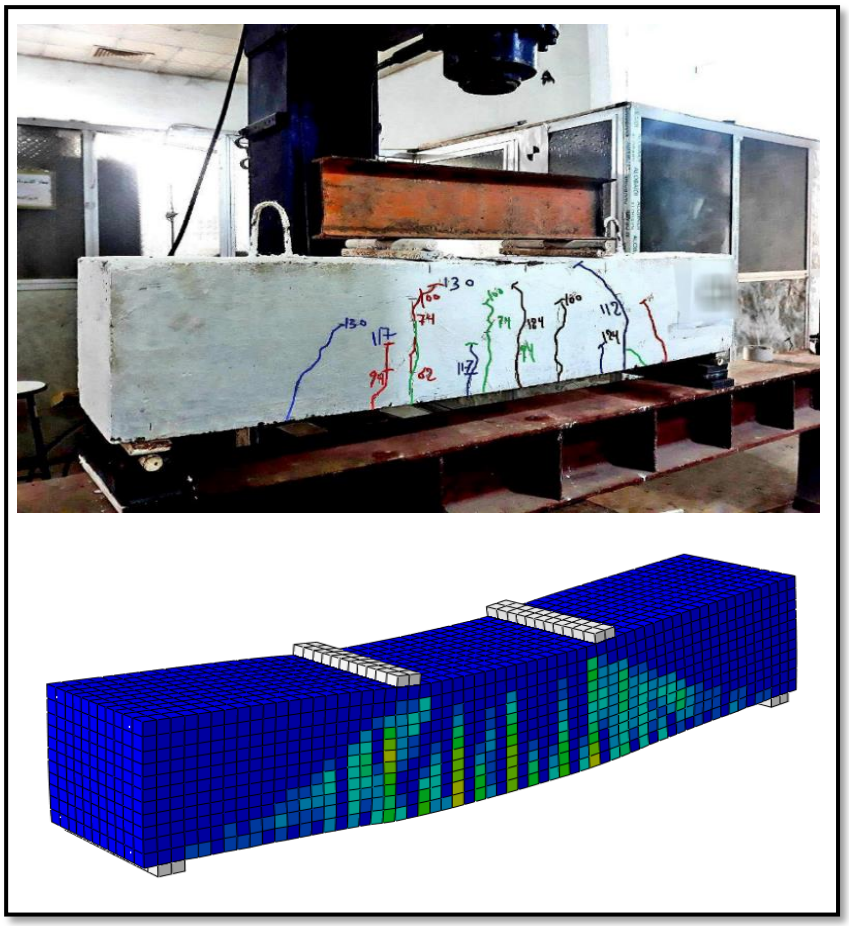

Plate 5. 1: Experimental and numerical cracks patterns for (HC)

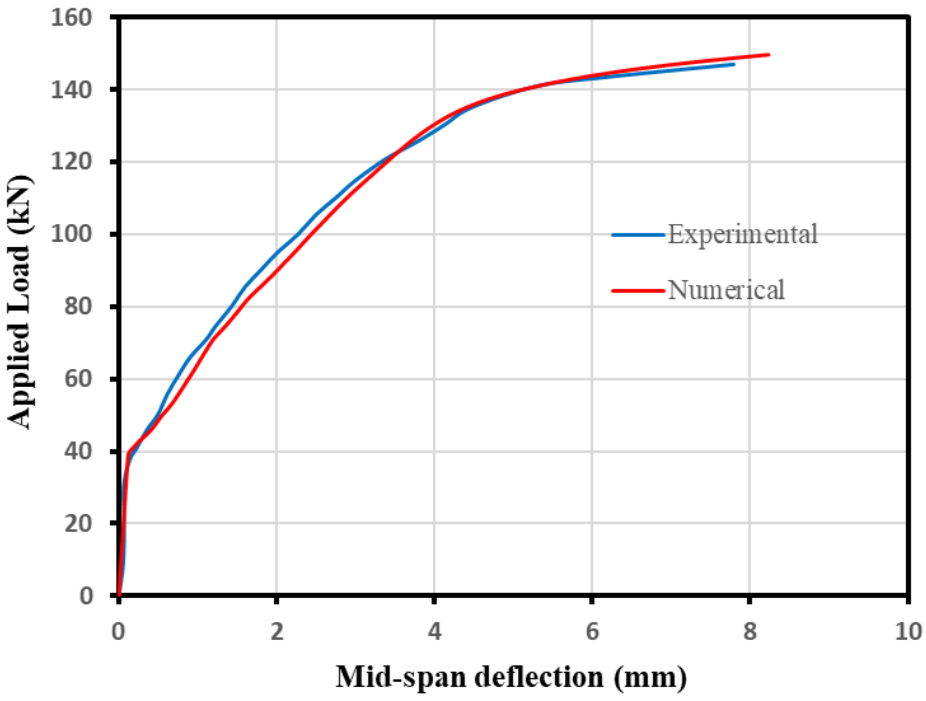

Fig. 5. 8: Experimental and numerical load-deflection curves for (H10MF)

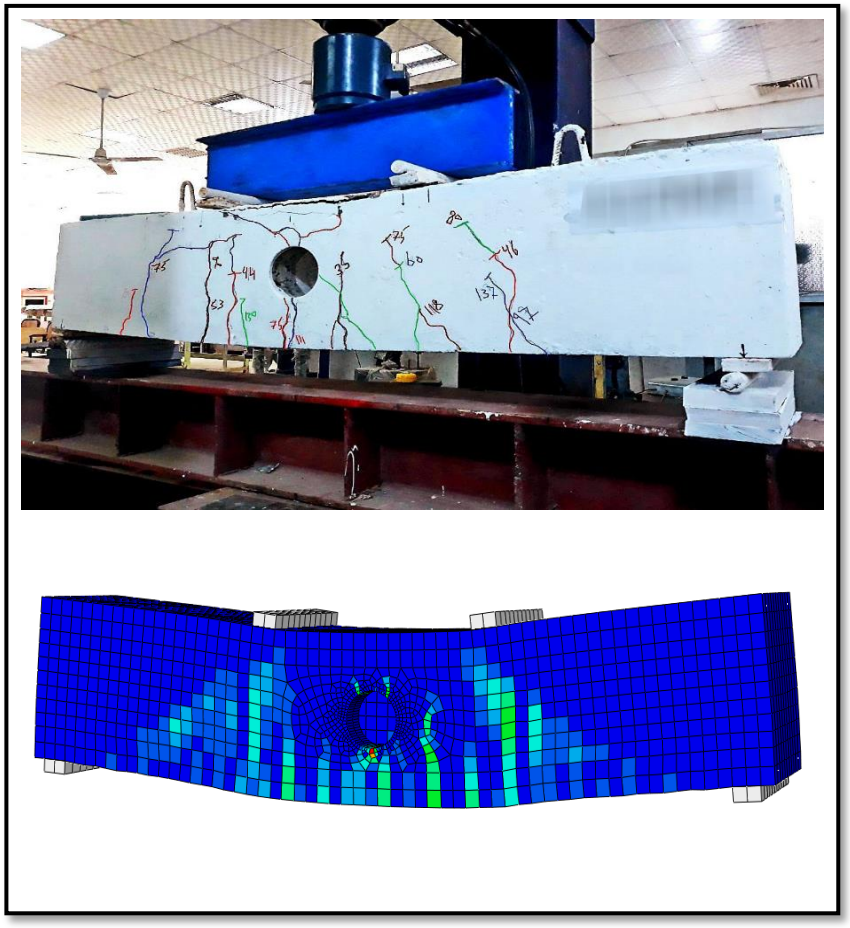

Plate 5. 2: Experimental and numerical cracks Patterns for (H10MF)

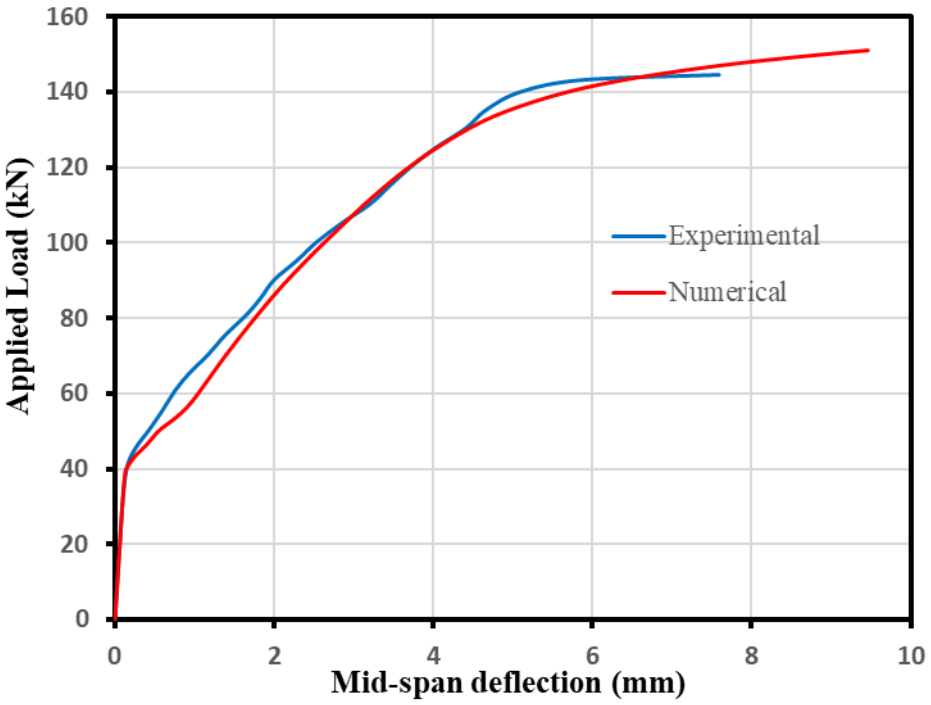

Fig. 5. 9: Experimental and numerical load-deflection curves for (H10SF)

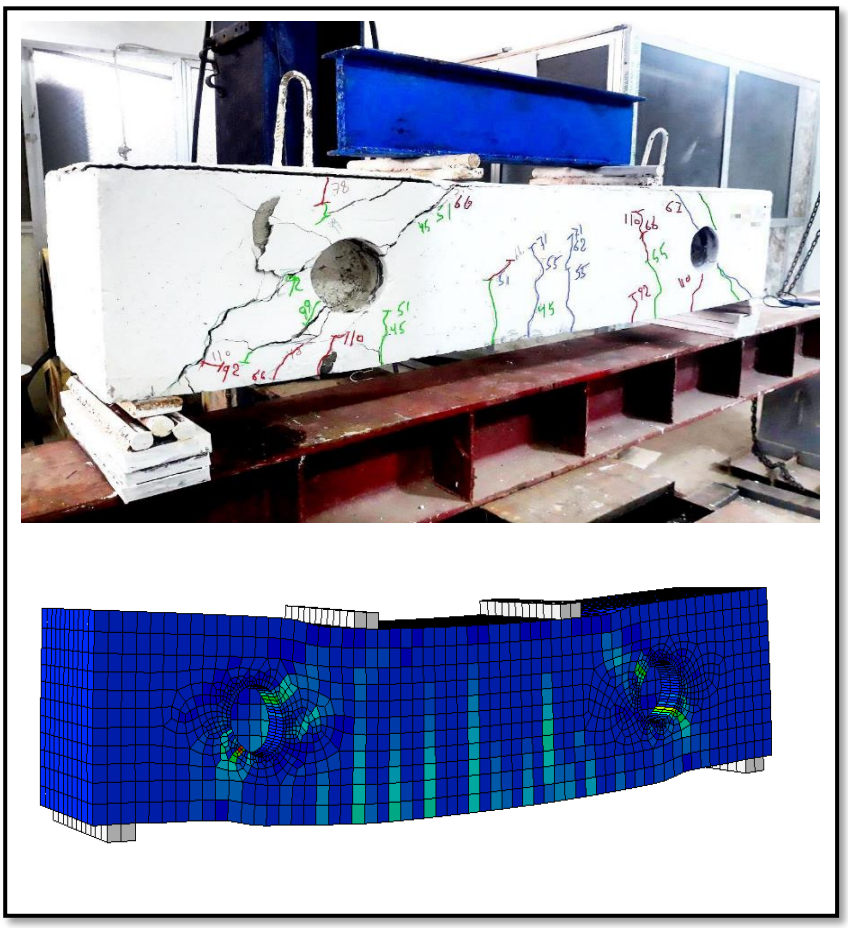

Plate 5. 3: Experimental and numerical cracks Patterns for (H10SF)

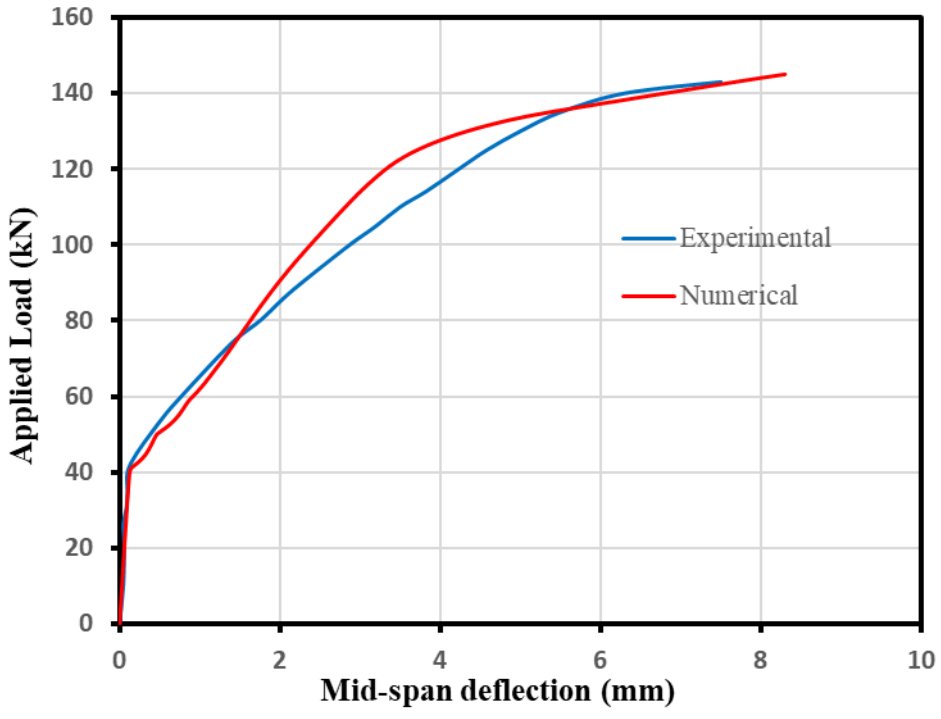

Fig. 5. 10: Experimental and numerical load-deflection curves for (H10SMF)

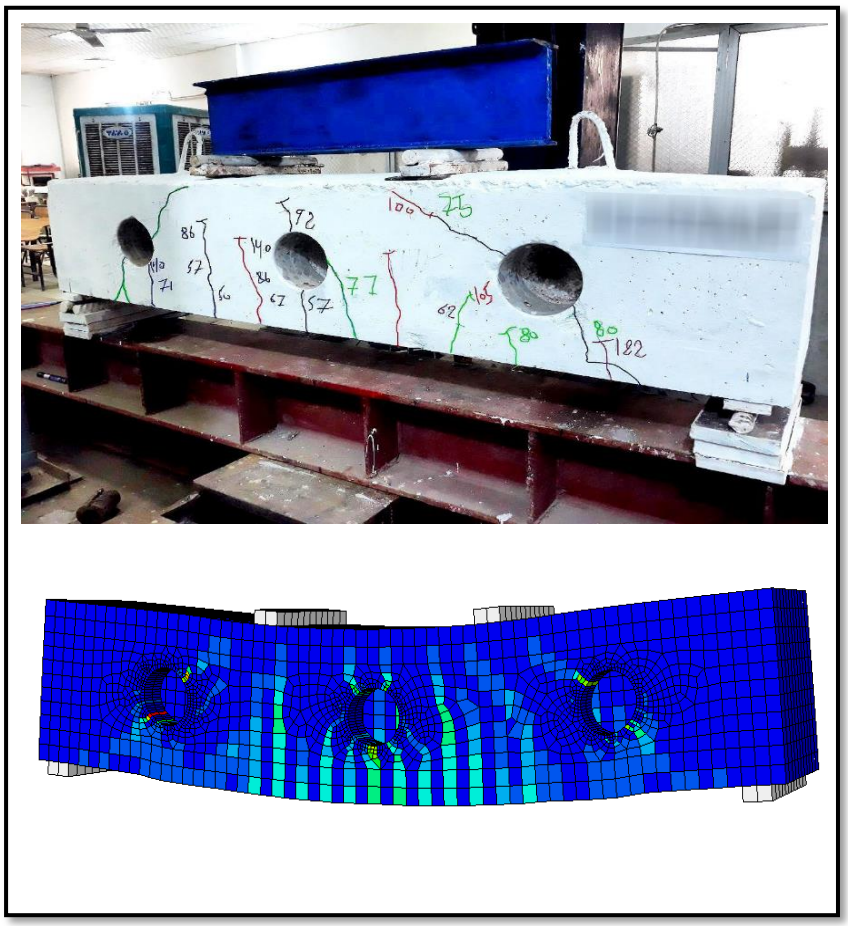

Plate 5. 4: Experimental and numerical cracks Patterns for (H10SMF)

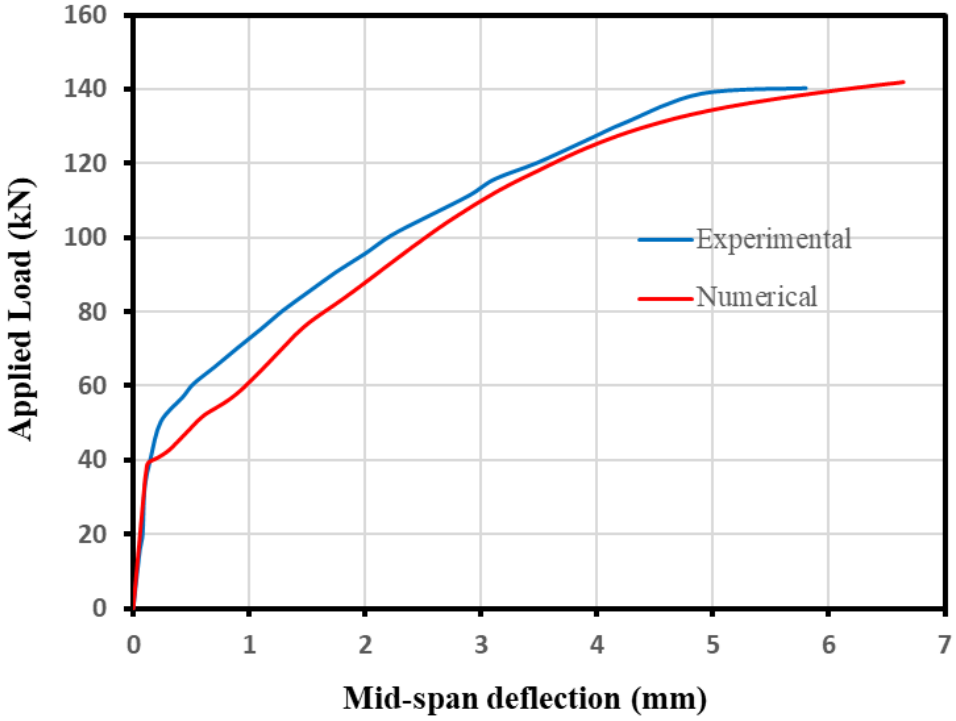

Fig. 5. 11: Experimental and numerical load-deflection curves for (H10MFR)

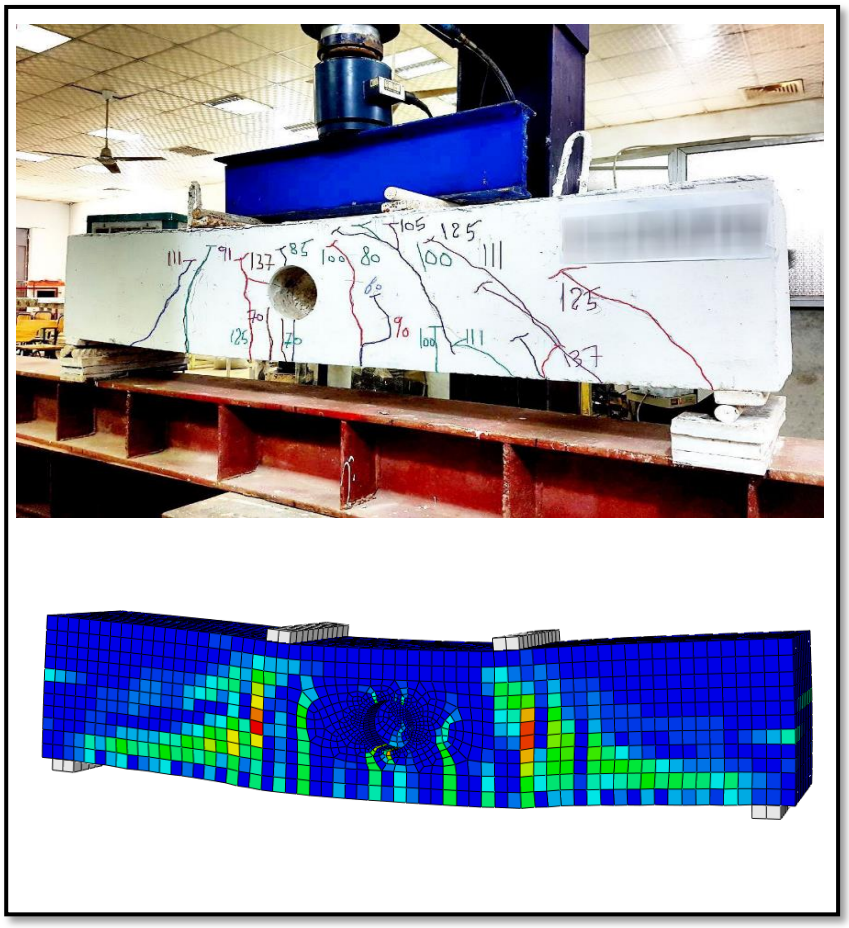

Plate 5. 5: Experimental and numerical cracks Patterns for (H10MFR)

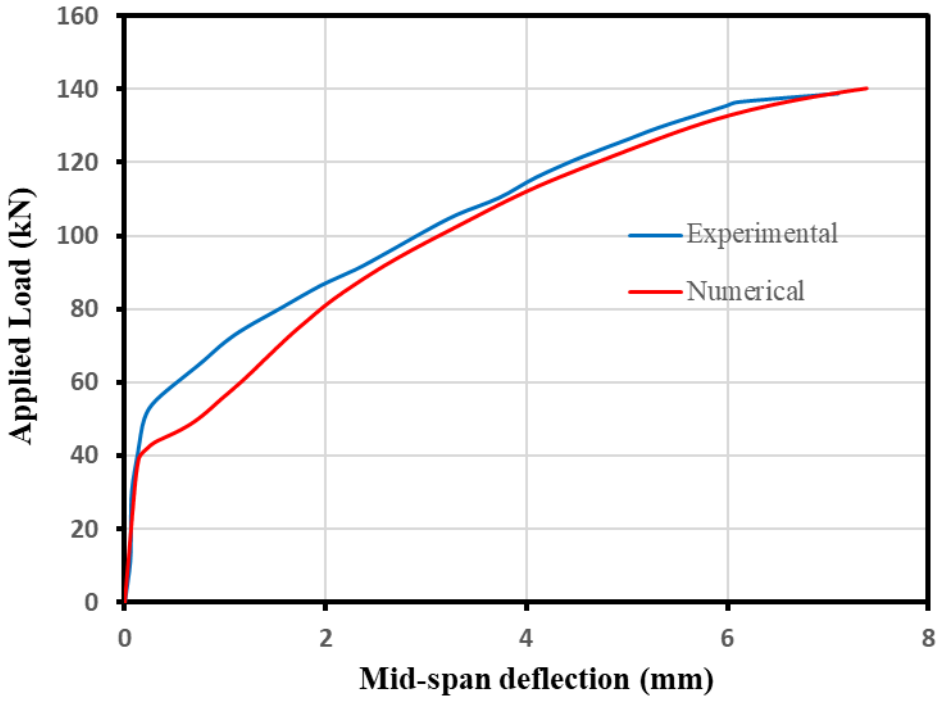

Fig. 5. 12: Experimental and numerical load-deflection curves for (H10SFR)

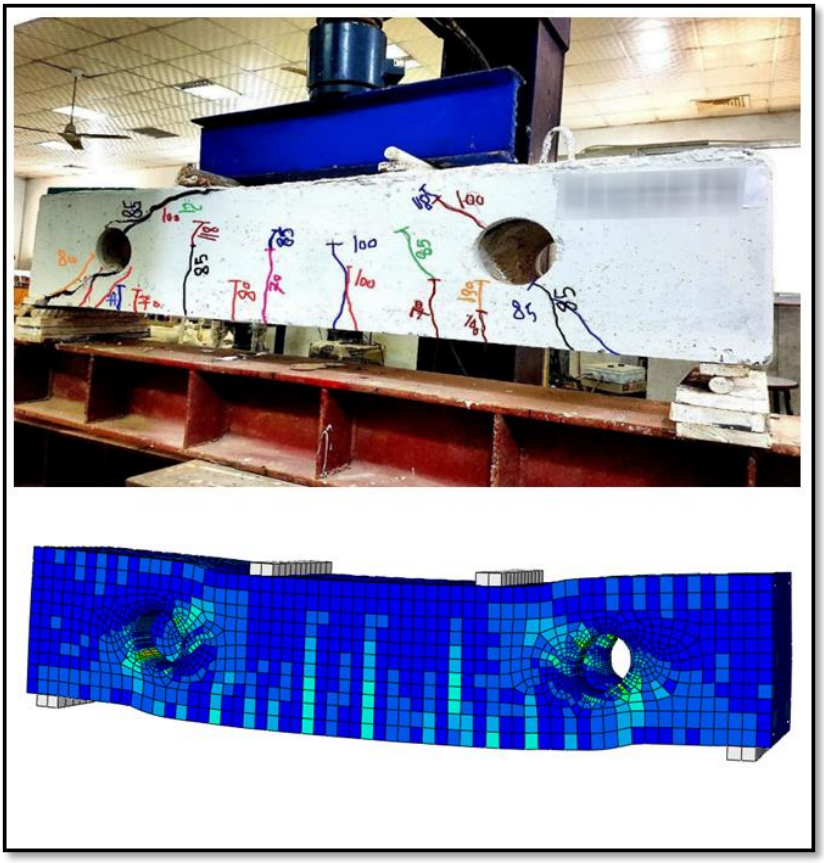

Plate 5. 6: Experimental and numerical cracks Patterns for (H10SFR)

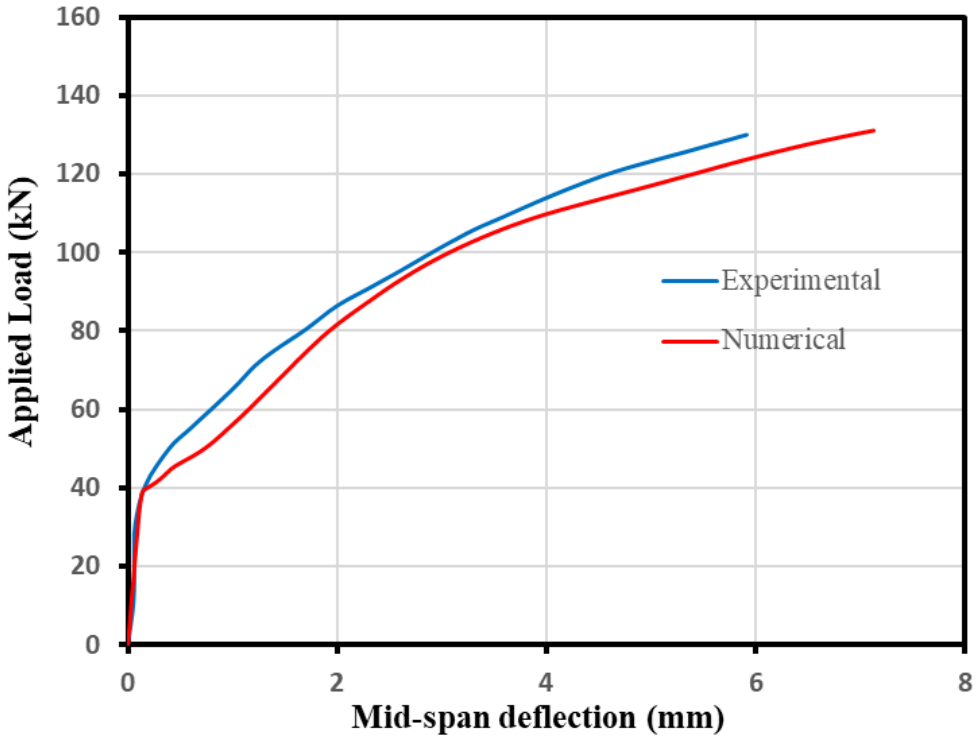

Fig. 5. 13: Experimental and numerical load-deflection curves for (H10SMFR)

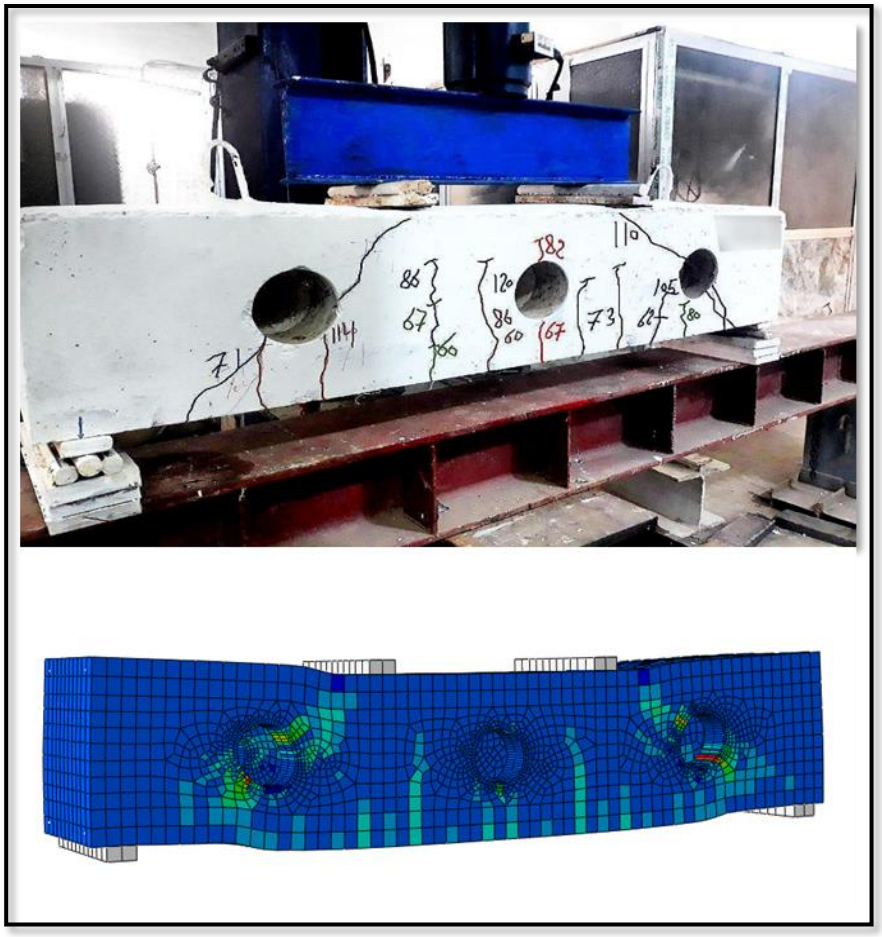

Plate 5. 7: Experimental and numerical cracks Patterns for (H10SMFR)

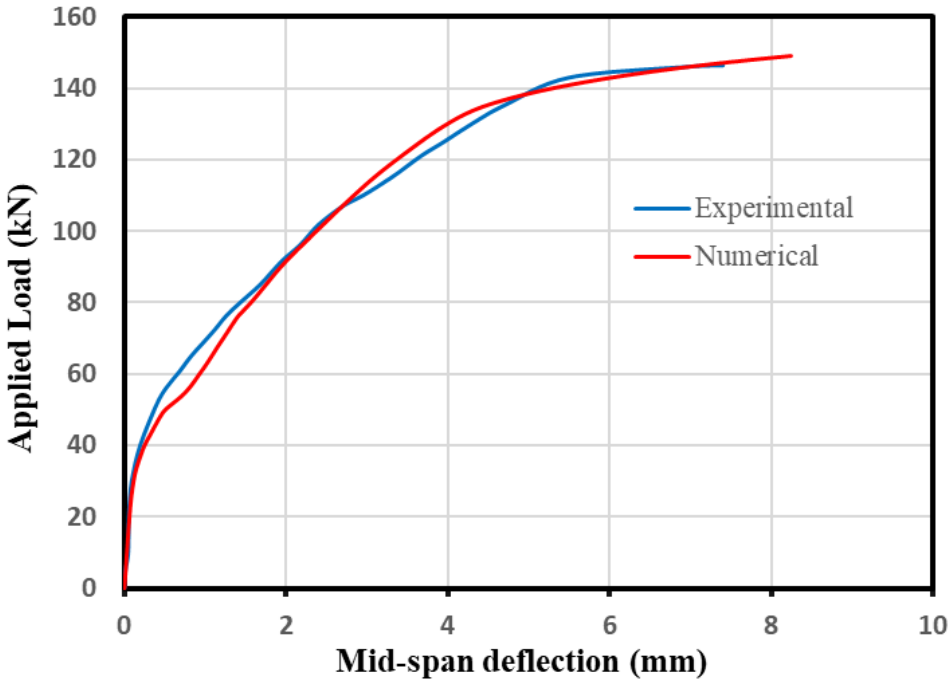

Fig. 5. 14: Experimental and numerical load-deflection curves for (H10MB)

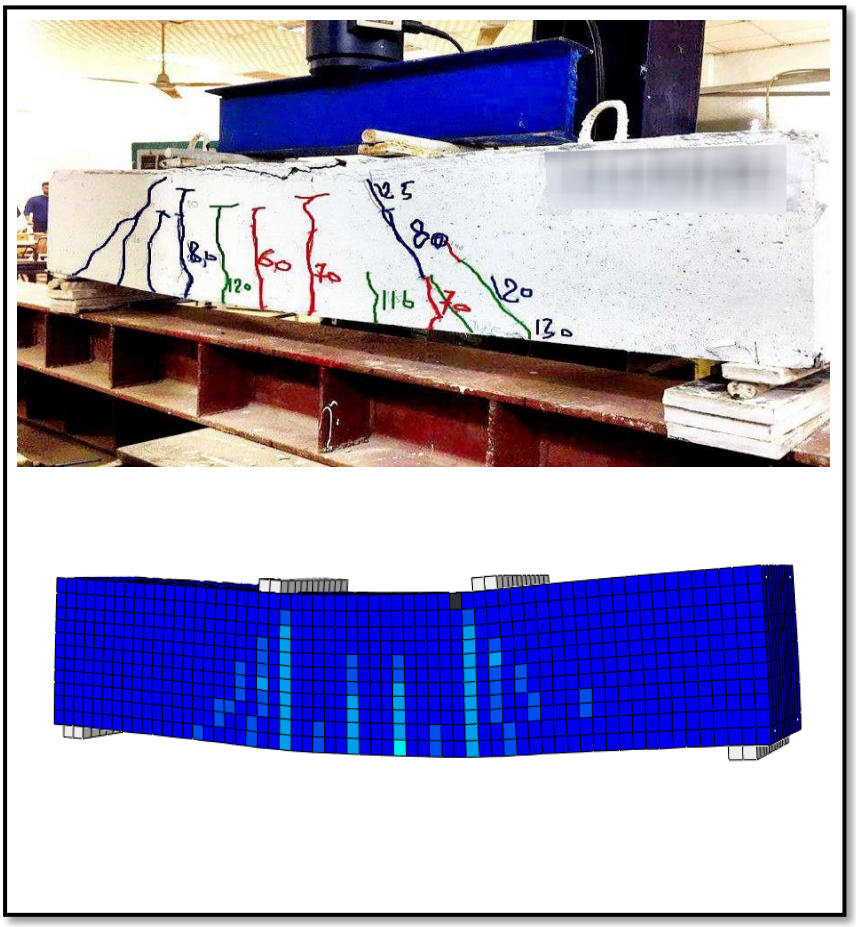

Plate 5. 8: Experimental and numerical cracks Patterns for (H10MB)

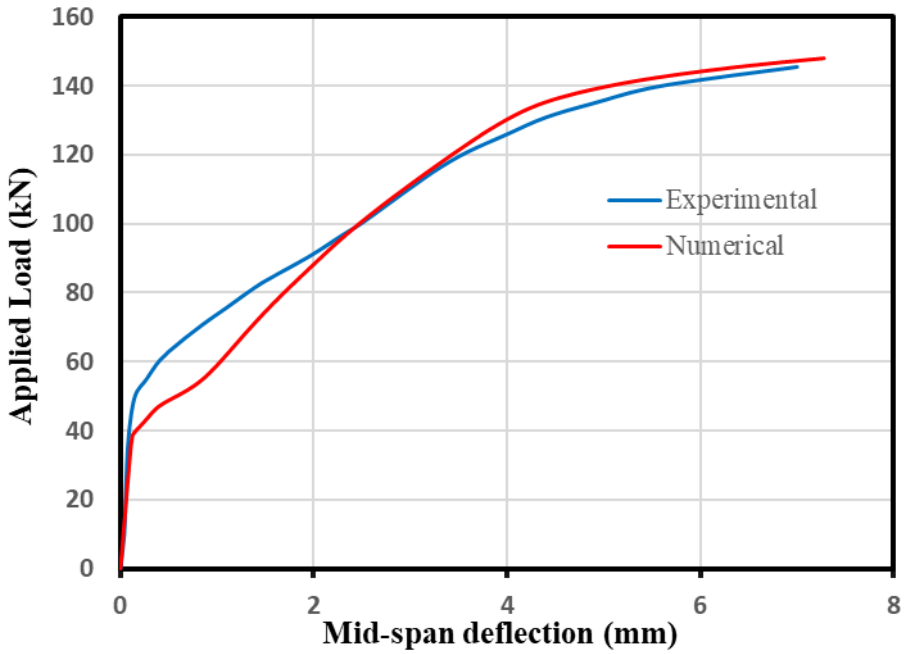

Fig. 5. 15: Experimental and numerical load-deflection curves for (H10SB)

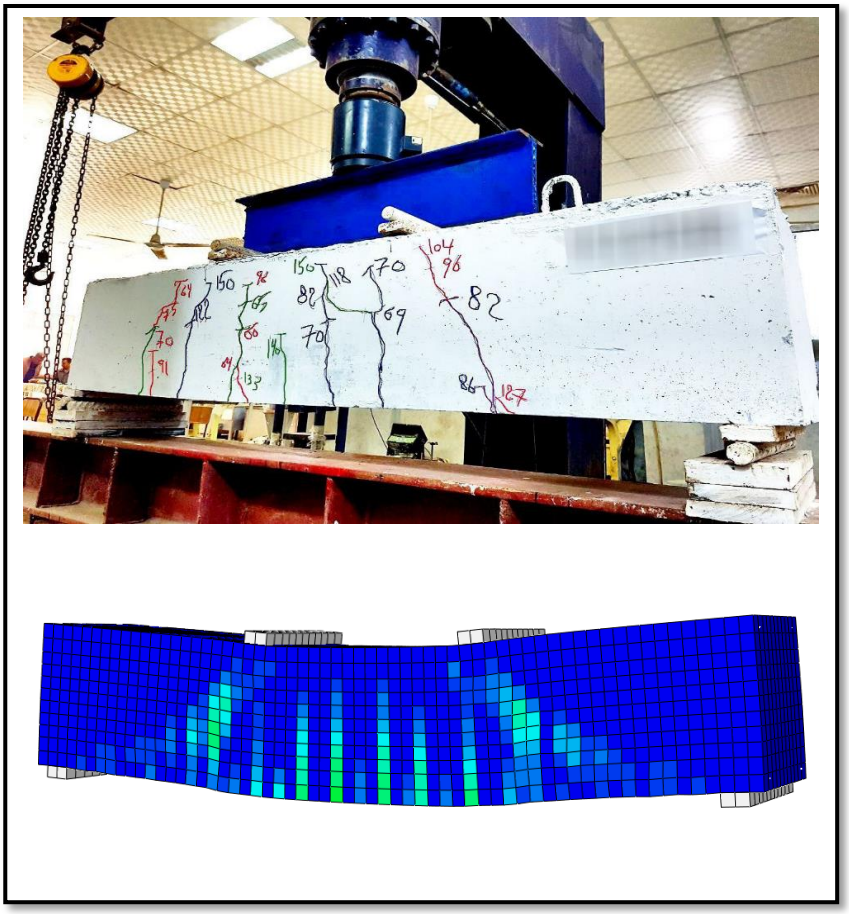

Plate 5. 9: Experimental and numerical cracks Patterns for (H10SB)

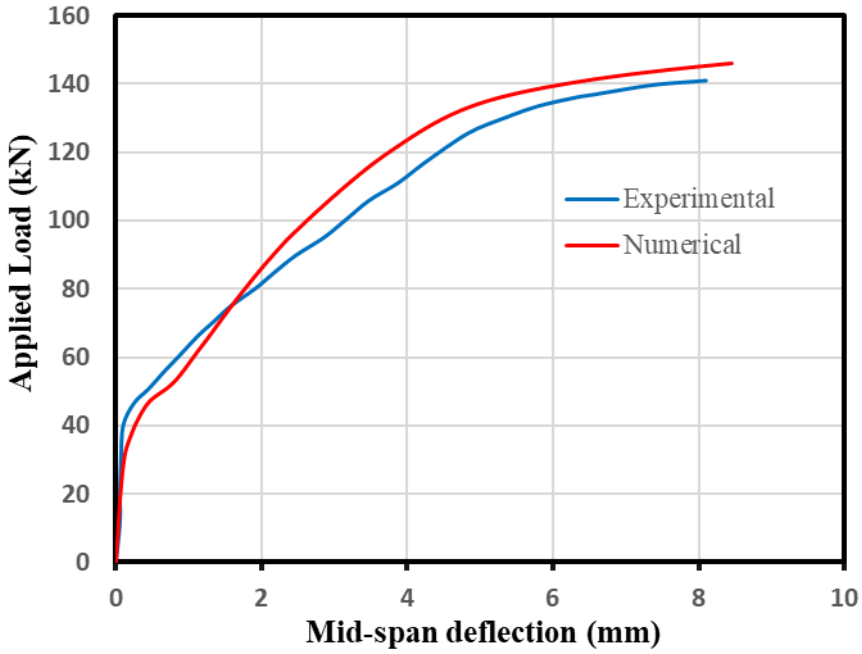

Fig. 5. 16: Experimental and numerical load-deflection curves for (H10SMB)

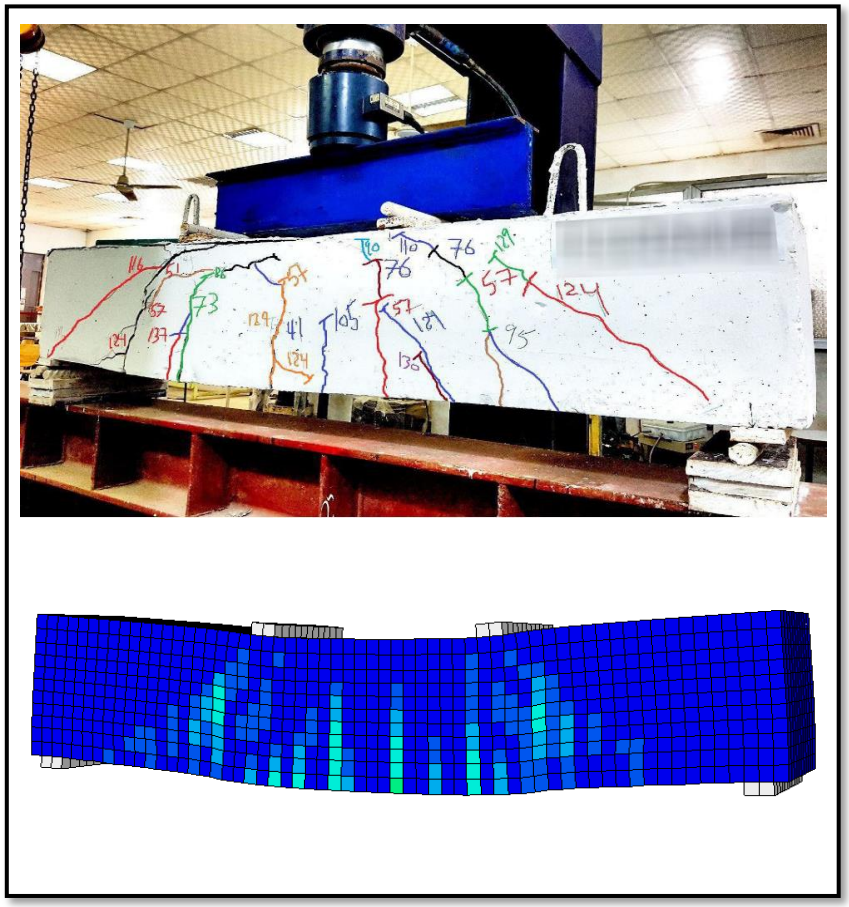

Plate 5. 10: Experimental and numerical cracks Patterns for (H10SMB)

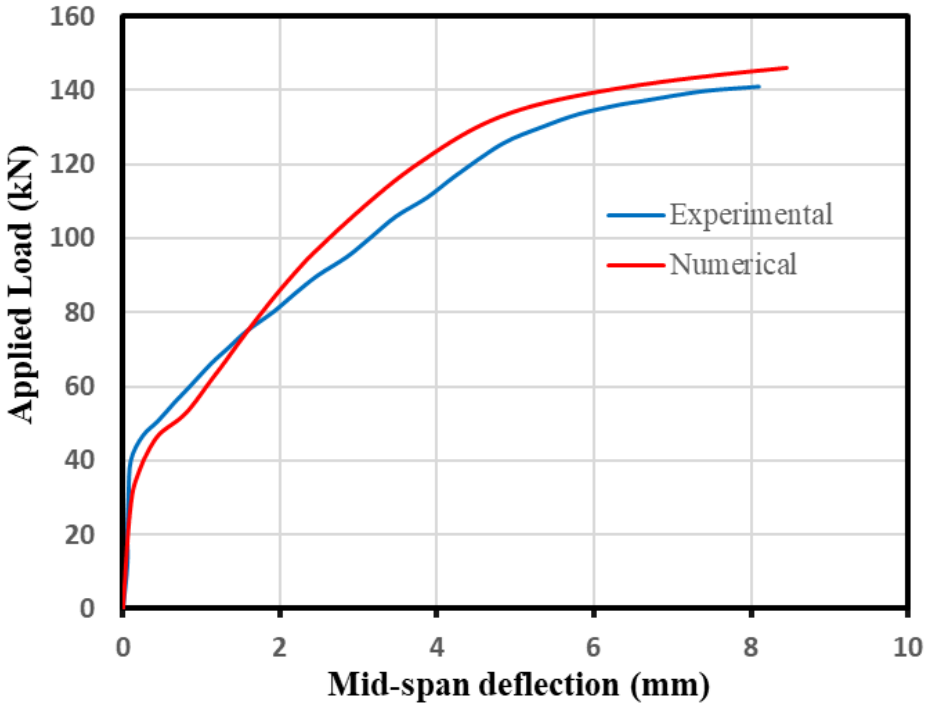

Fig. 5. 17: Experimental and numerical load-deflection curves for (H10MFR-CFRP)

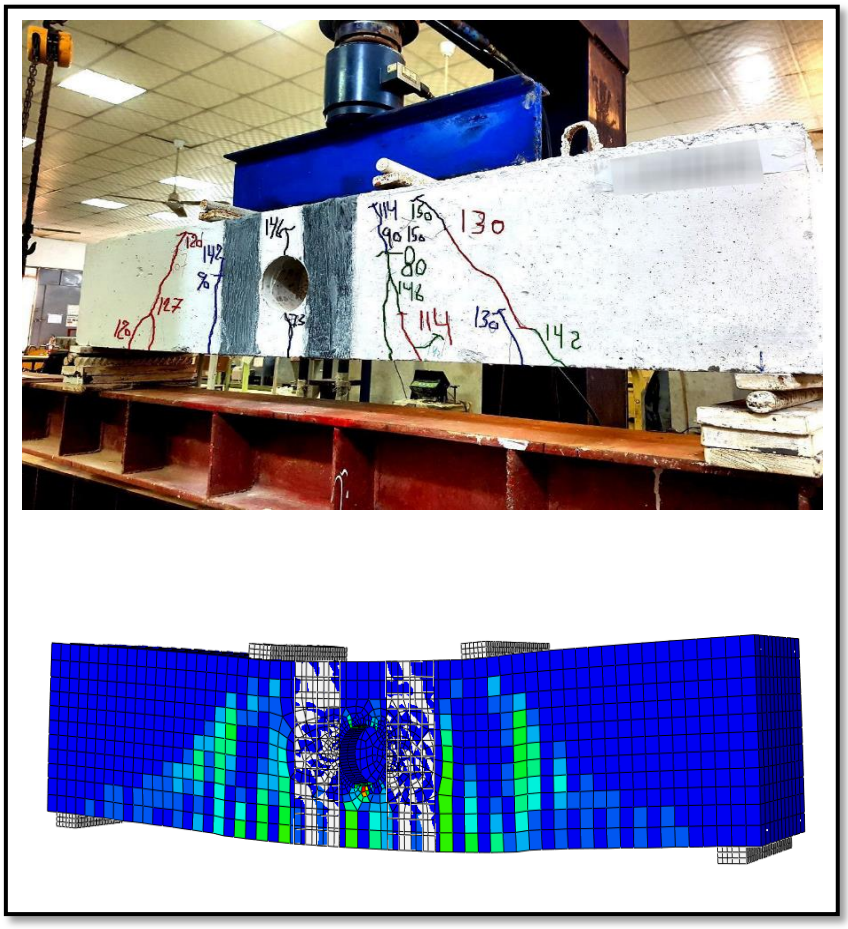

Plate 5. 11: Experimental and numerical cracks Patterns for (H10MFR-CFRP)

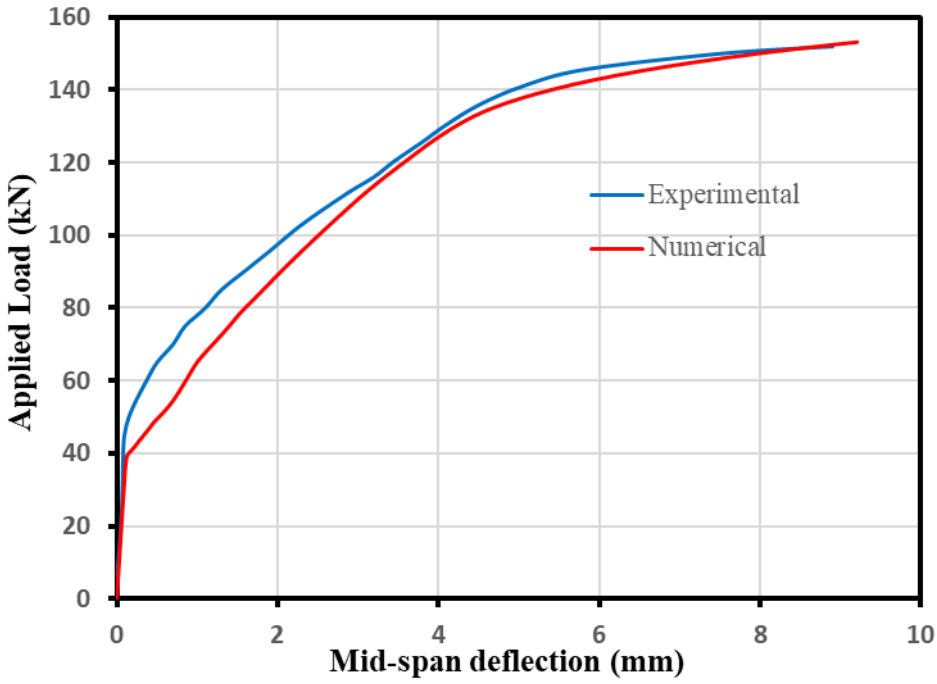

Fig. 5. 18: Experimental and numerical load-deflection curves for (H10SFR-CFRP)

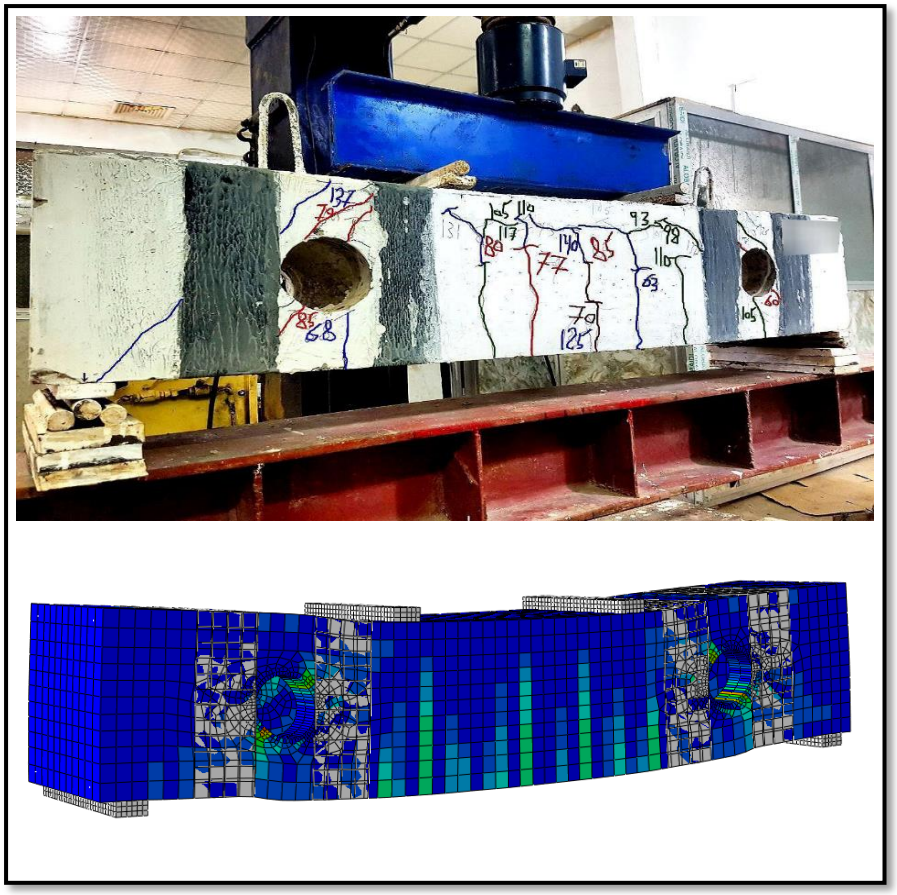

Plate 5. 12 Experimental and numerical cracks Patterns for (H10SFR-CFRP)

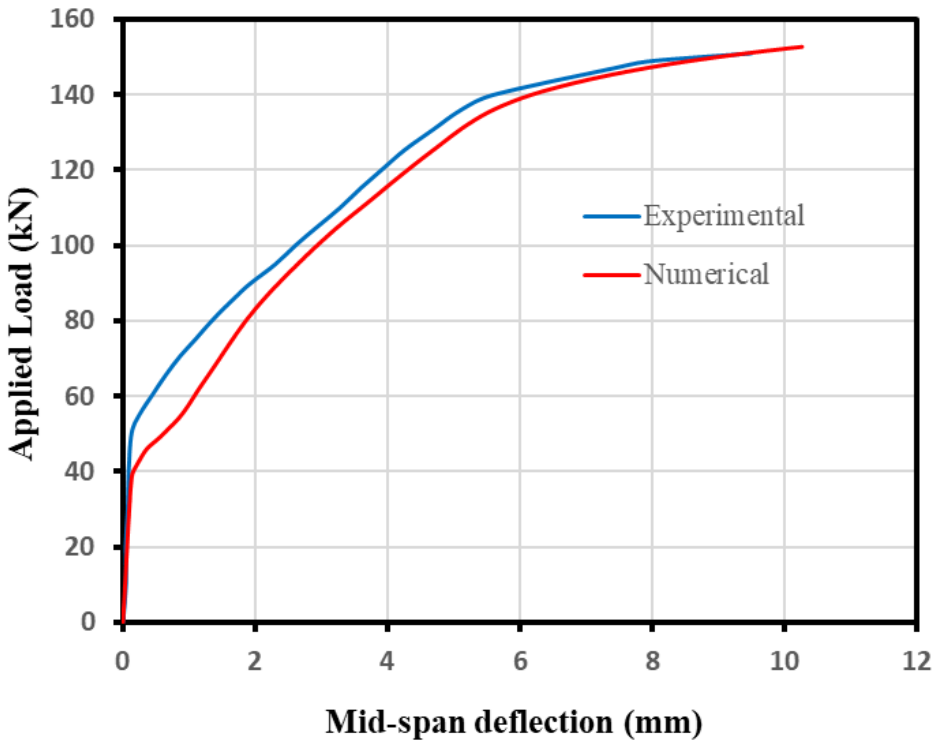

Fig. 5. 19: Experimental and numerical load-deflection curves for (H10SMFR-CFRP)

Plate 5. 13: Experimental and numerical cracks Patterns for (H10SMFR-CFRP)

5.4.2 Cracks Pattern

A comparison has been made between the pattern of the cracks at failure for the numerical models recorded in the ABAQUS program and the pattern of the cracks of the experimental specimens, as illustrated in the previous **Plates 5.1 to 5.13**. From these plates, good agreement was noticed between the experimental and the theoretical specimens.

5.4.3 Ultimate Load and Maximum Deflection

A comparison has been made between the ultimate experimental load and maximum deflection and those numerical that obtained from ABAQUS program, as given in **Table 5.2**. It can be concluded that a good agreement between the numerical and experimental results and that the mean difference in the ultimate load and the maximum deflection was 1.8% and 8.3% respectively. For this reason, the proposed model is reliable and can be used with confidence.

Table 5. 2: Experimental and numerical results of tested beams

Group	Specimen symbol		Ultimate Load (Pu) kN	$(Pu_{,FEA}\_Pu_{,EXP})*100$ / $Pu_{,EXP}$	Maximum Deflection (Δu) mm	$(\Delta u_{,FEA}\_\Delta u_{,EXP})*100$ / $\Delta u_{,EXP}$
	HC	EXP. FEA	155.0 157.4	1.55	11.7 12.3	5.10
Group 1	H10MF	EXP. FEA	147.0 149.7	1.84	7.79 8.20	5.20
	H10SF	EXP. FEA	144.5 151.0	4.50	7.59 9.50	25.0
	H10SMF	EXP. FEA	143.0 145.0	1.40	7.50 8.30	10.6
	H10MFR	EXP. FEA	140.3 141.9	1.14	5.80 6.60	13.8
	H10SFR	EXP. FEA	138.8 140.2	1.01	7.10 7.40	4.20
	H10SMFR	EXP. FEA	130.2 131.0	0.61	5.90 7.10	20.0
Group 2	H10MB	EXP. FEA	146.4 149.0	1.78	7.40 8.20	10.8
	H10SB	EXP. FEA	145.5 147.9	1.65	7.00 7.30	4.20
	H10SMB	EXP. FEA	141.0 146.0	3.55	8.10 8.50	4.90
Group 3	H10MFR-CFRP	EXP. FEA	152.0 153.2	0.66	8.90 9.20	3.40
	H10SFR-CFRP	EXP. FEA	151.0 152.7	1.13	9.50 10.3	8.40
	H10SMFR-CFRP	EXP. FEA	142.0 144.9	2.04	7.00 7.20	2.90
	Mean Difference			1.8		9.20

5.5 Parametric Study

To evaluate the impact of several essential parameters on the overall behaviour of the hollow reinforced SCC beams with an opening under the effect of two-point loading, a parametric study was performed by the numerical application (ABAQUS).

The selected parameters to be studied in this chapter could be summarised as follows:

1. Effect of opening diameter.
2. Effect of opening number.
3. Effect of concrete compressive strength.
4. Effect of strengthening schemes.

5.5.1 Effect of Opening Diameter

To study the effect of an opening diameter on the load-deflection response, ultimate load, and deflection of hollow reinforced SCC beams, two openings' locations were selected. The first location was in the mid-span of the web in the front and rear of the beam, while the other was near the supported in the front and rear of the beam. Five different (diameter/height) ratios (16.67%, 25%, 33.33%, 41.67%, and 50%) were selected for each opening's location to be analysed in the present study. The load mid-span deflection curves shown in **Figs. 5.20** and **5.21** revealed the effect of the diameter change. From **Fig. 5.20,** it could be noticed that there is a small difference in the stiffness of the specimens although the change in diameter is owing to the existing of the opening in the tension zone, which is negligible in the ultimate strength analysis process. A reduction in the ultimate load occurred with the increase in the diameter of the opening. On the other hand, the deflection of these beams increased in comparison with HC, as shown in **Table 5.3.** A remarkable difference can be noticed in **Fig. 5.21** in the load-deflection response of the specimens with two openings near the supports. Furthermore, a significant reduction in the ultimate load occurred with the increase in the diameter of the opening. Meanwhile, the beams suffered from higher deflection if compared with HC owing to the effect on the beam stiffness that occurred due to the increase in the opening diameter, as shown in **Table 5.3**.

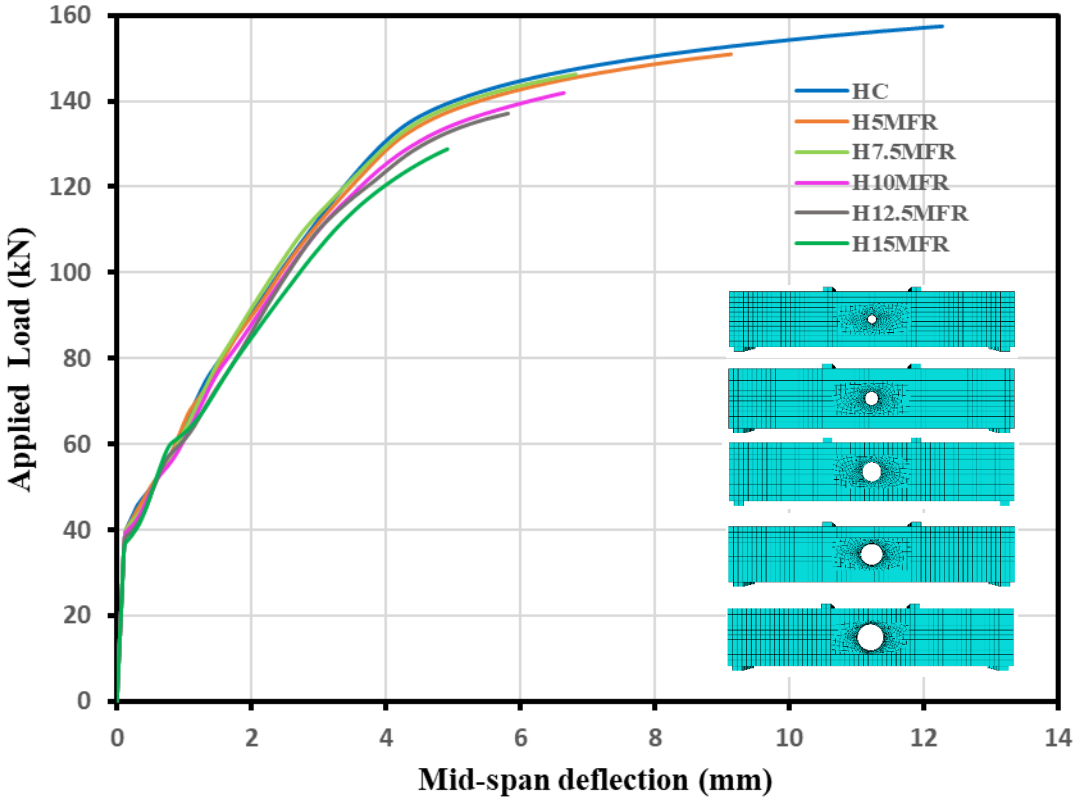

Fig. 5. 20: Effect of openings diameter on Load deflection curve for mid-span opening

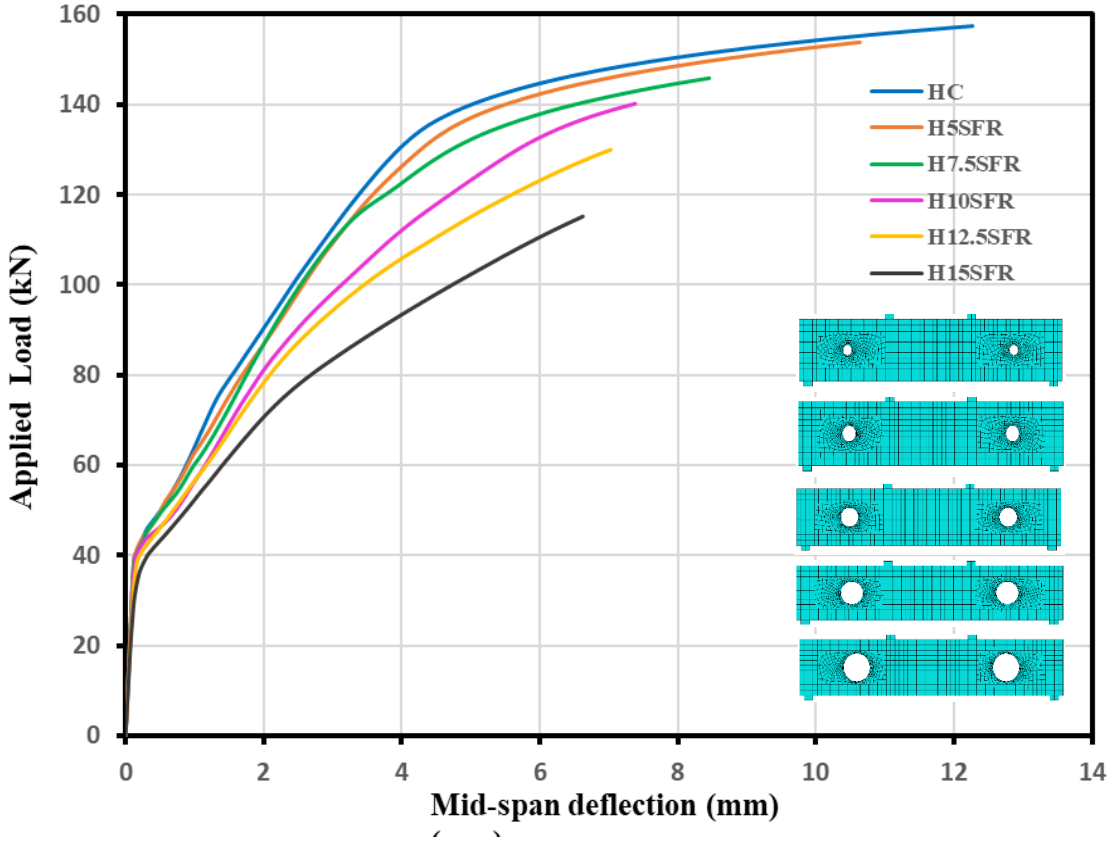

Fig. 5. 21: Effect of openings diameter on Load deflection curve for near supports opening

Table 5. 3: Effect of opening diameter on the ultimate load and maximum deflection

Opening location	Beam Symbol	Ultimate Load kN	Maximum deflection (mm)
	HC	157.4	12.3
Mid-span	H5MFR	150.9	9.10
	H7.5MFR	146.5	6.90
	H10MFR	141.9	6.60
	H12.5MFR	137.1	5.80
	H15MFR	128.9	4.90
Near supports	H5SFR	153.8	10.6
	H7.5SFR	145.9	8.50
	H10SFR	140.2	7.40
	H12.5SFR	130.0	7.00
	H15SFR	115.2	6.60

5.5.2 Effect of Openings' Number

The effect of changing the number of openings on the load-deflection response, ultimate load, and maximum deflection, was performed numerically by fixing the opening diameter to 100 mm. **Figure 5.22** exhibited the effect of change in the number of openings on the load-deflection curve response. The results revealed a significant difference in the stiffness of the beams, where the stiffness of all beams decreases with the increase in the number of opening. Meanwhile, a remarkable reduction has occurred in the ultimate load in contrast to the deflection as beams suffer from higher deflection due to the increase in the number of openings if compared with HC, as shown in **Table 5.4**.

Table 5. 4: Opening number effect on ultimate strength and maximum deflection

Number of opening	Ultimate Load kN	Maximum deflection mm
Without opening	157.4	12.3
One opening	141.9	6.6
Two openings	140.2	7.4
Three openings	131.0	7.1
Four openings	117.0	5.8
Five openings	101.0	4.4

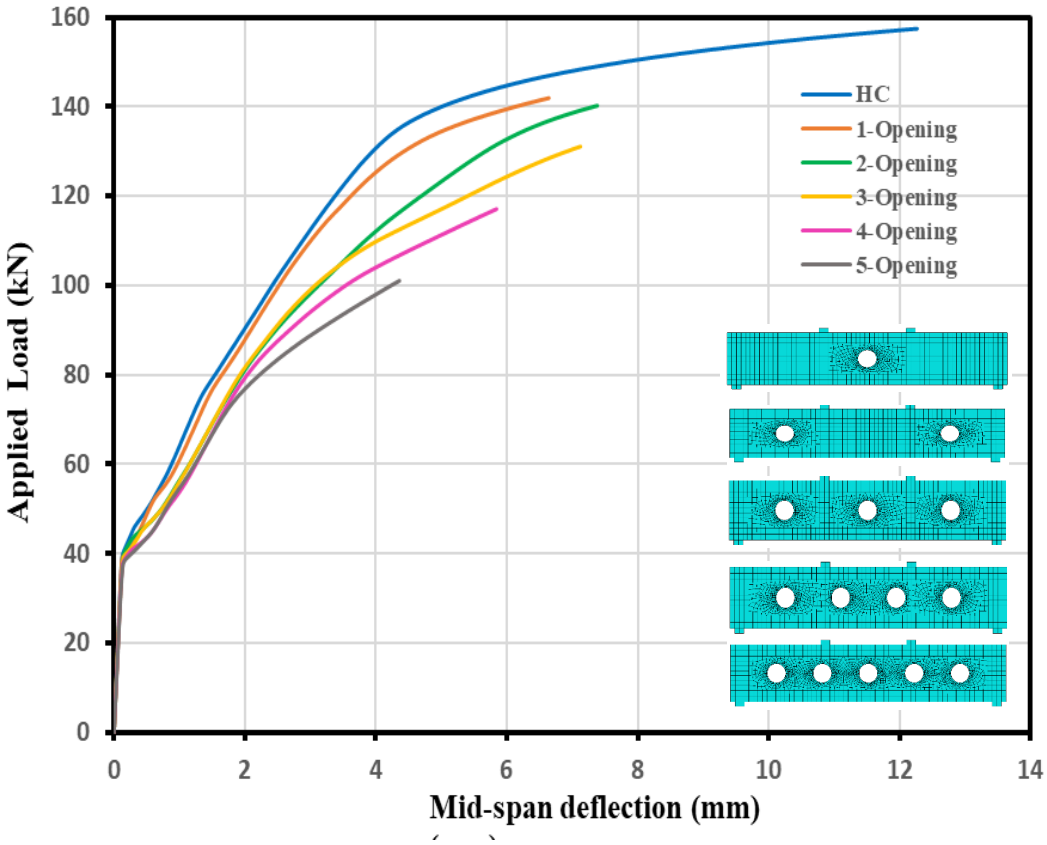

Fig. 5. 22: Effect of openings' number change on the load-deflection curves

5.5.3 Effect of Strengthening Schemes by CFRP

The effect of different strengthening schemes by CFRP on the load-deflection response, ultimate load, and deflection of reinforced SCC hollow beams with mid-span opening or near supports openings in front and rear of the web have been numerically studied. Various strengthening schemes have been proposed for both H10MFR and H10SFR specimens using U-wrapping and full wrapping with different layers of CFRP strips (one layer, two layers and three layers) with two strips of 0.167 mm thickness, and 100 mm width for each opening. Besides, a new scheme was used for both beams H10MFR and H10SFR, in which the CFRP strip was applied along the bottom flange of the hollow beams with 300 mm width. Furthermore, a scheme with inclined CFRP strips was used for H10SFR specimen only in which two layers of CFRP strips were used for each opening (the CFRP strips were inclined with 45 degrees, and perpendiculars on the cracks paths, with 0.167 mm thickness and 100 widths). **Figures 5.23 and 5.24** exhibited the effect of the different strengthen schemes on the load-deflection curve for both H10MFR and H10SFR specimens. These figures revealed that all the strengthening schemes with CFRP enhanced the ultimate load capacity, and post-cracking stiffness if compared with the unstrengthened one. The best strengthening scheme for

both H10MFR and H10SFR specimens was the bottom flange CFRP owing to the significant increase in the ultimate load and the function of cracking delay and concrete confinement owing to CFRP. Furthermore, the increases in the ultimate load and post cracking stiffness in specimen H10MFR were higher than those in specimen H10SFR. The effect of strengthening schemes on the ultimate load and maximum deflection is listed in **Table 5.5**.

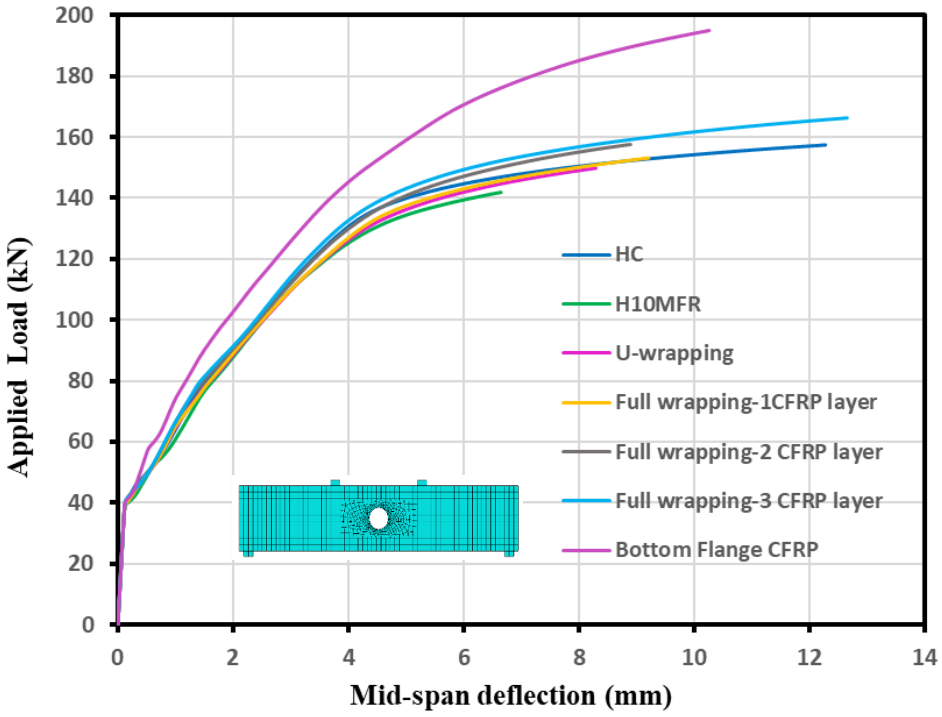

Fig. 5. 23: Effect of CFRP strengthening schemes on the load-deflection curve for H10MFR

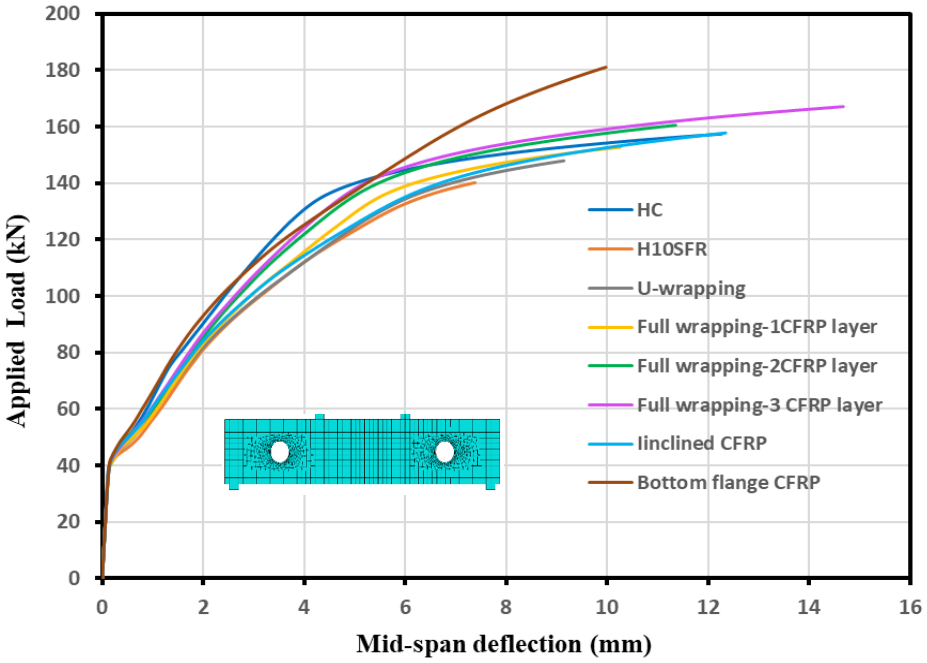

Fig. 5. 24: Effect of CFRP strengthening schemes on the load-deflection curve for H10SFR

Table 5. 5: Effect of strengthening schemes on ultimate load and maximum deflection

Beam Symbol	Strengthen Schemes	Ultimate Load kN	Maximum Deflection (mm)
HC	**Without strengthening**	157.4	12.30
H10MFR	Without strengthen ing	141.9	6.60
H10MFR	U-wrapping	149.8	8.30
	Full wrapping-1CFRP layer	153.2	9.20
	Full wrapping-2CFRP layers	157.6	8.90
	Full wrapping-3CFRP layers	166.3	12.6
	Bottom flange CFRP	195.0	10.3
H10SFR	Without strengthen	140.2	7.40
H10SFR	U-wrapping	147.9	9.10
	Full wrapping-1CFRP layer	152.7	10.3
	Full wrapping-2CFRP layers	160.5	11.4
	Full wrapping-3CFRP layers	167.1	14.4
	Bottom flange CFRP	181.1	10.0
	Inclined CFRP	157.8	12.3

5.5.4 Effect of Concrete Compressive Strength

The effect of changing the concrete compressive strength on the load-deflection response, ultimate load, and maximum deflection on the behaviour of hollow reinforced SCC beam with near supports opening in front and rear of the web were numerically carried out in this study. The diameter, location and number of opening were kept constant, and the compressive strength was changed (27.5, 32.5, 37.5, 42.5, 47.5 MPa). **Figure 5.25** illustrates the effect of compressive strength change on the load-deflection curve response. It is clear from the result that the stiffness and the ultimate load of the beams have a relative relationship with the compressive strength, in contrast with the deflection that has an inverse relationship with the

compressive strength. The ultimate load and maximum deflection values are presented in **Table 5.6.**

Table 5.6: Effect of compressive strength on ultimate load and maximum deflection

Compressive Strength	Ultimate Load kN	Maximum Deflection (mm)
f_{cu}-27.5	129.9	6.30
f_{cu}- -32.5	140.2	7.40
f_{cu}- -37.5	151.0	10.1
f_{cu}--42.5	164.3	13.2
f_{cu}- -47.5	175.1	18.8

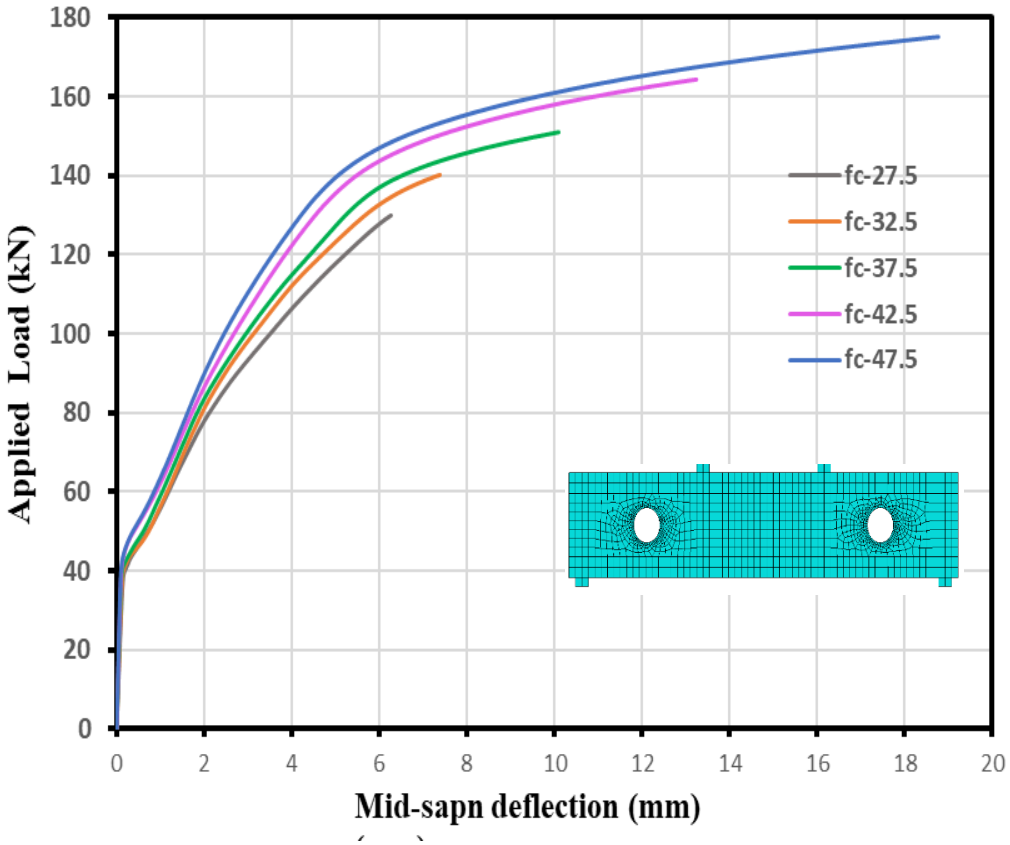

Fig. 5.25: Effect of compressive strength on the load-deflection curve

CHAPTER SIX
CONCLUSIONS AND RECOMMENDATIONS

6.1 Introduction

In this study, the behaviour of hollow reinforced SCC beams with and without an in-place circular opening that is non-strengthened or externally strengthened with CFRP strips was investigated. This study comprises two parts, the first part was an experimental program, and the second part was nonlinear finite element analysis by ABAQUS (2019) program to predict the ultimate load capacity and the overall behaviour. In this chapter, the main findings obtained from the experimental and analytical evidence are presented, in addition to some recommendations for further work.

6.2 Conclusions

The significant conclusions noticed from each phase of the experimental and numerical investigation are presented in this section.

6.2.1 Conclusions from Experimental Results

1. The creation of in-place circular openings in a beam could change the recorded mode of failure based on the location of the opening.
2. The location of openings has a remarkable effect on the ultimate strength of the beams in which the reductions were about (9.5%, 10.5 %, 16%) when the opening exists in front and rear of the web at flexure zone, shear zone, or both flexure, and shear zone, respectively if compared with HC.
3. The maximum decreases in the stiffness occurred in the beams H10MFR, H10SFR, and H10SMFR, which caused an increase in the deflection of these beams by (26%, 61% and 70%), respectively if compared with HC.
4. The reductions in the ultimate load for the strengthened beams H10MFR-CFRP, H10SFR-CFRP, and H10SMFR-CFRP were (1.9%, 2.6%, and 8.4%), respectively if compared with HC.
5. The external strengthening by CFRP strips enhanced the ultimate load capacity for H10MFR-CFRP, H10SFR-CFRP, and H10SMFR-CFRP by about (8.3 %, 8.8 %, and 9%), respectively when compared with the unstrengthened beams due to concrete confinement and the function of cracking delay owing to CFRP.

6. The external strengthening by CFRP strips for web openings succeeded in preventing cracks from reaching web openings and decreased the hairline cracks to a minimum number due to the redistributing process of stresses by CFRP laminates during loading.
7. The external strengthening by CFRP strips increased the stiffness of H10MFR-CFRP, H10SFR-CFRP, and H10SMFR-CFRP, which caused a decrease in the deflection of these beams by (22%, 44%, and 30%), respectively if compared with the unstrengthened beams.
8. The deflection ductility indices decreased marginally for all tested beams. The new values ranged from (1.53 to 3.17) if compared with the control beam, which made all beams to be more brittle than the control beam.

6.2.2 Conclusions from the Numerical Study

1. The FEA analysis by ABAQUS program was able to analyze the hollow reinforced SCC beams with in-place circular openings that are unstrengthened or strengthened by CFRP strips. The proposed model gave an excellent convergence with the experimental result in terms of ultimate strength, load-deflection curves, and failure mode.
2. The average differences in the ultimate load capacity and the maximum deflection between FEA and the experimental results of all specimens were nearly 1.8% for ultimate load and 9.2%, for maximum deflection, which ensures the precision of the numerical analysis.
3. The ultimate strength of the hollow reinforced SCC beam decreased with the increase in the (D/H) for mid-span opening by (4.1%, 7%, 9.9%, 12.9%, 18.2%) for ratios (16.67, 25, 33.33, 41.67, and 50), respectively when compared with control beam.
4. The ultimate strength of the hollow reinforced SCC beam with near supports openings decreased with the increase in the (D/H) of the openings by (2.3%, 7.4%, 11%, 17.4%, and 26.8%) for ratios (16.67, 25, 33.33, 41.67, and 50) respectively, if compared with control beam.
5. The increase in the openings' number decreased the ultimate strength of the hollow reinforced SCC beam by (9.8%, 10.9%, 16.8%, 25.7%, and 35.8%) for (one, two, three, four, and five) openings' number, respectively if compared with control beam.
6. The increase in the compressive strength of concrete increased the ultimate load capacity for all types of beams, in which the increase in the ultimate strength of the hollow reinforced SCC girder with near supports openings reached to 25% at 47.5 MPa.

7. The scheme of strengthening the bottom flange by CFRP was the best scheme from the ultimate strength viewpoint for both hollow reinforced SCC beams with a near support opening or mid-span opening. The increases in the ultimate strengths were (29.2% and 37.4%) for both beams, respectively, if compared with HC.

6.3 Recommendations for Future Research

1. Investigate experimentally the behaviour of hollow reinforced SCC beams with and without opening subjected to dynamic and impact loading.

2. Examine experimentally the behaviour of hollow girders that have in-place circular openings using a different type of concrete such as high strength and/or reactive powder concrete.

3. Explore the behaviour of reinforced SCC beams with in-place circular openings under repeated loads.

4. Investigate the effect of using different strengthening techniques such as external prestressing technique, and NSM technique on the behaviour of reinforced SCC beams with in-place circular openings.

5. Investigate the effect of type of FRP on the torsional behaviour of hollow reinforced SCC beams without openings experimentally.

6. Inspect the behaviour of damaged hollow reinforced SCC beams experimentally with in-place circular openings strengthened with CFRP laminates.

7. Finite element analysis for the behaviour of hollow pre-stressed SCC beams with in-place circular openings by using the ABAQUS program.

REFERENCES

Abo Dhaheer, M. S. *et al.* (2016) 'Proportioning of self–compacting concrete mixes based on target plastic viscosity and compressive strength: Part I - mix design procedure', *Journal of Sustainable Cement-Based Materials*, 5(4), pp. 199–216.

ACI 318-2014 ((2014)) 'Aci 318M-14', *Building Code Requirements for Structural Concrete*.

Ahmad, S., Umar, A. and Masood, A. (2017) 'Properties of Normal Concrete, Self-compacting Concrete and Glass Fibre-reinforced Self-compacting Concrete: An Experimental Study', *Procedia Engineering*, 173, pp. 807–813.

Ahmed, H. M. (2011) 'Properties of Self Compacting Concrete Containing Limestone Powder as Replacement of Sand' *Journal of Engineering and Development*, 15(3), pp. 117–130.

Al-bayati, N. (2017) 'Structural Behavior of Self-Compacting Reinforced Concrete Deep Beams Republic of Iraq Ministry of Higher Education and Scientific Research University of Technology', 34(April 2016), pp. 2310–2317.

Al-Shaarbaf, I. A. S., Al-Bayati, N. A. M. J. and Al-Kaisy, D. I. A. (2007) 'Nonlinear finite element analysis of reinforced concrete beams with large openings under flexure', *Engineering and Technology Journal*, 25(2), pp. 210–228.

Al-sheikh, S. A. (2014) 'Flexural behaviour of RC beams with opening', *Concrete Research Letters*, pp. 812–824.

Allam, S. M. (2012) 'Strengthening of RC beams with large openings in the shear zone', *International Science Index*, 6(January 2005), pp. 1–6.

Alsaeq, H. M. (2013) 'Effects of opening shape and location on the structural strength of RC deep beams with openings', *Proceedings of World Academy of Science, Engineering and Technology*, 7(78), p. 1344.

Alyhya, W. S. *et al.* (2015) 'A rational method for the design of self-compacting concrete mixes based on target plastic viscosity and compressive strength', *35th Cement & concrete science conference (CCSC35), Aberdeen, UK*, pp. 85–94.

American Society of Testing Materials ((2013)) 'ASTM C494 Standard Specification for Chemical Admixtures for Concrete', *Annual Book of ASTM Standards*.

Amiri, S., Masoudnia, R. and Akbar Pabarja, A. (2011) *The Study of the Effects of Web Openings on the Concrete Beams*, *Australian Journal of Basic and Applied Sciences*.

ASTM-C293 (2002) 'Standard Test Method for Flexural Strength of Concrete (Using Simple Beam with Third-Point Loading) ASTM C-78', *Astm*.

ASTM A615 (2016) 'Standard Specification for Deformed and Plain Carbon-Steel Bars for Concrete Reinforcement', *American Society for Testing and Materials*.

ASTM C496/C496M-11 (2011) 'ASTM C496-11 Standard Test Method for Splitting Tensile Strength of Cylindrical Concrete Specimens', *Annual Book of ASTM Standards Volume 04.02*.

Atta, A. M. and Khalil, A. E.-H. (2014) 'Strengthening of RC beams with an opening in the shear zone using external prestressing technique', *Magazine of Concrete Research*, 67(3), pp. 133–144.

Aykac, B. *et al.* (2014) 'Flexural behaviour and strength of reinforced concrete beams with multiple transverse openings', *ACI Structural Journal*, 111(2), pp. 267–277.

Aziz, A. H. (2016) 'Experimental and Theoretical Evaluation for Effect of Openings Location on Shear Strength of Rc Beams', *Journal of Engineering and Development*, 20(1), pp. 1–15.

Aziz, A. and Hashim, O. (2018) 'Torsional strength evaluation of reinforced SCC box beams strengthened internally by opened and closed transverse concrete diaphragms', *MATEC Web of Conferences*. Edited by T. S. Al-Attar, M. A. Al-Neami, and W. S. AbdulSahib, 162, p. 04009. doi: 10.1051/matecconf/201816204009

BS 1881-116: (1983) 'Testing concrete — compressive strength of concrete cubes', *British Standard Institution*.

BS EN 12350-8 (2008) 'Part 8: Self-compacting concrete - Slump-flow test', *British Standard*.

Carreira, D. J. and Chu, K. (1986) 'Stress-Strain Relationship for Plain Concrete in Compression', *ACI Structural Journal*, (82), pp. 797–804.

Chin, S. C., Shafiq, N. and Nuruddin, M. F. (2011) 'Strengthening of RC Beams Containing Large Opening at Flexure with CFRP laminates'*World Academy of Science, Engineering and Technology*, 5(12), pp. 2031–2037.

Chin, S. C., Shafiq, N. and Nuruddin, M. F. (2016) 'Behaviour of RC beams with CFRP-strengthened openings', *Structural Concrete*, 17(1), pp. 32–43.

De Corte, W. and Boel, V. (2010) 'Crack Width Analysis of Reinforced Self-Compacting Concrete Beams', *Key Engineering Materials*, 452–453, pp. 629–632.

Douglas, R. (2004) 'Properties of self-consolidating concrete containing type F fly ash', *Portland Cement Association, No. Item Code: SN2619*, (2619), pp. 1–84.

EFNARC (2005) 'The European Guidelines for Self-Compacting Concrete Specification, Production and Use May', *The European Guidelines for Self Compacting Concrete*.

Elsepahy, M. S. (2018) 'Experimental and Analytical Study of Strengthening Reinforced Concrete Beams with Openings'*International Journal of Applied Engineering Research*, ISSN, 13(7), pp. 4934–4950.

Garg, P., Bansal, P. and Bansal, S. (2017) 'Experimental Investigation on the Behavior of RC Beams Strengthened by Externally Placed BFRP Sheets'*International Research Journal of Engineering and Technology (IRJET)*, Vol 04, Issue: 05 pp. 1124–1130.

Gatia Abtan, Y. and Dhafer AbdulJabbar (2018) 'Structural Behavior of HS-SC Reinforced Concrete Beams with Longitudinal and Transverse Openings Strengthened with CFRP Laminates', *Journal of Engineering and Sustainable Development*, 2018(05), pp. 48–67.

Gatia Abtan, Y. and Dhafer AbdulJabbar, H. (2019) 'Experimental Study to Investigate the Effect of Longitudinal and Transverse Openings on the Structural Behavior of High Strength Self Compacting Reinforced Concrete Beams', *Journal of Engineering and Sustainable Development*, 2019(01), pp. 66–79.

Hassan, N. Z., Ismael, H. M., Salman, A. M. and Etal. (2018) 'Study Behavior of Hollow Reinforced Concrete Beams'*International Journal of Current Engineering and Technology*, 8(6), pp. 1640–1651.

Hauhnar, L., Rajkumar, R. and Umamaheswari, N. (2017) 'Behavior of Reinforced Concrete Beams With Circular Opening in the Flexural Zone Strengthened By Steel', *International Journal of Civil Engineering and Technology (IJCIET)*, 8(5), pp. 303–309.

Hemzah, S. A. (2014) 'Nonlinear Analysis For Behavior Of R . C. Horizontally Semicircular Curved Beams With Openings And Strengthened By CFRP Laminates'*international Journal Of Scientific & Technology Research* 8(3), pp. 136–145.

Horta, A. (2005) 'Evaluation of Self-Consolidating Concrete for Bridge Structure Applications'Master's Thesis, Georgia Institute of Technology, School of Civil & Environmental Engineering.

Huang, P. (2005) 'Performance Evaluation Method of Self-Consolidating Concrete', in *SCC'2005-China - 1st International Symposium on Design, Performance and Use of Self-Consolidating Concrete*. RILEM Publications SARL, pp. 429–438. doi: 10.1617/2912143624.045

Amiri, J V, H. M. (2004) 'Effect of Small Circular Opening on the Shear and Flextural Behavior and Ultimate Strength of Reinforced Concrete Beams Using Normal and High', *Journal Of School Of Engineering*, Volume 16(3239), p. Page(s) 37 To 52.

Keflegen, A. (2018) *Performance Of Self Compacting Concrete Used In Congested Reinforcement Structural Element*. Master Thesis, Addis Ababa Institute Of Technology.

Khayat, K. H. (1998) 'Use of Self-Consolidating Concrete in Canada', in *International Workshop on Self-Compacting Concrete*, (Vol. 23, p. 26).

Khayat, K. H. and Morin, R. (2003) 'Performance of self-consolidating concrete used to repair parapet wall in Montreal', in *International RILEM Symposium on Self-Compacting Concrete*. RILEM Publications SARL, pp. 913–919.

Khayat, K., Hu, C. and Monty, H. (1999) 'Stability of self-consolidating concrete, advantages, and potential applications', in *Self-Compacting Concrete: Proceedings of the First International RILEM Symposium*, pp. 143–152.

Kudatini, S. B. (2016) 'Experimental Investigation on Internally Strengthened RC Beam with Rectangular', pp. 15410–15417.

Lin, C. H. and Chen, J. H. (2012) 'Shear behaviour of self-consolidating concrete beams', *ACI Structural Journal*, 109(3), pp. 307–315.

Lopes, S. M. R. and Bernardo, L. F. A. (2009) 'Twist behaviour of high-strength concrete hollow beams-Formation of plastic hinges along the length', *Engineering Structures*. Elsevier Ltd, 31(1), pp. 138–149.

Luo, S. (2005) 'Research on the Bending and Shearing Properties of Self-Compacting Concrete Beams', in *SCC'2005-China - 1st International Symposium on Design, Performance and Use of Self-Consolidating Concrete*. RILEM Publications SARL, pp. 641–648.

Mansur, M. A., Huang, L. M., Tan, K. H. and Lee, S. L. (1992) 'Deflections of reinforced concrete beams with web openings', *ACI Structural Journal*, 89(4), pp. 391–397.

Mansur, M. A. (1998) 'Effect of openings on the behaviour and strength of R/C beams in shear', *Cement and Concrete Composites*, pp. 477–486.

Mansur, M. A., & Hasnat, A. (1979). Concrete beams with small opening under torsion. *Journal of the Structural Division*, *105*(11), 2433-2447.

Mansur, M. A., Tan, K. H. and Wei, W. (1999) 'Effects of creating an opening in existing beams', *ACI Structural Journal*, 96(6), pp. 899–905.

Naik, T. R., Kumar, R., Ramme, B. W. and Canpolat, F. (2012) 'Development of high-strength, economic self-consolidating concrete', *Construction and Building Materials*, 30, pp. 463–469.

Nie, X. F., Zhang, S. S., Teng, J. G. and Chen, G. M. (2018) 'Experimental study on RC T-section beams with an FRP-strengthened web opening', *Composite Structures*. Elsevier, 185(February 2017), pp. 273–285.

Okamura, H. and Ouchi, M. (1998) 'Self-compacting high-performance concrete', *Progress in Structural Engineering and Materials*, 1(4), pp. 378–383.

Okamura, H. and Ouchi, M. (2003) 'Self-Compacting Concrete', *Journal of Advanced Concrete Technology*, 1(1), pp. 5–15.

Okamura H, et. al. Mix-design for self-compacting concrete, Concrete Library of JSCE, No. 25, pp.107-120, June 1995.

Okrajnov-Bajic, R., Vasovic, D. and et al. (2009) 'Self-compacting concrete and its application in contemporary architectural practice', *Spatium*, (20), pp. 28–34.

Pimanmas, A. (2010) 'Strengthening R/C beams with opening by externally installed FRP rods: Behavior and analysis', *Composite Structures*. Elsevier Ltd, 92(8), pp. 1957–1976.

American Segmental Bridge (2005) *Wakota Bridge Update, Minnesota, SPRING , VOL. 46*. Available at: http://www.asbi-assoc.org/projects/project.cfm?articleID=5AE0D3B0-F1F6-B13E-8499DCE839DFCDC0&categoryIDs=44A57F74-F1F6-B13E-81940961706FF0A9&searchString=&mainPageNumber=7&resultsPerPage=20 (Accessed: 11 October 2019).

Ra'id, F. A., Al-Shaarbaf, I. and Al-Khafaji, J. (2016) 'Reinforced Self-Compacting Concrete Beams Under Torsion', *Journal of Engineering and Sustainable Development*. Al-Mustansyriah University, 20(2), pp. 82–99.

Sharifi, Y. (2012) 'Structural performance of Self-Consolidating Concrete used in reinforced concrete beams', *KSCE Journal of Civil Engineering*, 16(4), pp. 618–626.

Iraqi Specification No.5, "Portland Cement", Baghdad, (1984).

Iraqi Specification No.45, "Natural Sources for Gravel that is used in concrete and construction", Baghdad, (1984).

Material Data Sheet.(2015)'Sika ViscoCrete® -5930.pdf' Egypt-El Abour City: Feb, pp. 1–2.

Material Data Sheet. (2017)a 'Sikadur®-330', pdf Egypt-El Abour City (May), pp. 2–5.

Material Data Sheet. (2017b) 'SikaWrap ® -231 C Woven Unidirectional Carbon Fibre Fabric , (March), pp. 2–5.

Da Silva, P. R. and De Brito, J. (2015) 'Fresh-state properties of self-compacting mortar and concrete with combined use of limestone filler and fly ash', *Materials Research*, 18(5), pp. 1097–1108.

Tan, K. H. and Mansur, M. A. (1996) 'Design procedure for reinforced concrete beams with large web openings', *ACI Structural Journal*, 93(4), pp. 404–411.

Walraven, J. (2003) 'Structural aspects of self-compacting concrete', in *Proceedings of the 3rd international RILEM Symposium on SCC*, pp. 15–22.

Naik, T. R. *et al.* (2012) 'Development of high-strength, economical self-consolidating concrete', *Construction and Building Materials*, 30, pp. 463–469. doi: 10.1016/j.conbuildmat.2011.12.025.

BEAM Design

A.1 Checking Flexural Capacity of the Section

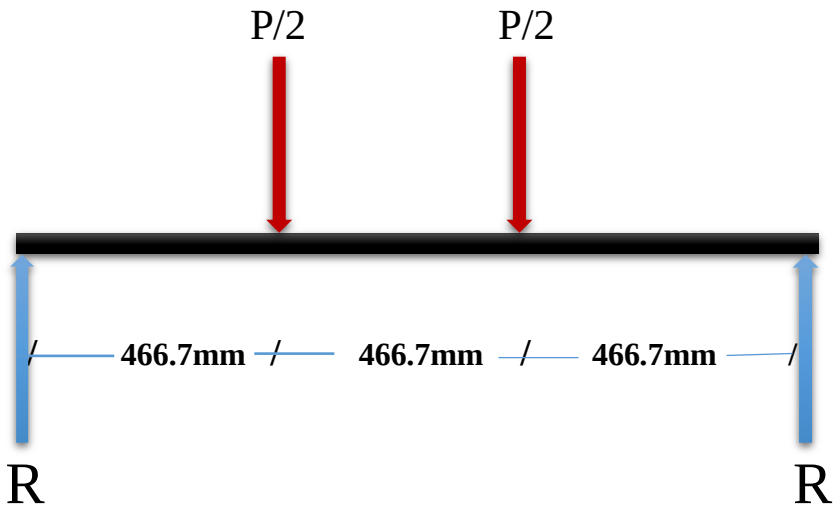

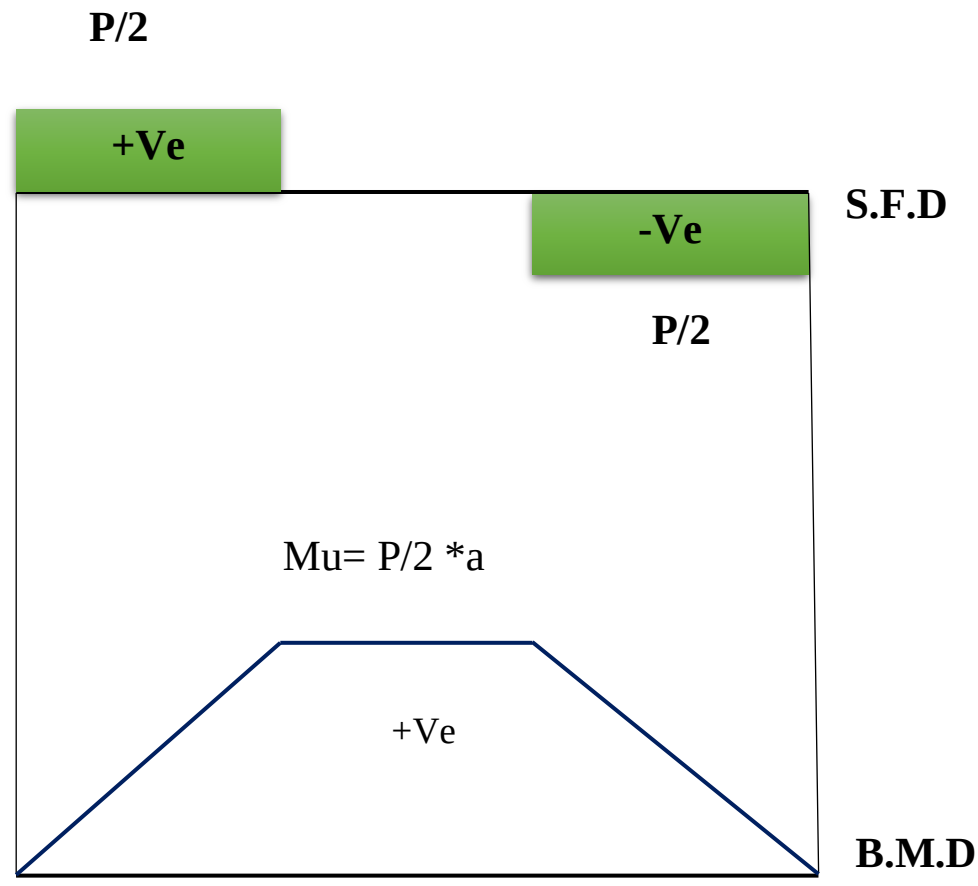

• **Beam Data**

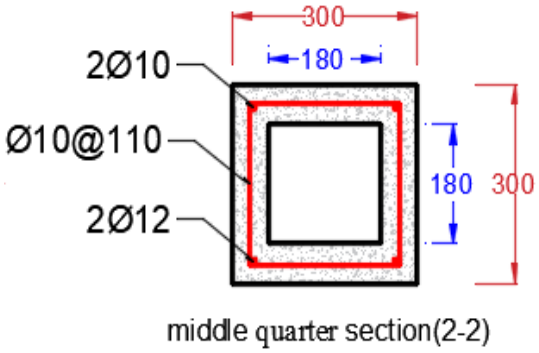

middle quarter section(2-2)

$$fy = 516MPa$$

$$d = 264mm$$

$$fc' = 25MPa$$

$$cover = 20mm$$

$$a = \frac{As * fy}{0.85\, fc' * b}$$

$$a = \frac{226.2 * 516}{0.85 * 25 * 300} = 18.3mm \rightarrow a < hf$$

∴The beam is rectangular

$$Mn = As * fy * (d - \frac{a}{2})$$

$$Mn = 113 * 2 * 516 * (264 - \frac{18.3}{2}) * 10^{-6} = 30kN.m$$

$$Mn = \frac{Pu}{2} * a$$

$$30 = \frac{Pu}{2} * \frac{1.4}{3} = 129kN \rightarrow Pu = 12.9Ton$$

A.2 Checking Shear Capacity of the Section

$$Vc = 0.17\sqrt{fc'} * bw * d$$

$$= 0.17\sqrt{25} * (264 * 120) * 10^{-3} = 27kN$$

$$Av = 2 * \frac{\pi}{4} * 10^2 = 157mm^2$$

$$Vs = \frac{Av * fy * d}{s} = \frac{157 * 516 * 264}{90} * 10^{-3} = 238kN$$

$$Vu = Vs + Vc$$

$$Vu = 238 + 27 = 265kN$$

A.3 Design of External Strengthening by CFRP Laminates for Beam with Front and Rear Opening

$$Vu = 64.65kN$$

$$Vc = 0.17\sqrt{fc'} * bw * d$$

$$Vc = 0.17 * \sqrt{25} * (120 * 264 - 100 * 60 * 2) * 10^{-3}$$

$$Vc = 17kN$$

$$A_{CFRP} = \frac{Shear\ force}{\text{Fibre tensile strength}}$$

$$A_{CFRP} = \frac{(64.65 - 17) * 1000}{4000} = 11.9mm^2$$

$$Minimum\ CFRP\ width = \frac{8.64}{0.167} = 71.3mm$$

Used CFRP width = 100 mm full wrapping on each side of the opening

Appendix-B
Materials properties

B.1 Cement

Table B.1: Cement chemical properties *

Chemical Properties	Test Result	Iraqi specification No. 5/1984 %
SiO_2 %	21.7	----
AL_2O_3 %	3.6	----
Fe_2O_3 %	4.5	----
CaO %	65.2	----
MgO %	1.6	≤ 5%
SO_3 %	2.1	≤2.5%ifC3A< 5% ≤2.8%ifC3A> 5%
I.R %	0.66	≤1.5 %
L.O.I %	3.46	≤4%
C_3A %	1.91	----
L.S.F %	0.94	0.66-1.02
Fe_2O_3 - AL_2O_3 %	----	----
NA_2O - K_2O %	----	----

* These tests were carried out in the Karbala Construction Laboratory.

Table B.2: Cement physical properties *

Physical Properties	Test Result	Iraqi specification No. 5/1984 %
Setting Time, min,	125 Initial 185 final	≥45 ≤600
Fineness (Blaine), m^2/kg	376	≥230
Compressive strength at 3 days (MPa)	29	>15
Compressive strength at 7 days (MPa)	36	>23

* These tests were carried out in the Karbala Construction Laboratory.

B.2 Fine Aggregate (Sand)

Table B.3: Test results of fine aggregate*

Sieve size (mm)	Cumulative Passing %	Cumulative passing % Limits of Iraqi specification No. 45/1984, zone(3)
10	100	**100**
4.75	97	**90 - 100**
2.36	91	**85 - 100**
1.18	85	**75 – 90**
0.60	76	**60 – 79**
0.30	45	**12 – 40**
0.15	10	**0 – 10**
Materials passing from sieve 75 µ %= 3.6% (specification requirements up to 5%)		
SO_3 content=0.364% (specification requirements up to 0.5%)		

* These tests were carried out in the Karbala Construction Laboratory.

B.3 Coarse Aggregate (Gravel)

Table B.4: Test results of coarse aggregate*

Sieve size(mm)	passing %	Specification limits Iraqi specification No.45/1984
37.5	100	**100**
20	98	**95– 100**
14	----	**----**
10	43	**30 – 60**
5	3	**0 – 10**
Mechanical wear =16.1% ((specification requirements up to 35%)		
Materials passing from sieve 75 µ %= 0.29% (specification requirements up to 3%)		
SO3 content=0.03% (specification requirements up to 0.1%)		

* These tests were carried out in the Karbala Construction Laboratory.

B.4 Limestone Powder

Table B.5: Chemical composition of limestone dust*

Oxide	Content %
CaO	60.01
Fe_2O_3	0.2
Al_2O_3	0.61
SiO_2	1.22
MgO	0.32
SO_3	0.1
L.O.I	36.5

* These tests were carried out in the Karbala Construction Laboratory.

Table B.6: Physical properties of Limestone dust*

Physical properties of Limestone dust	
Physical form	Fine aggregate gradation zone (2)
Colour	White
Absorption	20%

* These tests were carried out in the Karbala Construction Laboratory.

B.5 Superplasticizer (Sika ViscoCrete-5930)

Table B.7: Technical data of sika viscocrete®-5930*

Property	Description or Value
Basis	An aqueous solution of modified polycarboxylates
Appearance	Turbid liquid
Density (kg /lt)	1.095
Boiling	100 ^{0} C
PH	7-9
Recommended dosage	0.2-0.8 % litter by weight of cement for NC 0.8-2 % litter by weight of cement for SCC

(*) Provided by the manufacturer

B.6 Sika Wrap®-300 C

Table B.8: Properties of sika wrap®-300 C (Carbon Fibre Fabric)* Material Data Sheet (2017)

Fibre type	High strength carbon fibres
Fibre orientation	0◦ (unidirectional). The fabric is equipped with individual weft fibres which prevent Loosening of the roving (heat set process).
Dry Fibre Density	1.82 g/cm^3
Fabric design thickness	0.167 mm
Tensile strength of fibres	4 000 MPa
Tensile modulus of fibres	230 000 MPa
Elongation at break	1.7 %
Fabric length/roll	≥ 100m
Fabric width	500mm

* Provided by the manufacturer

B.7 Epoxy Resin (Sikadur-330)

Table B.9: Properties of sikadur-330 (Impregnating Resin)* Material Data Sheet, (2017)

Appearance	Comp. a: white Comp. b: grey
Density	1.31 kg/l (mixed)
Mixing ratio	A : B = 4 : 1 by weight
Open time	30 min (at + 35◦C)
Viscosity	Pasty, not flowable
Application temperature	+ 15◦C to + 35◦C (ambient and substrate)
Tensile strength	30 MPa (cured 7 days at +23◦C)
Flexural E-modulus	3800 MPa (cured 7 days at +23◦C)

* Provided by the manufacturer

C.1 ABAQUS

In this work, the Concrete Damage plasticity model was chosen for the simulation of hollow self-compacting concrete beams with in-place openings the properties of concrete that were used in this model is listed in the table below

Table C. 1: General properties of concrete

Specimen symbol	Compressive strength (MPa)	Young modules (MPa)	Poisson Ratio
HC			
H10MF			
H10SF			
H10SMF			
H10MFR			
H10SFR			
H10SMFR	32.5	26794	0.18
H10MB			
H10SB			
H10SMB			
H10MFR-CFRP			
H10SFR-CFRP			
H10SMFR-CFRP			

Table C. 2: Concrete damaged plasticity parameters of concrete

Dilation angle	Eccentricity	Fb0/fc0	k	Viscosity parameter
40	0.1	1.16	0.667	0.0001

For defining the stress-strain curve of concrete this study used model **Carreira and Chu**, (**1986**) as follow as illustrated in **Fig C.1**

$$\frac{f_c}{f'_c} = \frac{\beta\,(\epsilon/\epsilon'_c)}{\beta - 1 + (\epsilon/\epsilon'_c)^{\beta}} \qquad (1)$$

$$\beta = \frac{1}{1 - \dfrac{f'_c}{\epsilon'_c E_{it}}} \qquad (2)$$

for $\beta \geq 1.0$ and $\epsilon \leq \epsilon_u$

Where:

fc`: is the maximum stress obtained from cylinder test (MPa)

€`: is the strain corresponding with the maximum stress

Ec: is the modulus of elasticity.

(3 : is a material parameter that depends on the shape of the stress-strain diagram

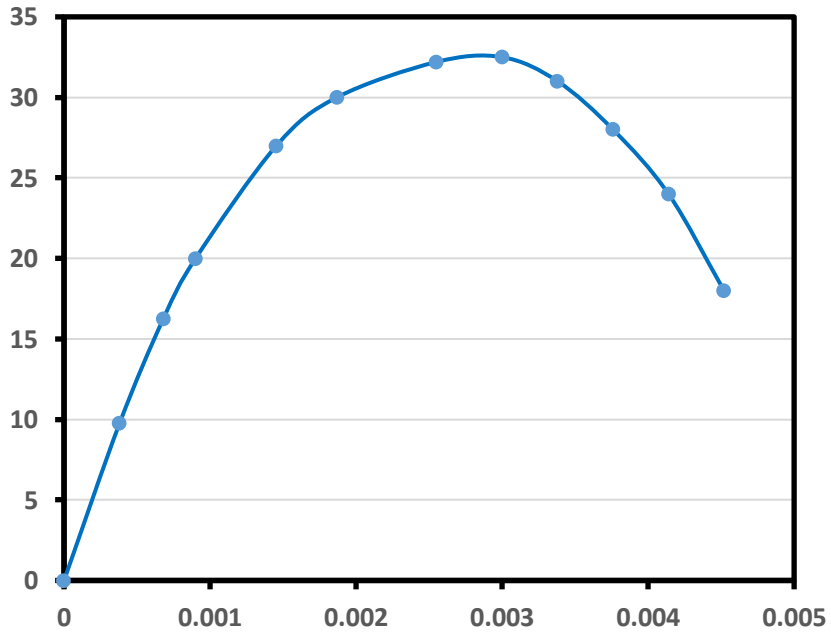

Fig. C. 1: Stress-strain relationship model used in this study

Table C. 2: Stress-strain relationship model used in this study Carreira and Chu, (1986)

Number	Yield stress for concrete (MPa)	Plastic strain for concrete (mm)
1	9.75	0
2	16.25	0.0003
3	20	0.000521
4	27	0.001074
5	30	0.001489
6	32.2	0.00217
7	32.5	0.00262
8	31.5	0.003
9	29	0.00338
10	24	0.00376

Table C. 3: Plastic properties of steel

Material	Diameter (mm)	Yield stress fy (MPa)	Plastic strain fu (mm)
Steel bar	10	450	0
		500	0.018
Steel bar	12	510	0
		610	0.1

Table C. 4: Properties of CFRP laminate

Material	Dry Fibre Modulus of Elasticity in Tension(MPa)	Dry Fibre Tensile Strength (MPa)	Laminate Nominal Thickness (mm)
CFRP	230 000	4 000	0.167

C.2 Mises Stresses for H10MFR Strengthening Schemes

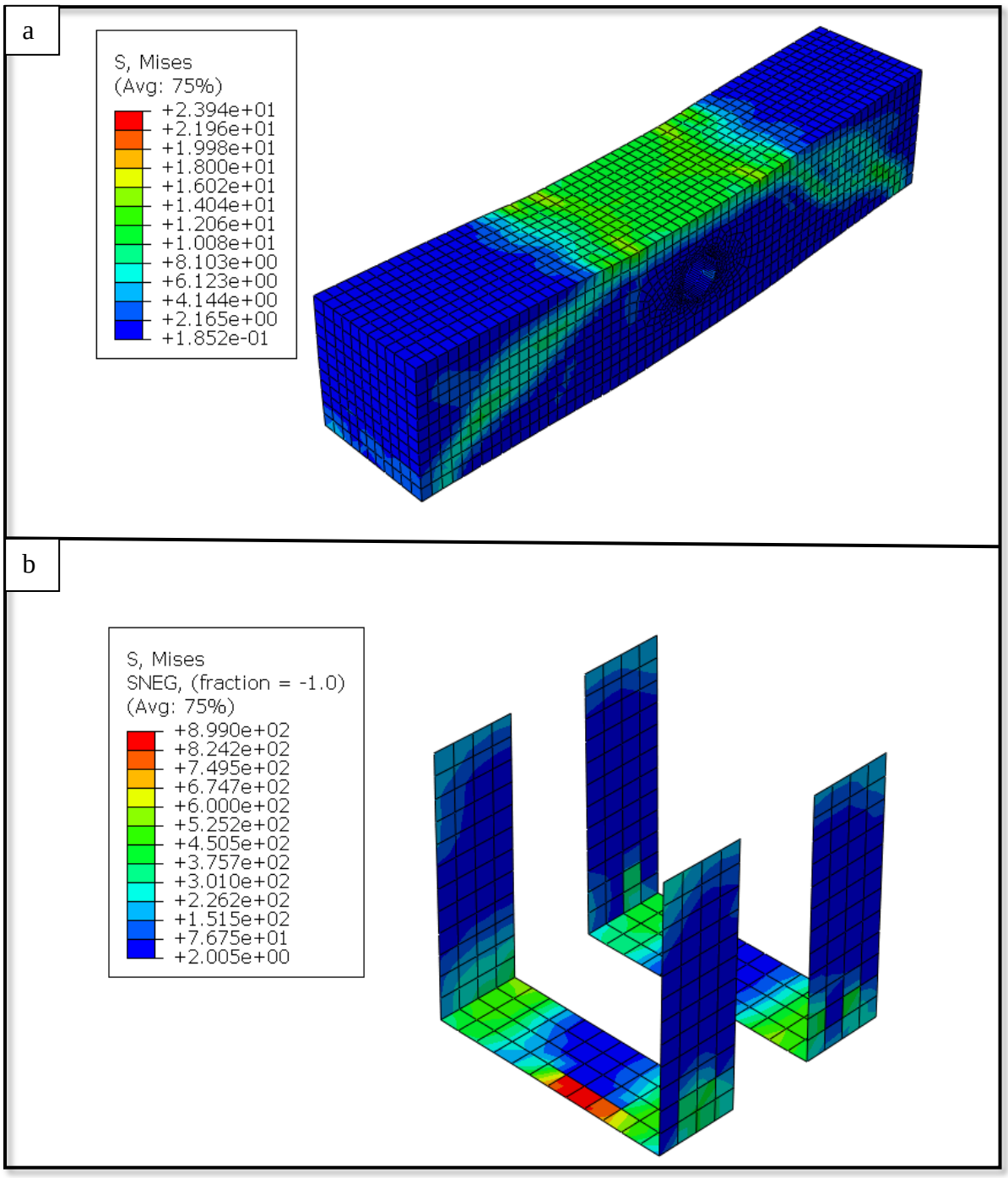

Fig. C. 2: Stresses distribution in a u-wrapping scheme for H10MFR

a) Stresses in concrete

b) Stresses in CFRP

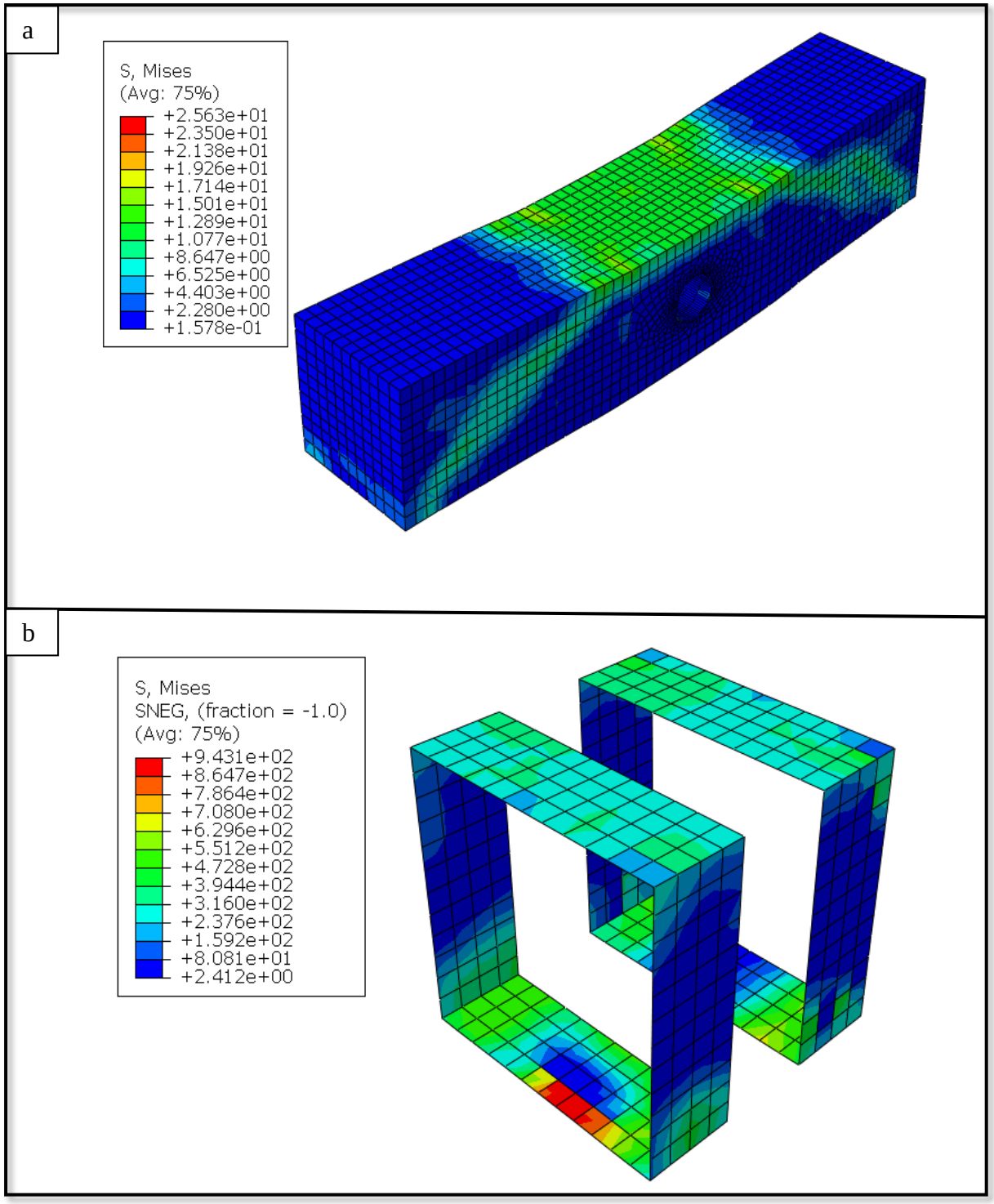

Fig. C. 3: Stresses distribution in full wrapping-1CFRP layer scheme for H10MFR

a) Stresses in concrete

b) Stresses in CFRP

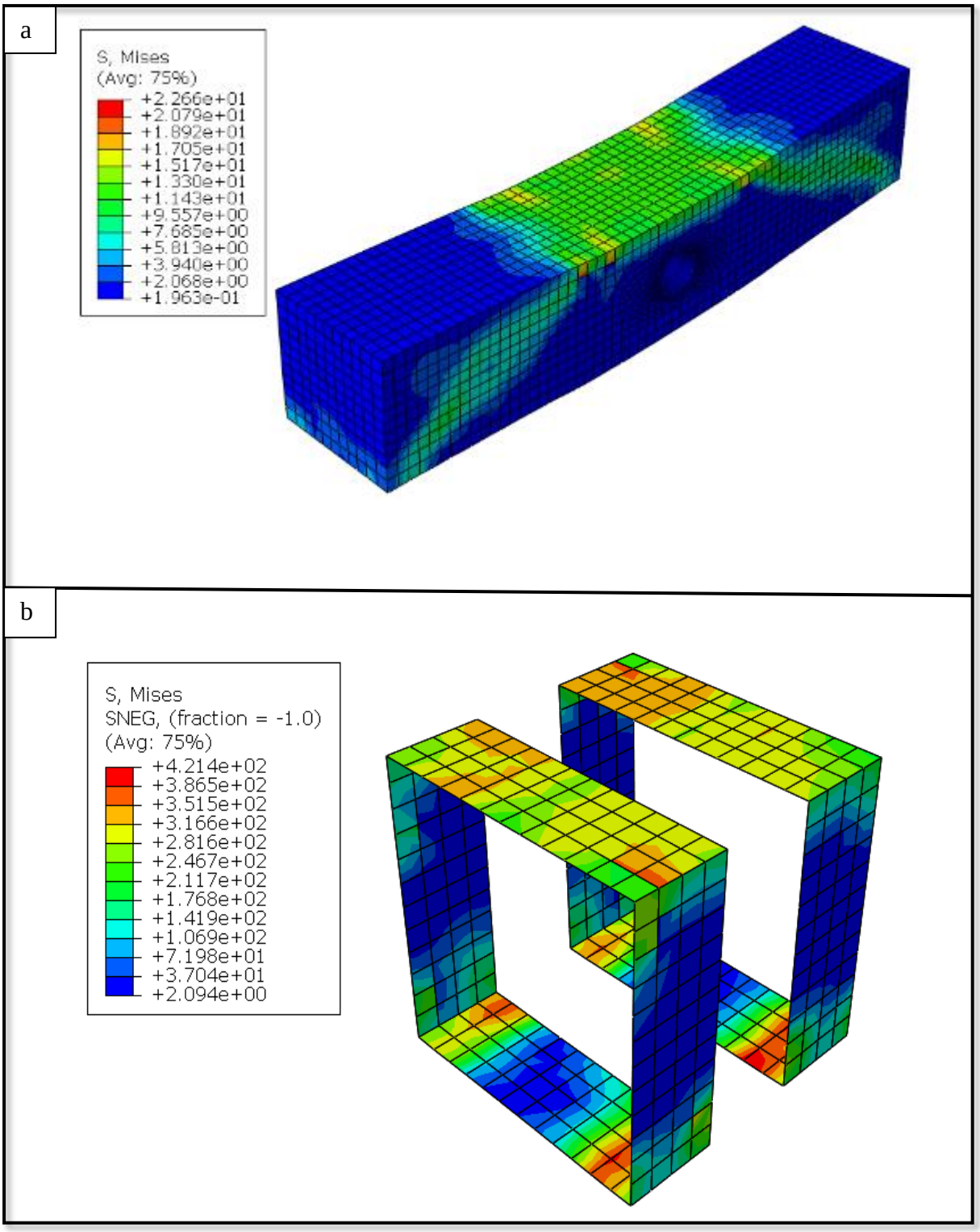

Fig. C. 4: Stresses distribution in full wrapping-2CFRP layer scheme for H10MFR

a) Stresses in concrete

b) Stresses in CFRP

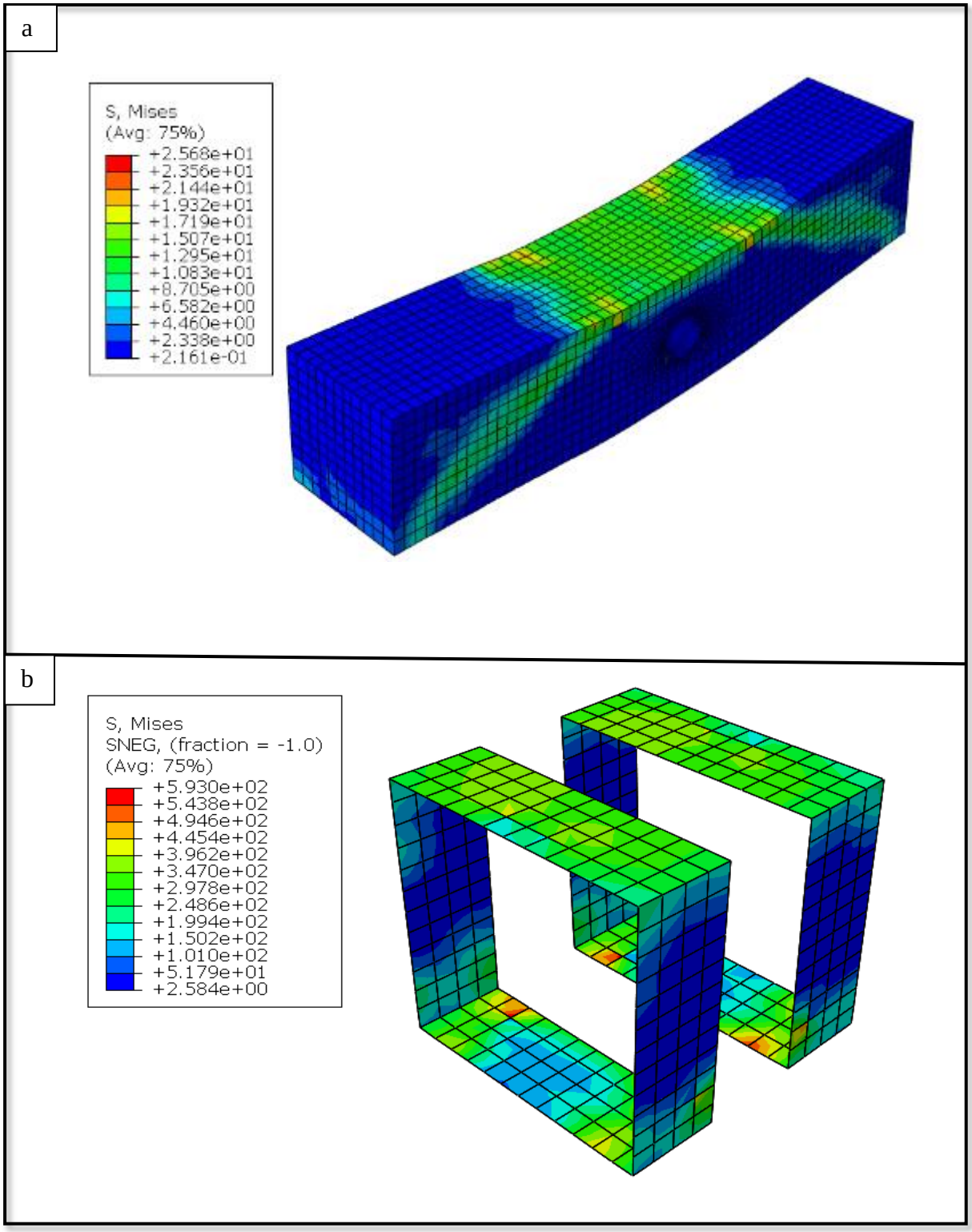

Fig. C. 5: Stresses distribution in full wrapping-3CFRP layer scheme for H10MFR

a) Stresses in concrete

b) Stresses in CFRP

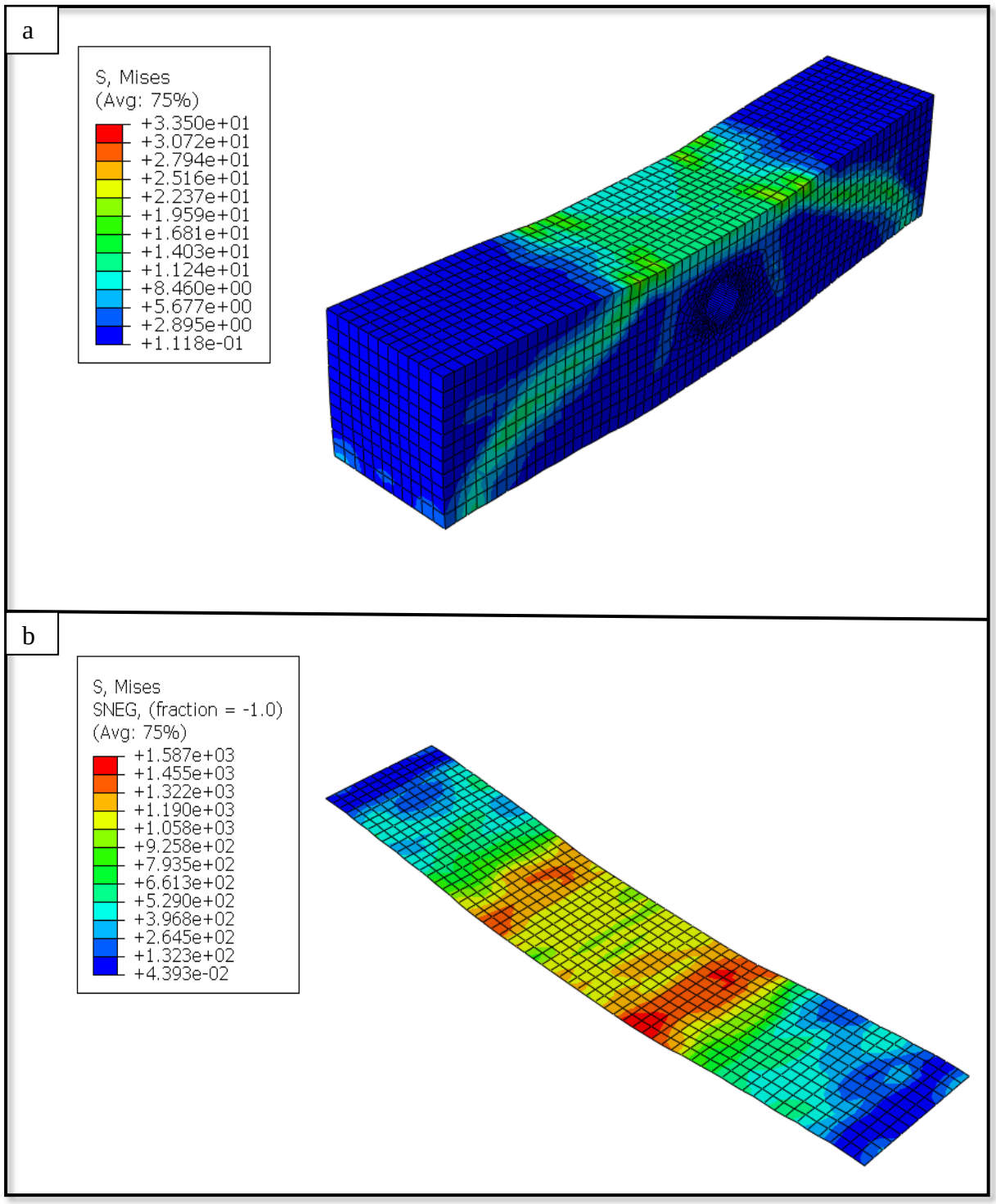

Fig. C. 6: Stresses distribution in a bottom-CFRP scheme for H10MFR

a) Stresses in concrete

b) Stresses in CFRP

C.3 Mises Stresses for H10SFR Strengthening Schemes

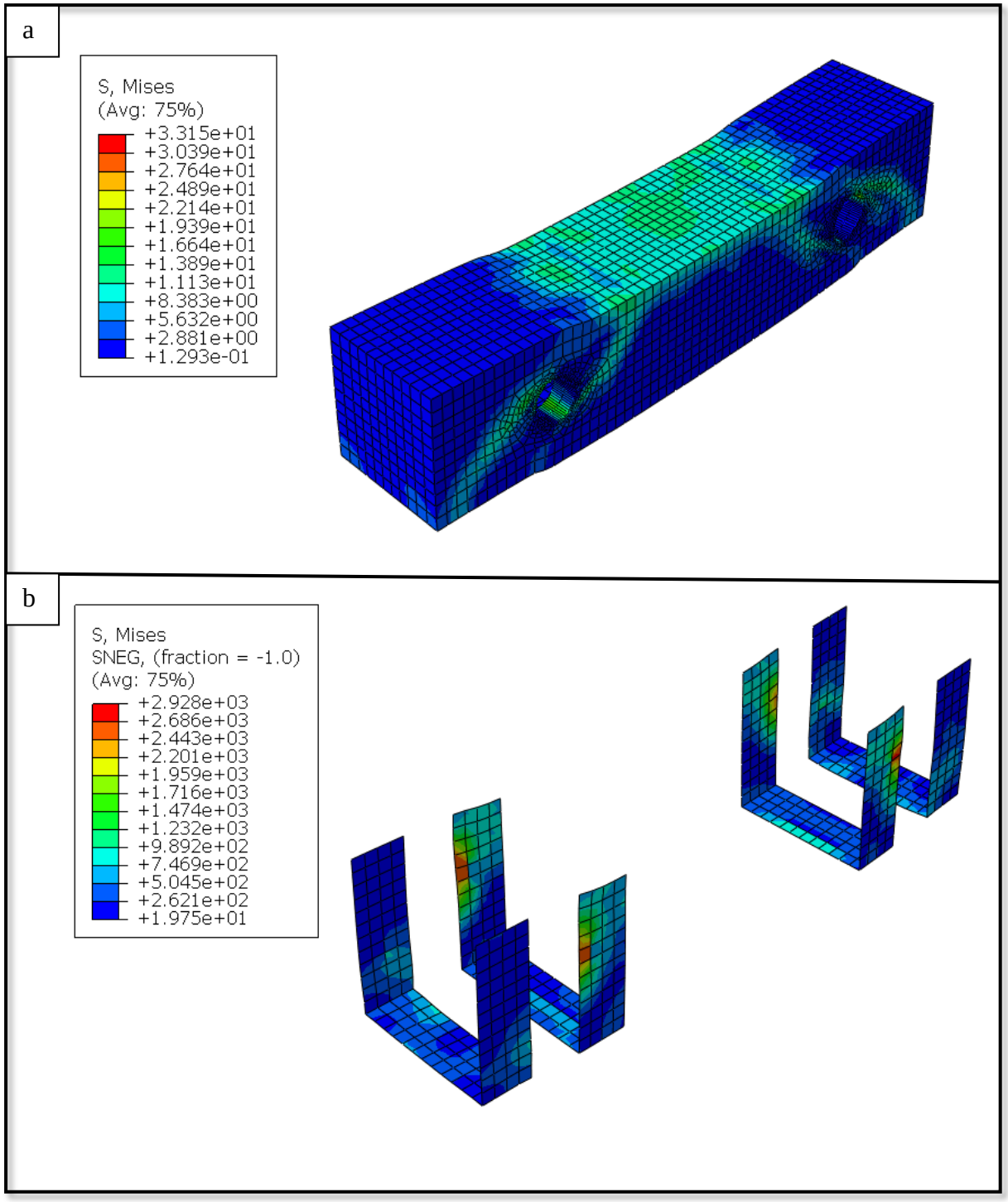

Fig. C. 7: Stresses distribution in a u-wrapping scheme for H10SFR

a) Stresses in concrete

b) Stresses in CFRP

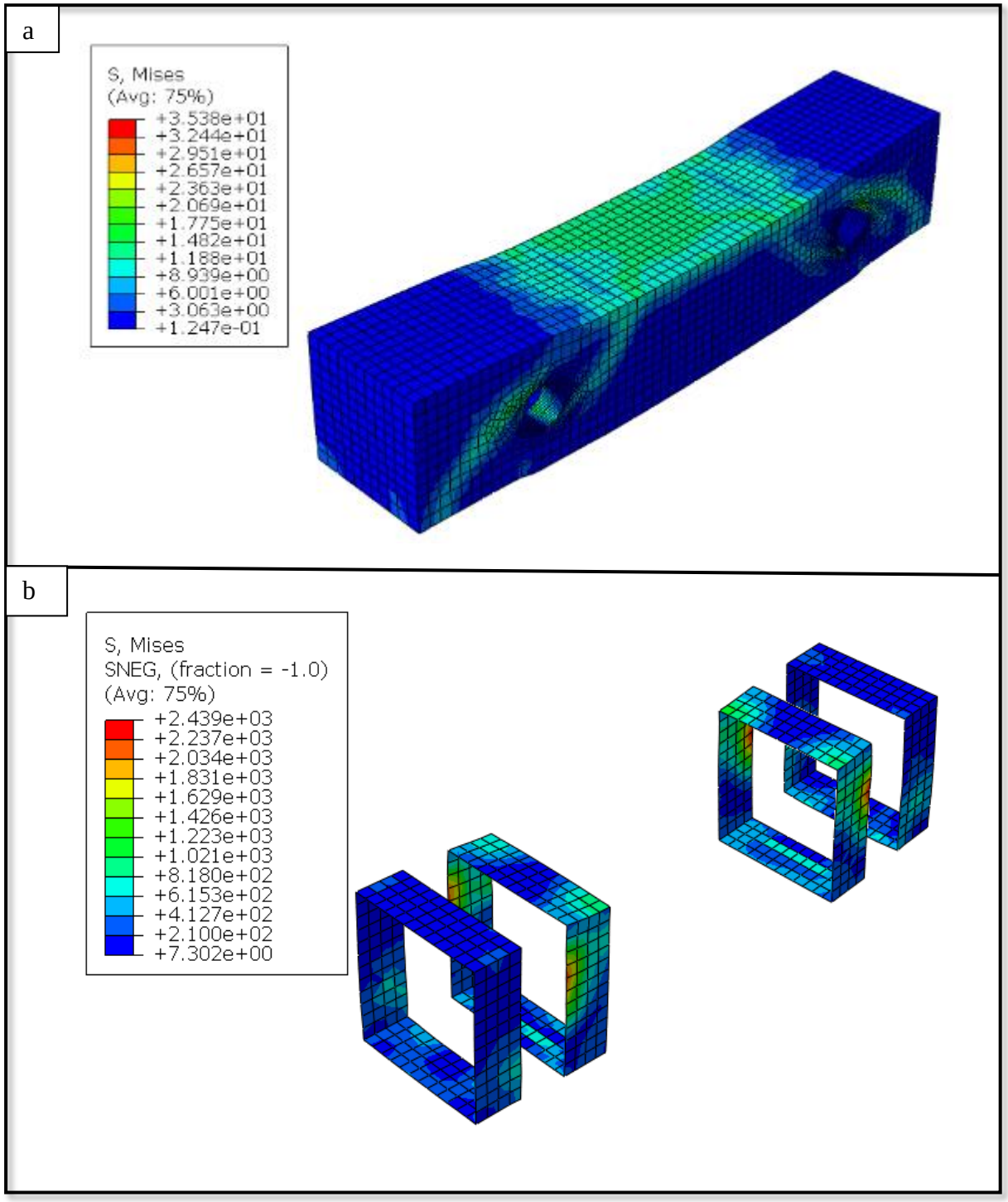

Fig. C. 8: Stresses distribution in full wrapping-1CFRP layer scheme for H10SFR

c) Stresses in concrete

d) Stresses in CFRP

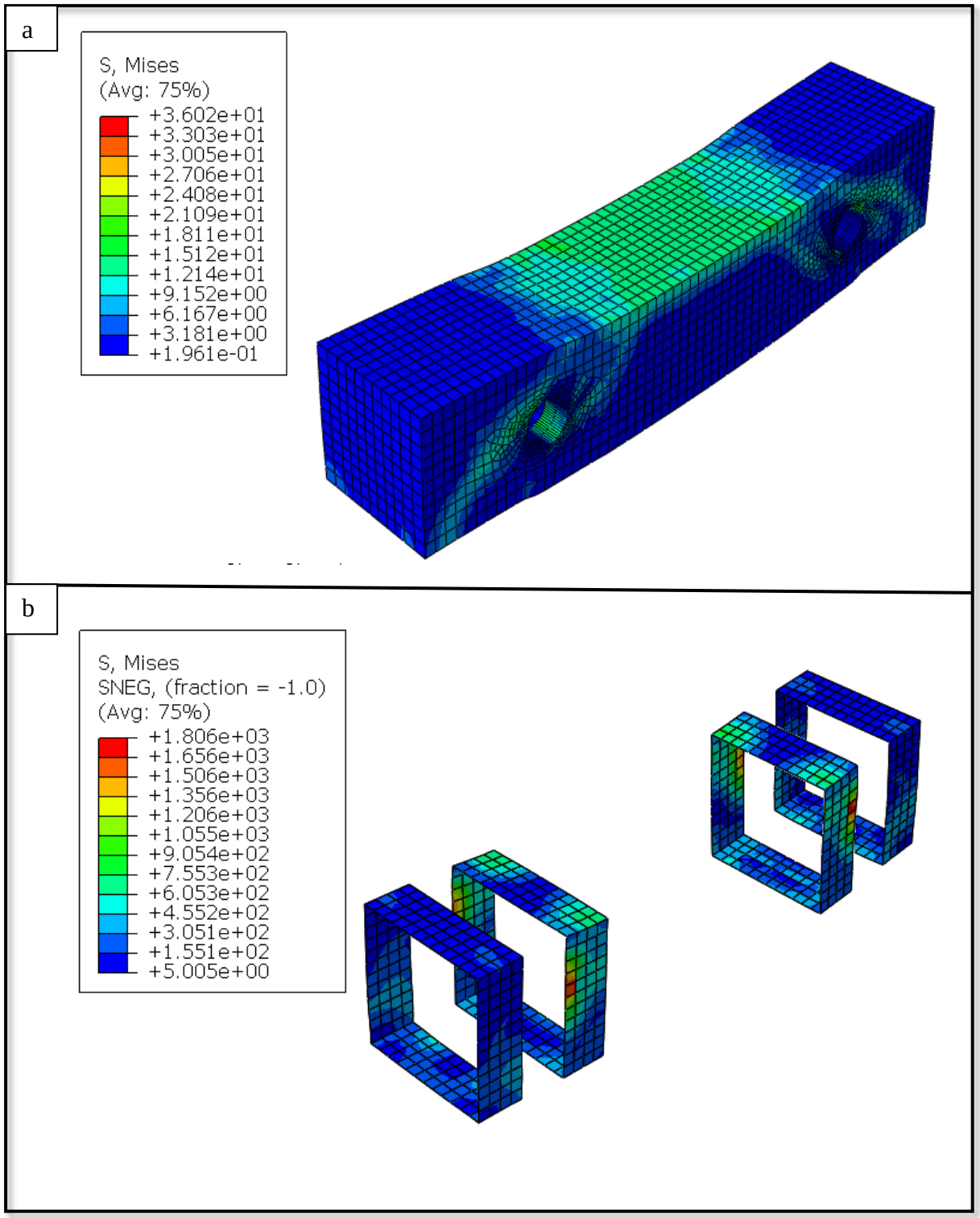

Fig. C. 9: stresses distribution in full wrapping-2CFRP layer scheme for H10SFR

e) Stresses in concrete

f) Stresses in CFRP

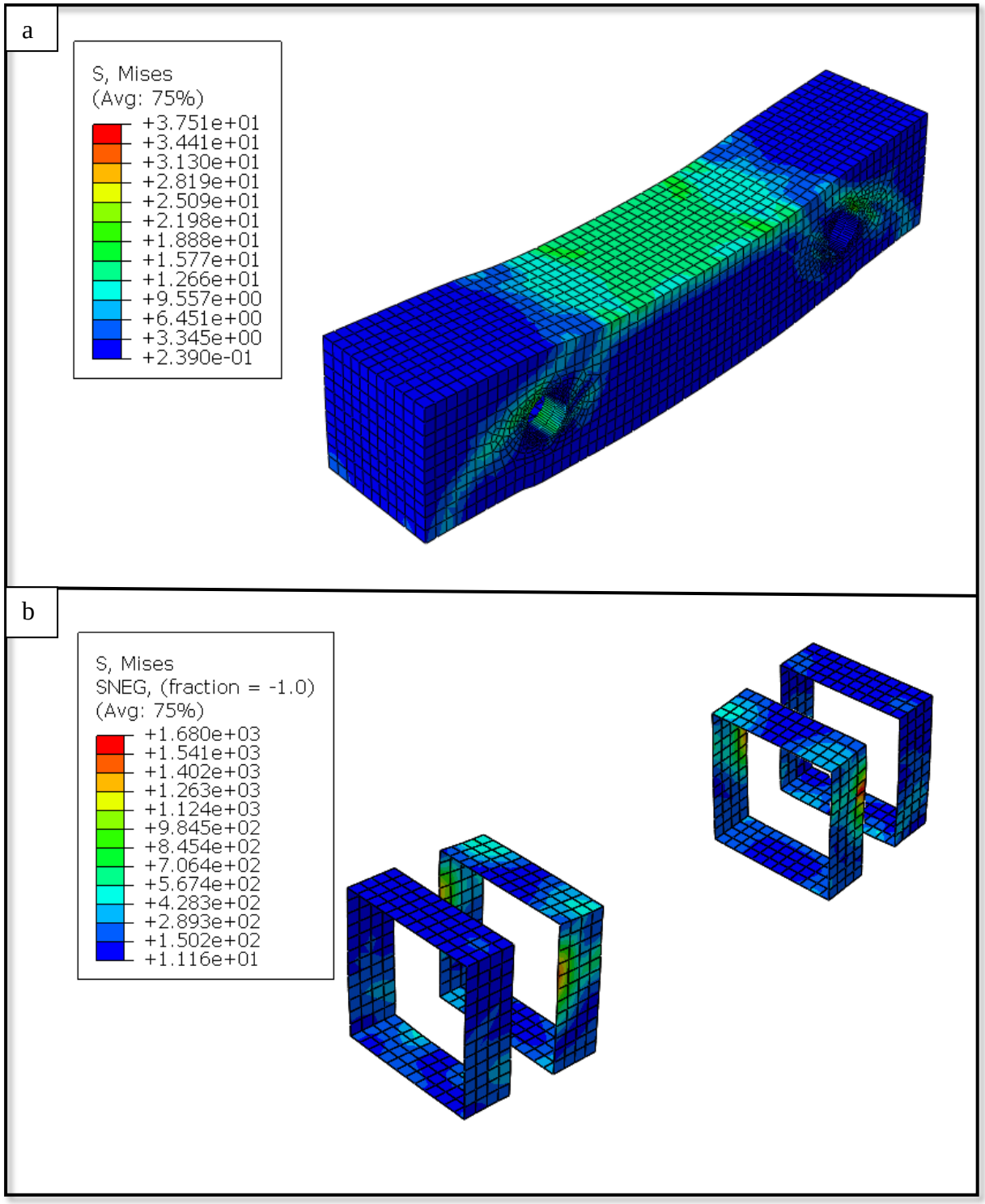

Fig. C. 10: Stresses distribution in full wrapping-3CFRP layer scheme for H10SFR

a) Stresses in concrete

b) Stresses in CFRP

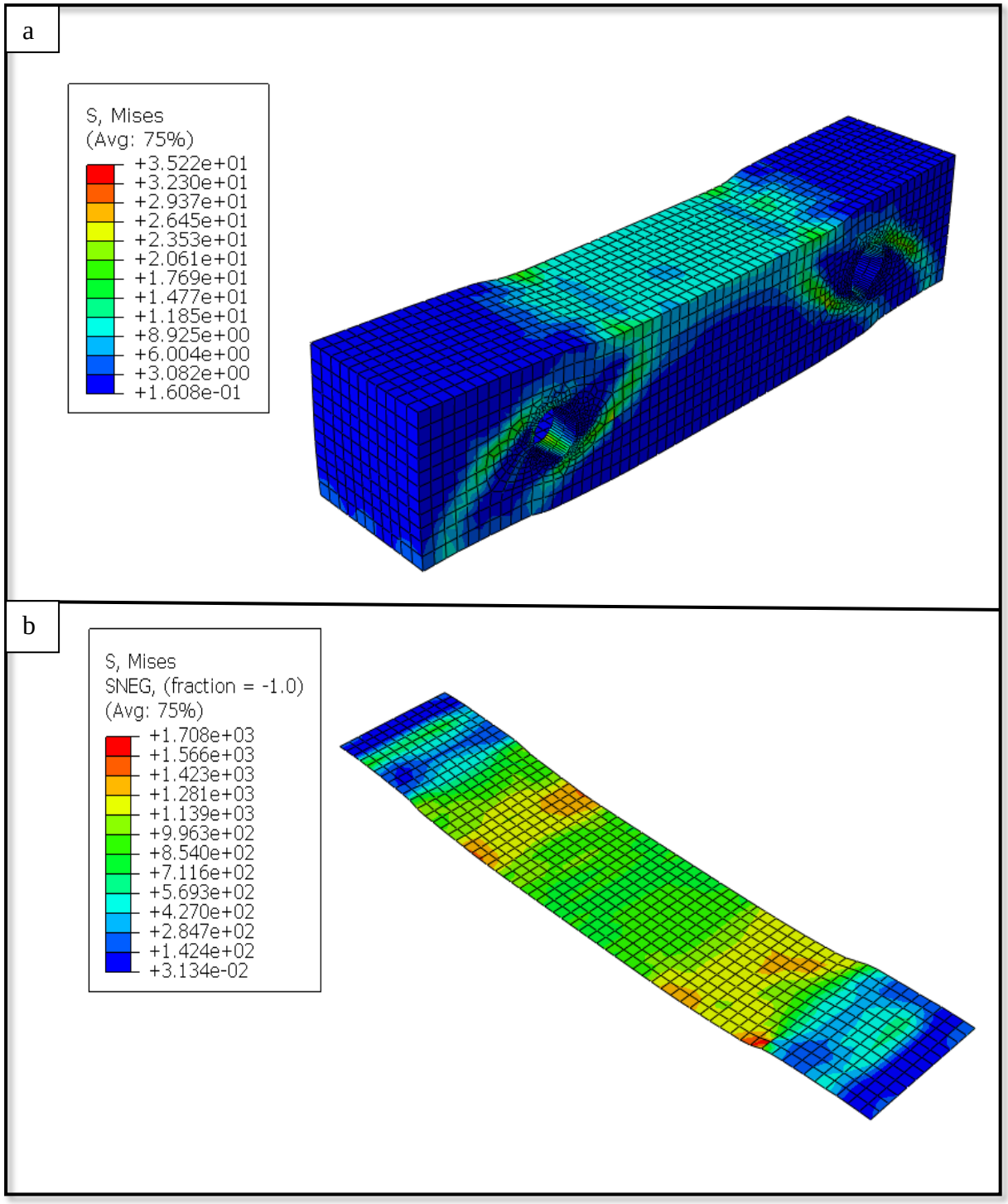

Fig. C. 11: Stresses distribution in a bottom-CFRP scheme for H10SFR

a) Stresses in concrete

b) Stresses in CFRP

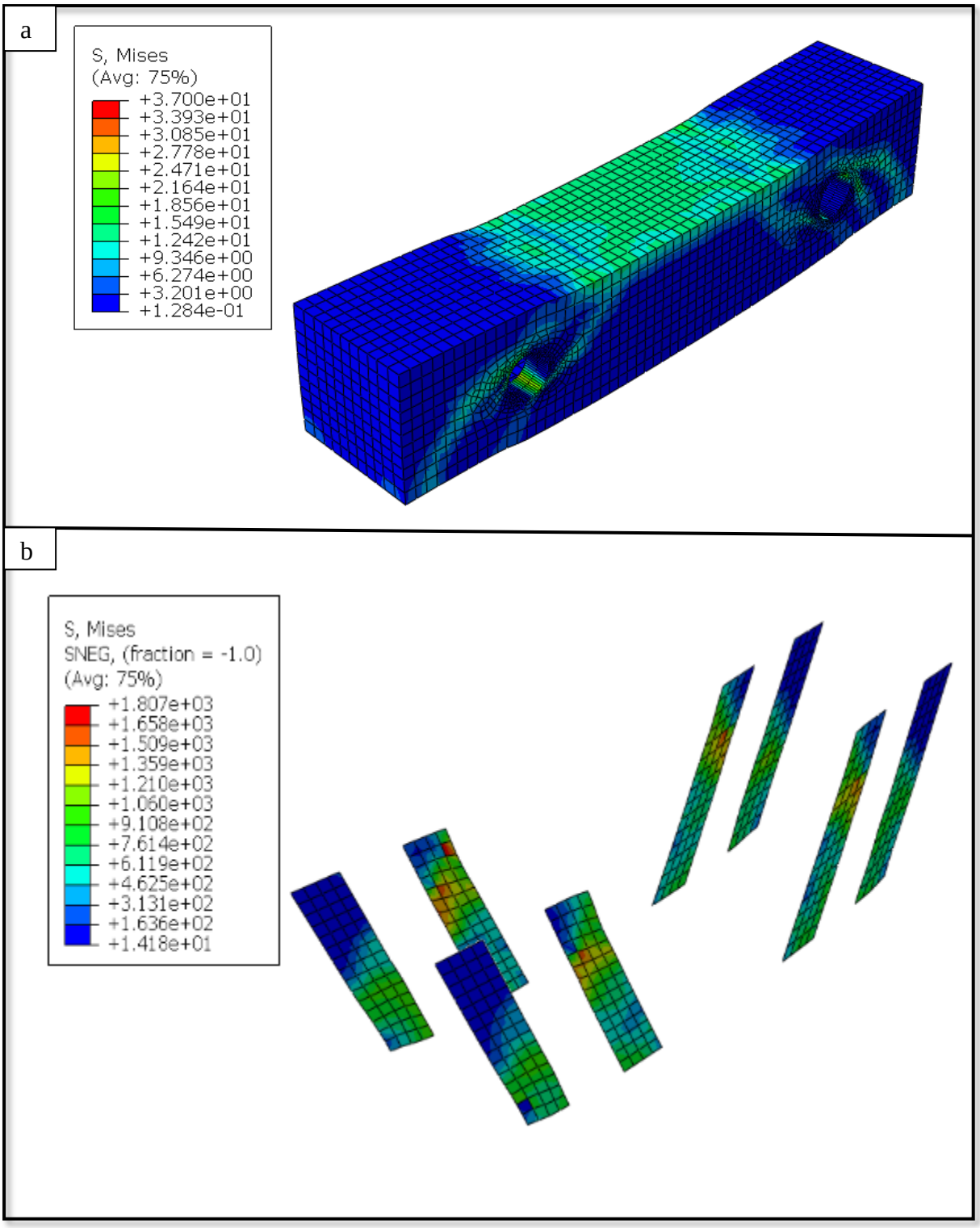

Fig. C. 12: Stresses distribution in an inclined-CFRP scheme for H10SFR

a) Stresses in concrete

b) Stresses in CFRP

الخلاصة

هدف البحث هو دراسة السلوك الانشائي لأعتاب مجوفة مصنوعة من خرسانة ذاتية الرص تحتوي على فتحات موقعية مستعرضه غير مقواة او مقواة باستعمال شرائط اللدائن الكربونية المسلحة من خلال تنفيذ عمل مختبري ونظري بواسطة برنامج الاباكوس 2019.

اشتمل البرنامج العملي على صب أربعة عشر عتبا خرسانيا مجوفا باستخدام خرسانة مسلحة مرصوصه ذاتياً وقد تم اختبارها تحت حميلين مركزيين ومتماثلين مع خصائص انشائية متطابقة (الأبعاد، تسليح الانثناء، مقاومة الانضغاط الخرسانية، وحجم الفتحة). تم تصنيف الاعتاب إلى ثلاث مجموعات بالإضافة إلى عتبين بدون فتحات كأعتاب مرجعية لغرض المقارنة. تضمنت المجموعة الأولى ستة أعتاب مع فتحة في الامام أو في الامام والخلف من الجذع، في حين احتوت المجموعة الثانية على ثلاثة أعتاب ذات فتحات في الحافة السفلية للعتب. اما المجموعة الثالثة، فقد تضمنت ثلاثة أعتاب مع فتحة في الأمام والخلف من الجذع مقواة باستعمال شرائط اللدائن الكربونيه المسلحة. اهم المتغيرات التي تمت دراستها هي عدد الفتحات ومواقعها.

بينت النتائج المختبرية للمجموعة الأولى من العينات أن استحداث فتحات في منطقة الثني أو منطقة القص أو كليهما تسبب في انخفاض في أحمال الفشل النهائية بنسب تراوحت ما بين (5.2٪- 16 ٪). علاوة على ذلك ، لوحظ زيادة في انحراف العينات بنسب مختلفة تقع ما بين (20٪ -70 ٪) بسبب الانخفاض في صلابة هذه العينات من (16٪-41٪) بالمقارنة مع العتب المجوف المرجعي. بينما تراوحت نسب الانخفاض في عينات المجموعة الثانية في أحمال الفشل النهائية من (5.5٪ - 9 ٪). علاوة على ذلك ، فإن جميع الأعتاب في المجموعة الثانية عانت من انحرافات عليا تراوحت ما بين (28٪ -63 ٪) بسبب الانخفاض في صلابة هذه الأعتاب من (22٪ -39٪) بالمقارنة مع العتب المجوف المرجعي. في المقابل ، تراوحت نسب الانخفاض في أحمال الفشل النهائية للعينات في المجموعة الثالثة من (1.9٪-8.4٪) ، بينما كانت الزيادة في مقدار الانحراف من (22- 43٪) بسبب الانخفاض في جساءة هذه الاعتاب من (18٪ -23٪) إذا ما قورنت بالعتب المجوف المرجعي . بالأضافه الى ذلك حسنت التقويه بأستخدام شرائط اللدائن الكربونيه المسلحة من صلادة الانحناء والالتواء للعتب بعد التشقق وكذلك أخرت ظهور التشققات أذا ما قورنت بالاعتاب غير المقواة في المجموعة الاولى. فيما يتعلق بالمجموعة الأولى من الأعتاب، تراوحت قيم مؤشرات المطيلية من (1.5-2.8) إذا ما قورنت بالعتب المرجعي، في حين تراوحت قيم المجموعة الثانية من (2.16-2.5) إذا ما قورنت بالعتب المرجعي. من ناحية أخرى، تم تسجيل قيم عالية لمؤشرات المطيلية للمجموعة الثالثة من الأعتاب وتراوحت القيم ما بين (2.35-3.17) مقارنة مع الحزم غير المقواة في المجموعة الأولى.

تم أجراء تحليل غير خطي بأستخدام تحليل العناصر المحدودة باستخدام برنامج الاباكوس لأجراء التحقق لتعرض الأعتاب الخرسانية المجوفة ذاتية الرص بوجود او عدم وجود فتحات موقعية غير مقواة او مقواة باستعمال شرائط اللدائن الكربونية المسلحة. كما تم أجراء دراسة نظرية جديدة ذات متغيرات مختلفة. تم أفتراض أن هناك ترابط تام بين الكونكريت وحديد التسليح وأيضا بين سطح الخرسانه و شرائط اللدائن الكربونية المسلحة. بينت النتائج ان هناك تقارب جيد بين النتائج العملية والنظرية من حيث الحمل النهائي، الأنحراف الاقصى، ومنحنيات انحراف الحمل، ونمط الفشل. كان معدل الاختلاف في الحمل النهائي والانحراف الأقصى مساويا لـ 1.8٪ و 9.2٪ على التوالي وهذا يمكن ان يضمن صحة النتائج العددية. كشفت

نتائج تحليل العناصر المحدودة للأعتاب ايضا أن أحمال الفشل النهائية للأعتاب المجوفة ذات الفتحات انخفضت مع زيادة قطر الفتحة من 4.1٪ إلى 18.2٪ للفتحة الموجودة في وسط العتب ومن 2.3٪ إلى 26.8٪ للفتحات الموجودة بالقرب من المساند إذا ما قورنت مع العتب المرجعي. بالاضافة الى ذلك، فقد بينت النتائج التحليليه ان الزيادة في عدد الفتحات ذات القطر نفسه قد ادت إلى انخفاض في أحمال الفشل النهائية من 9.8٪ إلى 35.8٪ إذا ما قورنت مع العتب المرجعي.علاوة على ذلك ، ازداد الحمل النهائي للعتب المجوف الحاوي على فتحات قريبة من المساند ذات قطر متماثل عند زيادة مقاومة الانضغاط للخرسانه. كان مخطط تقوية الحافة السفلية بواسطة شرائط اللدائن الكربونية المسلحة هو الأفضل من حيث التحمل الاقصى للأعتاب المجوفة الحاوية على فتحات قريبة على المساند أو في وسط العتب حيث كانت الزيادات في القوة النهائية من (29.2-37.4 ٪) لكلا العتبين على التوالي ، إذا ما قورنت بالأعتاب غير المقواة.

جمهورية العراق
وزارة التعليم العالي و البحث العلمي
جامعة كربلاء/ كلية الهندسة
قسم الهندسة المدنية

السلوك الانشائي للأعتاب الصندوقيه الخرسانيه ذاتية الرص الحاويه على فتحات موقعيه

رسالة مقدمة الى
قسم الهندسة المدنية في كلية الهندسة/ جامعة كربلاء
كجزء من متطلبات نيل شهادة الماجستير في علوم الهندسة المدنية – هندسة البنى التحتية
من قبل

سيف علي حسن
(بكالوريوس في الهندسة المدنية – 2016)
اشراف
أ.م.د. سجاد عامر حمزه
م.د. وجدي شبر صاحب

2020 م 1441 هـ